ABSTRACT

Title of Dissertation: IMPACT OF RECENT FOREST MANAGEMENT AND DISTURBANCES ON CARBON DYNAMICS IN THE GREATER YELLOWSTONE ECOSYSTEMS

Feng Zhao, Doctor of Philosophy, 2015

Dissertation directed by: Dr. Chengquan Huang, Research Professor, Department of Geographical Sciences
Dr. Ralph Dubayah, Professor, Department of Geographical Sciences

Protected areas are recognized worldwide as being important components of climate change mitigation and adaptation strategies. With increasing interests in quantifying greenhouse gas emissions and potentially managing forests to increase the rate of carbon sequestration, there are urgent needs to quantify impact of forest management and disturbances on carbon dynamics.

The overall goal of this study is to quantify the impact of recent forest management and disturbances on forest carbon dynamics in GYE, by integrating forest inventory, remote sensing data and carbon modeling approach. Four specific goals for this study include: (1) Develop a method to compare historical and current fire regimes using time series remote sensing data and a landscape succession model; (2) Assess post-fire and post-harvest forest recovery in GYE using time series remote

sensing data; (3) Characterize recent forest management and disturbance history (1984-2011) in GYE using local management record and time series remote sensing data; (4) Quantify the impact of recent forest management and disturbances on carbon dynamics in GYE by linking forest inventory, time series remote sensing and carbon modeling.

This dissertation is a synthesized analysis of the impact of recent forest management and disturbance on carbon dynamics in GYE, by integrating forest inventory, remote sensing and C modeling approach. The results of this study could contribute to a better understanding of management-disturbance-carbon interactions over ecosystems with complex management regimes and environmental gradients, such as GYE. This study provides a comprehensive and consistent annualized record of forest disturbances, post-disturbance forest recovery, carbon stocks, and relative impact of forest management and disturbance on carbon dynamics in GYE. Such a record would be useful for informed forest management and policy making, ecosystem conservation and restoration, biodiversity protection and carbon assessment in this region. With the availability of input data nationwide, this approach can be applied to the rest of U.S. for many research and management purposes.

IMPACT OF RECENT FOREST MANAGEMENT AND DISTURBANECS ON CARBON DYNAMICS IN THE GREATER YELLOWSTONE ECOSYSTEMS

by

Feng Zhao

Dissertation submitted to the Faculty of the Graduate School of the
University of Maryland, College Park, in partial fulfillment
of the requirements for the degree of
Doctor of Philosophy
2015

Advisory Committee:
Dr. Chengquan Huang, Chair
Professor Ralph Dubayah, Co-chair
Dr. Zhiliang Zhu
Professor George Hurtt
Professor Joseph Sullivan

Dedication

To my parents, Haimin Zhao and Gaimei Shao, my sister, Yang Zhao and my husband, Ran Meng.

Thank you for your love and support.

Acknowledgements

At times our own light goes out and is rekindled by a spark from another person. Each of us has cause to think with deep gratitude of those who have lighted the flame within us.

--- Albert Schweitzer

I would first like to thank and acknowledge my advisors Dr. Chengquan Huang and Dr. Ralph Dubayah. Thanks to both of you for providing me the opportunity to study and work here with you and live my dream as an environmental scientist. Cheng, thank you for being a strict and hands-on mentor. I would always remember the long discussions we had over my dissertation and I hope someday I will grow into a mentor as sharp, patient and supportive as you do. Ralph, thank you for being an insightful and genuine advisor. I got many of the best comments/suggestions/questions from you. With absolute respect and admiration, I am proud to be both of your students.

My special thanks go to my committee members, Dr. Zhiliang Zhu, Dr. George Hurtt and Dr. Joseph Sullivan. Z, thank you for always being there for me and empowering me with your kind encouragement. Your keen insights on frontier research directions helped shaping up my dissertation and future research goals. George, thank you for being an inspiring teacher, both in class and for my research, and teaching me to think about research from bigger pictures. Joe, thank you for taking time to discuss my research with me and supporting me as my Dean's representative.

I am sincerely thankful for all the help and support I get from many outstanding faculty and researchers, Dr. Shunlin Liang, Dr. Sean Healey, Dr. Robert Keane, Dr. James McCarter, Christopher Garrard, Alexander Hernandez, Roy Renkins, Katherine Rice, Dr. Guoqing Sun, Dr. Tatiana Loboda, Dr. Mengxue Li, Dr. Bo Jiang, Dr. Yi Peng, Dr. Tao He, Dr. Zhiyu Zhang, Dr. Dongdong Wang, Dr. Anu Swatantran, and Dr. Louis Giglio. Thank you all for taking aside time and helping with my questions/concerns, and I am grateful for all your kind support and suggestions.

I would like to say thanks to my dear lab mates and group members, Dr. Wenli Huang, Dr. Huiran Jin, Danxia Song, Weishu Gong, Pui-Yu Ling, Panshi Wang, Dr. Rui Zhang, Dr. Maosheng Zhao, Dr. Feng A. Zhao, Dr. Xin Tao, Dr. Yingchun Liu and Dr. Khaldoun Rishmawi. Going to the lab with you guys around has been an important part of my daily life and thank you all for making it colorful and enjoyable. A big thank you to departmental administrative working professionals, Bob Crossgrove, Dr. Rachel Berndtson, Wilhelmina Johnson, Liz Smith, Shannon Bobbitt, Christine Kang, Meei Ching Ma, Jenny Hu, Fernando Ramirez for their kindness and patience with all my requests and inquiries.

I am also thankful for friendship and supports from all my fellow graduate students and dear friends, LeeAnn King, Jie Zhang, Dr. Janet Nackoney, Cheng Fu, Dr. Xiao-Peng Song, Dr. Min Feng, Dong Chen, Dr. Hao Tang, Yaoqi Zhang, Dr. Xiaoming Liu, Dr. Yuntao Dong, Dr. Amanda Whitehurst, Praveen Noojipady, and many more. My life in the U.S. also feels more welcoming and at home thanks to Aunt Zhun Cheng, Uncle and Aunt Guoqing Tian, Xili Luo, Aunt Xiaoyan Song and

Aunt Chaoling Zheng. Although I cannot list all names here, I will be remembering all the kindness and warmness I received from everyone.

I feel grateful every day for my loving family. My parents, parents-in-law, my husband, sister, niece, and brother-in-law. This long-distance separation makes me realize that family is invaluable to my personal well-being. With your endless love and support, I know I can be brave for whatever lies before me.

Finally, thanks to the U.S. Geological Survey and Ann Wylie Dissertation Fellowship for providing financial support for this dissertation work.

Table of Contents

List of Tables

List of Figures

Chapter 1: Introduction

1.1 Background

Understanding effects of land management on capacity and vulnerability of carbon stocks and sequestration is a key requirement of the Energy Independence and Security Act of 2007. Protected areas are recognized worldwide as being important components of climate change mitigation and adaptation strategies because of their governance structures, permanence, and management effectiveness (Soares-Filho et al. 2010). Different types of protected areas have different management goals and strategies that can result in different forest disturbance and recovery history. As a result, forest carbon density, fluxes, and future sequestration potentials likely will be different among these areas.

National Parks, Wilderness Areas, and National Forests are all considered as protected areas, albeit with different levels of protection (Dudley 2008). Several national parks and wilderness areas were established in the Greater Yellowstone Ecosystem (GYE) between 1872 and 1976 (Clark et al. 1991). As mandated by the U.S. National Parks Act in 1872, maintenance of ecological integrity has become the first priority of the U.S. National Park Service (Everhart 1972). More recently, the potential contribution of these parks to climate change mitigation has become a question of policy and management interest. The prime directive of the National Park Service (NPS) is to "conserve the scenery and the natural and objects and the wildlife therein … leave them unimpaired for the enjoyment of future generations" (National Park Service Organic Act 1916). Therefore logging is prohibited within the parks, and

naturally ignited wildland fires may burn freely as an ecosystem process. The management of U.S. wilderness shares similar policies as the National Parks. Under the National Forest Management Act of 1976, national forests are managed for multiple uses, including timber, wildlife and so on. Certain amounts of harvest are allowed, but all fires are suppressed to protect public and property safety (Burroughs and Clark 1995). Although cooperation is ongoing on various fronts, in general national parks and national forests implement very different land management strategies that result in different disturbance and harvest patterns. While private lands are not subject to these management practices, some of them may also be regulated under laws of different levels – from federal laws such the Clean Water Act, Clean Air Act, Endangered Species Act, Federal Insecticide, Fungicide and Rodenticide Act to state law and local management plans (Cubbage and Siegel 1985).

Disturbance events (natural or anthropogenic) play important roles in determining world biome distribution (Bond et al. 2005), ecosystem composition and structure (Turner 2010), and the cycling of carbon and nutrients (Bradford et al. 2013; Kurz et al. 2008). Standing replacing disturbances such as wildland fires and clear-cutting typically result in short-term forest carbon losses, followed by carbon gains from forest recovery after the disturbances (McKinley et al. 2011). Recovery from past disturbances is an integral process of carbon and nutrient cycles (Houghton et al. 1999; Pan et al. 2011). Inclusion in the forest recovery process from disturbances is critical to calculating regional C fluxes and can better inform policy makers on both the importance and uncertainty of disturbances on regulating the regional and global carbon cycle (Goetz et al. 2012). Therefore, the frequency of the natural disturbances

and management activities that alter the spatial-temporal dynamics of disturbance and recovery regimes can have major effects on regional, national and global carbon dynamics(Hurtt et al. 2002).

1.1.1 Comparing current and historical fire regimes

Previous forest management and human activities would likely have altered forest disturbance regimes in many ecosystems in the western U.S., especially fires (Covington and Moore 1994; Keane et al. 2002b). Assessing departures of current fire regimes from historical (before human management) conditions is critical for fire and climate change research, fire management, prioritizing fuel treatment and thus understanding the effects of fire on carbon balance (Bowman et al. 2009). Effective wildland fire management is partly reliant on accurate and consistent comparison of historical and current fire regimes at multiple spatial and temporal scales (Hardy et al. 2001; Keane et al. 2003). Landscape fuel treatment can be prioritized, designed, and scheduled to restore and manage the forests by understanding the causal mechanisms creating historical and current fire regimes. For example, land managers use such information to quantitatively determine the condition of fire-dependent ecosystems and whether management actions designed to improve the health of the ecosystems are achieving their desired outcome (Hann and Bunnell 2001; Hardy et al. 2001). For policy applications, fire regime calculations are useful and often necessary for measuring goals of federal wildland fire management policies such as consistent management standards across geography and land management units and guidance for fuel treatments or community assistance (Council 2009). Informed fire management is also emerging as a critical tool for implementing climate change

policies (such as the Climate Action Plan[1]) to adapt to and mitigate effects of climate change (Brown et al. 2004; Spittlehouse and Stewart 2004).

Recently, methods have been developed to compare characteristics of current and historical fire regimes across major ecosystems in North America. One measurement called Fire Regime Condition Class (FRCC) is a classification based on the amount of change or departure by fire attributes and vegetation, developed to represent departure of present-day fire regime conditions from a defined reference period – that is, whether a landscape is still within the natural or historical range and variation (HRV) (Hann et al. 2004; Hann and Bunnell 2001). Directly estimating the departures of current to historical fire regimes over large areas has been difficult owing to discrepancies between historical fire records which tend to be simple-point records and contemporary observations, which tend to rely on remote sensing-based maps covering a relatively short time span. The LANDFIRE[2] project (Rollins 2009) used vegetation departure as a surrogate for fire departure. Maps were produced for the U.S. depicting attributes of current vegetation such as successional patterns and trends that have departed from simulated historical vegetation reference conditions as the result of altered fire regimes. Despite continued efforts by the LANDFIRE project, a consistent FRCC calculation with a reasonable spatial scale and geographic scope is still difficult (Hann and Bunnell 2001; Hardy et al. 2001).

Landscape fire succession models that spatially predict fire regimes have been demonstrated to be a suitable tool for developing fire regime maps (Keane et al. 2003). Several previous efforts have used landscape fire succession models (such as

[1] http://www.whitehouse.gov/sites/default/files/image/president27sclimateactionplan.pdf

[2] LANDFIRE: LANDFIRE Vegetation Departure layer. U.S. Department of Interior, Geological Survey. [Online]. Available: http: //landfire.cr.usgs.gov/viewer/

SEM-LAND and LANDIS) to compare historical and current fire regimes (Chang et al. 2008; Li et al. 2005). Although these studies have made substantial contributions to our understanding of fire regime departures simulated with landscape models, two gaps remain in the literature. First, contemporary fire records used in these studies for simulating current fire regimes were either incomplete or of a short time interval (about 10 years of fire records), and therefore might not be sufficient to capture long-term variability of fire characteristics. Second, spatial ranges examined by these studies have tended to be at the landscape level (several square kilometers) with extensive parameterization and computation efforts. For regional or national applications, landscape fire succession models are needed, with more simplified parameterization while retaining enough spatial and temporal information for forest management activities such as fire management and fuel treatment.

1.1.2 Characterizing recent forest disturbance history

Developing methods to document the disturbance records is important to understanding the feedback effects of forest disturbances on patterns of carbon and nutrient cycling (Liu et al. 2011; Marks and Bormann 1972), and managing the long term health of forests (Turner 2010). Time series remote sensing data are useful for tracking ecosystem disturbances in a variety of studies (Huang et al. 2010; Kennedy et al. 2010a). However, efficiently identifying and separating disturbance types such as wildfire and harvest still remain a technical challenge. Recently, new attribution techniques have been introduced for use with time series Landsat and other satellite images (Loboda et al. 2012; Neigh et al. 2014; Schroeder et al. 2011). However, few efforts have gone into separating disturbance types from time series disturbance pools

using machine learning algorithms. Technically, machine learning algorithms (such as support vector machine (SVM)) are well suited for applications of detecting and differentiating disturbances (Huang et al. 2002; Pal and Mather 2005), but few success stories have been reported.

1.1.3 Assessing post-disturbance forest recovery

Remote sensing techniques provide an effective tool for examining forest disturbance and recovery over large areas. In particular, a series of Landsat systems have been imaging the earth's surface since 1972, creating time series Landsat observations that are highly valuable for tracking land change history for over four decades. While numerous change detection algorithms have been developed (Lu et al. 2004; Singh 1989), with some having demonstrated successes in mapping forest disturbances over large areas (e.g. Huang et al. 2007; Masek et al. 2008; Potapov et al. 2009), characterizing post-disturbance forest recovery is challenging. Depending on local environmental conditions and post-disturbance management practices, it often takes years to decades for trees to grow back following a stand clearing disturbance event. It is difficult to determine at any time point during this process whether young trees had started growing back and whether their height and density exceeded the threshold values of forest according to a particular definition.

With the opening of the Landsat archive for no cost access in 2008 (Woodcock et al. 2008), many algorithms have been developed for monitoring vegetation dynamics using dense time series Landsat observations (Huang et al. 2010; Kennedy et al. 2010a; Zhu et al. 2012). One of the algorithms, the Vegetation Change Tracker (VCT), was designed for both detecting forest disturbance and tracking post-

disturbance recovery (Huang et al. 2010) using annual or biennial Landsat time series stacks (LTSS) (Huang et al. 2009a). While the disturbance products derived using this LTSS-VCT approach has been validated extensively across the United States (Huang et al. 2009b; Huang et al. 2015; Huang et al. 2011; Thomas et al. 2011), the ability of this approach for characterizing post-disturbance recovery has yet to be assessed.

1.1.4 Quantifying impact of management and disturbance on C dynamics

Studies conducted on tracking disturbances and management actions, tracking recovery, and assessing changes of fire regime would lead to data and processes necessary for modeling the effects of these disturbances and management on ecosystem balance. Lands of different ownerships are often managed with different strategies. For example, national parks, national forests, and private land owners typically have different management strategies.

Many previous modeling efforts have been made to quantify the impact of forest fire and harvest on regional, national and global C dynamics (Girod et al. 2007; Hurtt et al. 2002). There are several modeling tools which use either hypothetical landscapes or generalized conditions on real landscapes to infer carbon dynamics in forested ecosystems (Arora and Boer 2005; Turner et al. 2015). Recent advances in remote sensing of vegetation condition and change (Huang et al. 2010; Kennedy et al. 2010b; Zhu et al. 2012), along with new techniques linking remote sensing with inventory records, have allowed investigations that are much more tightly constrained to actual landscape conditions. These new capabilities are built into the Forest carbon Management Framework (ForCaMF), which is being used by the National Forest

System not only to model, but to monitor across very specific management units, the impact of different kinds of disturbance on carbon storage.

1.2 Research Objectives

The primary goal of this study is to derive quantitative understanding of the impact of land management practices and disturbance history on forest C dynamics in Greater Yellowstone Ecosystem (GYE) region. This is achieved through four tasks. The first is to develop new methods for comparing historical and current fire regime conditions over a large portion of the Northern Rocky Mountains, using time series remote sensing data and a landscape succession model. The other three tasks are designed to quantify forest harvest, disturbance, and recovery history, and the impact of such history on forest carbon dynamics in the Greater Yellowstone Ecosystem (GYE) region. Specifically,

1) Develop new methods for comparing historical and current fire regime conditions over a large portion of the Northern Rocky Mountains, using time series remote sensing data and a landscape succession model

2) Characterize recent forest management and disturbance history (1984-2011) in GYE using local management record and time series remote sensing data.

3) Assess post-fire and post-harvest forest recovery in GYE using time series remote sensing data.

4) Quantify the impact of recent forest management and disturbances on carbon dynamics in GYE by linking forest inventory, time series remote sensing and carbon modeling.

In Chapter 2, I develop and describe a new method to produce fire regime conditions class (FRCC) maps by comparing historical and current fire regimes using a landscape succession model. Historical and current fire characteristics were derived from pre-EuroAmerican Settlement fire record (tree ring, lake sediments etc.) and 27-year remote sensing based fire maps, respectively. The FRCC assessment method proposed in this study can be applied in other areas of the U.S. and will help reveal contemporary fire dynamics and serve for future fire and fuel studies and other forest management applications.

In Chapter 3, I discuss how disturbances are tracked and maps are produced for the annual forest fire, harvest and other disturbances in GYE from local management records and time series Landsat images. The Vegetation Change Tracker (VCT) algorithm is first used to produce annual disturbance maps and the Support Vector Machine (SVM) algorithm is then applied to separate forest disturbance types such as wildfires, harvests and other disturbances in GYE. Robust validations of the mapped forest disturbance and disturbance type maps are performed. Annual disturbance rates are calculated for each disturbance type, and the mapped forest disturbance statuses are further analyzed by land ownership and ecoregions.

In Chapter 4, I assess the post-fire and post-harvest forest recovery in GYE using time series remote sensing data. Annual forest disturbance and recovery maps are produced by VCT algorithm and disturbance types are based on maps generated from Chapter 3. The accuracy of the VCT recovery product is validated using high-resolution images from Google Earth and National Agricultural Imagine Program (NAIP). Then the validated recovery products are used to assess recovery rates

following fires and harvests in GYE. Random forests models are built to understand whether and how recovery vs no-recovery is affected by different environment factors such as climate and topography.

In Chapter 5, I quantify and analyze the impact of recent forest management and disturbances on the carbon dynamics in GYE by linking forest inventory, time series remote sensing and carbon modeling. Initial forest conditions are summarized and analyzed, stratifying by land ownership and ecoregions. Initial carbon conditions are modeled by linking Landsat spectral and topographic information with Forest Inventory and Analysis (FIA) plot measured aboveground live C. Average C accumulation curves are derived from FIA plots for each forest type and disturbance conditions. Time series C removal and emissions from harvests and fires are produced and uncertainties associated with the input data are quantified using Monte Carlo simulations.

Chapter 6 concludes the main findings and contributions of this dissertation. Future study directions are also discussed based on the results and limitations of current work.

Chapter 2: A Method for Comparing Historical and Current Fire Regimes

2.1 Introduction

Fire is a key ecological process that recycles nutrients, regulates vegetation succession, controls plant regeneration, and maintains biodiversity in many forest ecosystems (Bowman et al. 2009; Scott et al. 2013). Fire regime is the temporal and spatial expression of fire for specific ecosystems, and often can be described and classified by fire frequency and severity (Brown and Smith 2000; Heinselman 1981; Morgan et al. 2001). Fire frequency is the number of fire events at a point (point frequency) or within an area and a time period (rotation period) (Morgan et al. 2001). Point fire frequencies, such as mean fire return intervals (Heinselman 1973) represent patterns as aggregates of point samples. Fire rotation period, on the other hand, incorporates reconstructed or mapped fire perimeters and are defined as the length of time necessary to burn an area equivalent to a specific study area or landscape (Heinselman 1981; Morgan et al. 2001). The severity of fire has been described by the degree of tree mortality (Morgan et al. 1996), degree to which fires consume organic biomass on and within the soil (Lenihan et al. 1998; Ryan and Noste 1985), heat penetrating into the soil (Ryan and Noste 1985; White et al. 1996), or a combination of these fire effects (Turner et al. 1994).

Assessing departure of current to historical (pre-EuroAmerican settlement) fire regimes is critical for fire and climate change research, fire management, prioritizing fuel treatment and policy making (Bowman et al. 2009). Previous studies suggest that historical fire regimes may have been altered as a result of increased

anthropogenic activities including active fire suppression, land-use change, population increases and climate change (Covington and Moore 1994; Keane et al. 2002c). Recent studies have also noted that changes in fire regimes may lead to major shifts in vegetation, landscape structure, and ecological functions including productivity (Baker 1992). Effective wildland fire management is partly reliant on accurate and consistent comparison of historical and current fire regimes at multiple spatial and temporal scales (Hardy et al. 2001; Keane et al. 2003). Landscape fuel treatment can be prioritized, designed, and scheduled to restore and manage the forests by understanding the causal mechanisms creating historical and current fire regimes. For example, land managers use such information to quantitatively determine the condition of fire-dependent ecosystems and whether management actions designed to improve the health of the ecosystems are achieving their desired outcome (Hann and Bunnell 2001; Hardy et al. 2001). For policy applications, fire regime calculations are useful and often necessary for measuring goals of federal wildland fire management policies such as consistent management standards across geography and land management units and guidance for fuel treatments or community assistance (Council 2009). Informed fire management is also emerging as a critical tool for implementing climate change policies (such as the Climate Action Plan[3]) to adapt to and mitigate effects of climate change (Brown et al. 2004; Spittlehouse and Stewart 2004). This study was conducted with these potential applications in consideration.

[3] http://www.whitehouse.gov/sites/default/files/image/president27sclimateactionplan.pdf

Recently, methods have been developed to compare characteristics of current and historical fire regimes across major ecosystems in North America. One measurement called Fire Regime Condition Class (FRCC) is, a classification based on the amount of change or departure by fire attributes and vegetation, developed to represent departure of present-day fire regime conditions from a defined reference period – that is, whether a landscape is still within the natural or historical range and variation (HRV) (Hann et al. 2004; Hann and Bunnell 2001). Directly estimating the departures of current to historical fire regimes over large areas has been difficult owing to discrepancies between historical fire records which tend to be simple-point records and contemporary observations, which tend to be remote sensing-based maps covering a relatively short time span. The LANDFIRE[4] project (Rollins 2009) used vegetation departure as a surrogate for fire departure. Maps were produced for the U.S. depicting attributes of current vegetation such as successional patterns and trends that have departed from simulated historical vegetation reference conditions as the result of altered fire regimes. Despite continued efforts by the LANDFIRE project, a consistent FRCC calculation with a reasonable spatial scale and geographic scope is still difficult (Hann and Bunnell 2001; Hardy et al. 2001).

Landscape fire succession models that spatially predict fire regimes have been demonstrated to be a suitable tool for developing fire regime maps (Keane et al. 2003). Several previous efforts have used landscape fire succession models (such as SEM-LAND and LANDIS) to compare historical and current fire regimes (Chang et al. 2008; Li et al. 2005). Although these studies have made substantial contribution to

[4] LANDFIRE: LANDFIRE Vegetation Departure layer. U.S. Department of Interior, Geological Survey. [Online]. Available: http: //landfire.cr.usgs.gov/viewer/

our understanding of fire regime departures simulated with landscape models, two gaps remain in the literature. First, contemporary fire records used in these studies for simulating current fire regimes were either incomplete or of short time interval (about 10 years of fire records), and therefore might not be sufficient to capture long-term variability of fire characteristics. Second, spatial ranges examined by these studies have tended to be at landscape level (several square kilometers) with extensive parameterization and computation efforts. For regional or national applications, landscape fire succession models are needed, with more simplified parameterization while retaining enough spatial and temporal information for forest management activities such as fire management and fuel treatment.

We present here the methods and results of a study on comparing current and historical fire regime conditions, with potential forest management applications. The specific objectives of this study were to 1) Use time series (1984 - 2010) remote sensing product (Monitoring Trends of Burn Severity, MTBS) to quantify current fire characteristics in the study region; 2) introduce a new method that uses a landscape fire succession model to examine and compare current and historical fire regime conditions for a large study area in the Northern Rocky Mountains. With the availability of LANDFIRE and a remote sensing based fire product nationally, this method can be applied to other study regions in U.S.

2.2 Methods

2.2.1 Study area

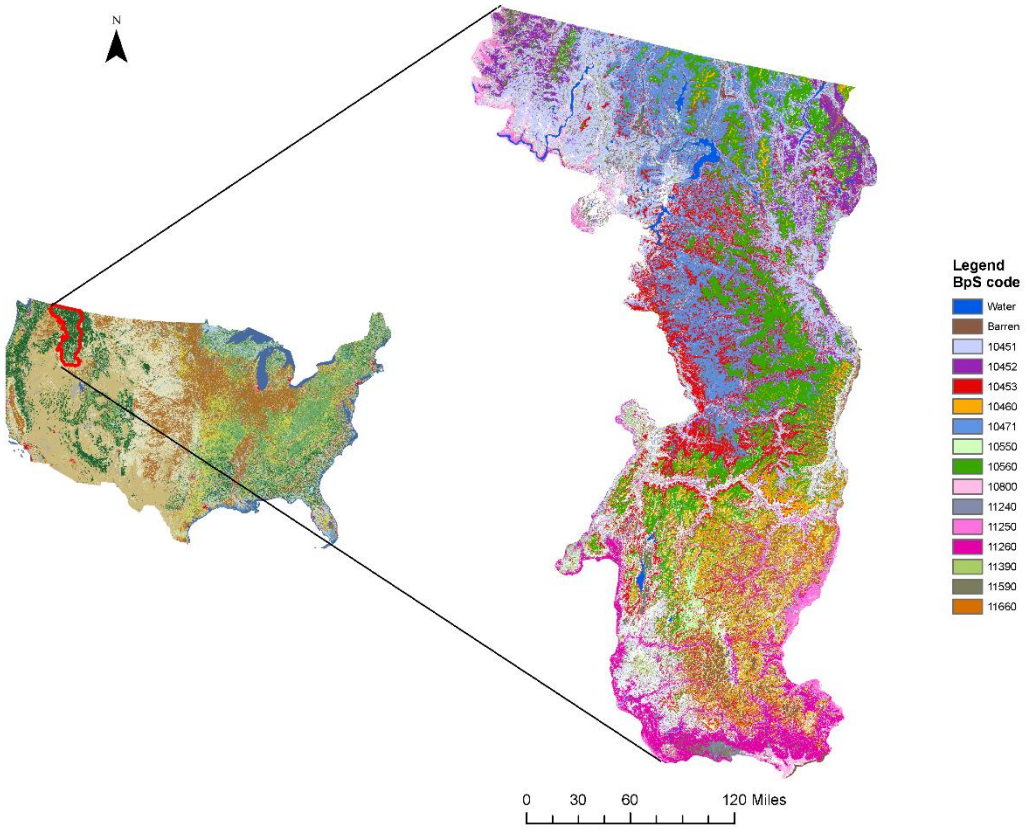

Figure 2- 1 The geographic location of the study area and lists of major biophysical settings (BpS) IDs.
10451: Northern Rocky Mountain Dry-Mesic Montane Mixed Conifer Forest - Ponderosa Pine-Douglas fir; 10452: Northern Rocky Mountain Dry-Mesic Montane Mixed Conifer Forest - Larch; 10453: Northern Rocky Mountain Dry-Mesic Montane Mixed Conifer Forest - Grand Fir; 10460: Northern Rocky Mountain Subalpine Woodland and Parkland; 10471: Northern Rocky Mountain Mesic Montane Mixed Conifer Forest; 10550: Rocky Mountain Subalpine Dry-Mesic Spruce-Fir Forest and Woodland; 10560: Rocky Mountain Subalpine Mesic-Wet Spruce-Fir Forest and Woodland; 11660: Middle Rocky Mountain Montane Douglas-fir Forest and Woodland; 10800: Inter-Mountain Basins Big Sagebrush Shrub land; 11240: Columbia Plateau Low Sagebrush Steppe; 11250: Inter-Mountain Basins Big Sagebrush Steppe; 11260: Inter-Mountain Basins Montane Sagebrush Steppe; 11390 Northern Rocky Mountain Lower Montane-Foothill-Valley Grassland; 11590: Rocky Mountain Montane Riparian Systems.

Table 2- 1 List of major vegetated biophysical settings (BpS) ID, BpS name and percent of area in the study region. Only vegetation types that cover above 1% are shown for simplicity.

BpS ID	BpS Name
10451	Northern Rocky Mountain Dry-Mesic Montane Mixed Conifer Forest - Ponderosa Pine-Douglas-fir
10452	Northern Rocky Mountain Dry-Mesic Montane Mixed Conifer Forest - Larch
10453	Northern Rocky Mountain Dry-Mesic Montane Mixed Conifer Forest - Grand Fir
10460	Northern Rocky Mountain Subalpine Woodland and Parkland
10471	Northern Rocky Mountain Mesic Montane Mixed Conifer Forest
10550	Rocky Mountain Subalpine Dry-Mesic Spruce-Fir Forest and Woodland
10560	Rocky Mountain Subalpine Mesic-Wet Spruce-Fir Forest and Woodland
11660	Middle Rocky Mountain Inter-Mountain Basins Big Sagebrush Steppe Montane Douglas-fir Forest and Woodland
10800	Inter-Mountain Basins Big Sagebrush Shrub land
11240	Columbia Plateau Low Sagebrush Steppe
11250	Inter-Mountain Basins Big Sagebrush Steppe
11260	Inter-Mountain Basins Montane Sagebrush Steppe
11390	Northern Rocky Mountain Lower Montane-Foothill-Valley Grassland
11590	Rocky Mountain Montane Riparian Systems

This study used zone 10 of the LANDFIRE project mapping zones as the study region (Figure 2-1), which comprises a large portion of the Northern Rocky Mountains. The study region covers a broad range of environmental gradients (Table 2-1) including significant variability in geology, landform, climate, vegetation, and land use (Habeck and Mutch 1973; Weaver 1980). In the order of increased elevation, major forest types include mid-Montane forest (e.g. Ponderosa Pine and Douglas fir), high-Montane forest (e.g. Engelmann Spruce), and subalpine forest (e.g. Subalpine Fir and Whitebark Pine). Findings from fire history studies indicated that the Northern Rocky Mountains were dominated by fire regimes of 30 to 200 years frequency and varied severities (Arno et al. 2000). In Northern Rocky Mountains, mixed-severity regimes covered about 50 percent of the area now in national forest

lands, nonlethal regimes occupied about 30 percent of this area and stand replacement regimes included about 20 percent (Arno 1980; Arno et al. 2000). Nonlethal regimes are primarily confined to forests where ponderosa pine was historically dominant. Mixed severity regimes were found across a broad range of forest types, including some of those dominated by Douglas fir and Western Larch, Lodgepole Pine and Whitebark Pine, as well as some relatively moist Ponderosa pine stands. Other areas of these same forest types were characterized by stand-replacement fire regimes (Arno et al., 2000).

2.2.2 Methods overview

We used the LANDscape SUccession Model version 4.0 (LANDSUMv4) (Keane et al. 2006; Keane et al. 2002a) to simulate both the historical and current fire regimes in the study region (Figure 2-2). The historical time period was defined as 'pre-EuroAmerican settlement' (before 1900s), the same as it was defined in the LANDFIRE project. Current time range was defined as 1984 to 2010, which was the mapping period of the MTBS data.

LANDSUMv4 is a spatially explicit landscape vegetation dynamics model for simulating fire and succession on fine scale landscape for land management applications (Keane et al. 2006; Keane et al. 2002a). Two main components of the model are succession and disturbances. LANDSUMv4 model simulates succession within a polygon or patch using a multiple pathway succession modeling approach (Keane et al. 2006; Kessell et al. 1981). This approach simulates succession as a deterministic process and assumes all pathways of successional development would eventually converge to a climax plant community called a Potential Vegetation Type

(PVT) (Pfister and Arno 1980). Disturbances, such as fires, are modeled in LANDSUMv4 as a stochastic process (Barrett 2001; Keane et al. 2006; Steele et al. 2006). There are two phases of fire simulation: the initiation phase and the effect phase. Fires are initiated for a polygon using a stochastic approach based on fire probabilities specified for PVT and succession class combinations in a Scenario Input File. The effects of an initiated fire disturbance are simulated as a change in succession age, succession class, or both (Keane et al. 2006).

LANDSUMv4 requires seven key tabular input files and two map files for its execution (Keane et al. 2006). Tabular input files include Simulation Input File, Attribute Input File, Disturbance Input File, Spatial Disturbance Input File, Scenario Input File, Vegetation Fix Input File, Vegetation File, and Management Plan Input File. The two map files required by LANDSUMv4 are a DEM (Digital Elevation Model) Input Layer and a Polygon Input Layer. Appendix A provides more information on the role of each input file and map.

Table 2- 2 Major model parameters used for simulating historical and current fire regimes in LANDSUMv4 model.

Parameters	Historical fire regime	Current fire regime
Average fire size (ha)	31.3	97.9
Ratio between dry, normal and wet year in a decade	2:5:3	4:4:2
Fire probabilities	Historical fire records (e.g. tree ring ,lake sediments) and literature	Fire probability calculated from MTBS data
Simulation time (years)	1500	1500
Spatial resolution (m)	90	90

Table 2-2 listed key model parameters used for historical and current fire regime simulations. Since fire and weather conditions are the only variables that have been changed between the study time periods, we kept the other simulation parameters constant throughout the historical and current fire regime simulations. Historical fire regime parameters were obtained from the LANDFIRE group. Current average fire size was calculated from MTBS data and National Interagency Fire Center fire records from 1984 to 2010. Current wind speed was held constant as the historical value. The ratio between dry, normal and wet year in a decade, which was the controlling factor for climate, was calculated from the Palmer Drought Severity Index (PDSI) from 1984 to 2010. As discussed above, historical and current fire probabilities were calculated from historical fire records and contemporary remote sensing product, respectively. We experimented with different spatial (30m and 90m) and temporal resolutions (1,500 years and 10,000 years) for both the historical and current fire regime simulations. After comparing these simulation results, we decided to adopt the 30 meter spatial resolution and 1,500 years simulation to save computer time while still retaining the most spatial and temporal information.

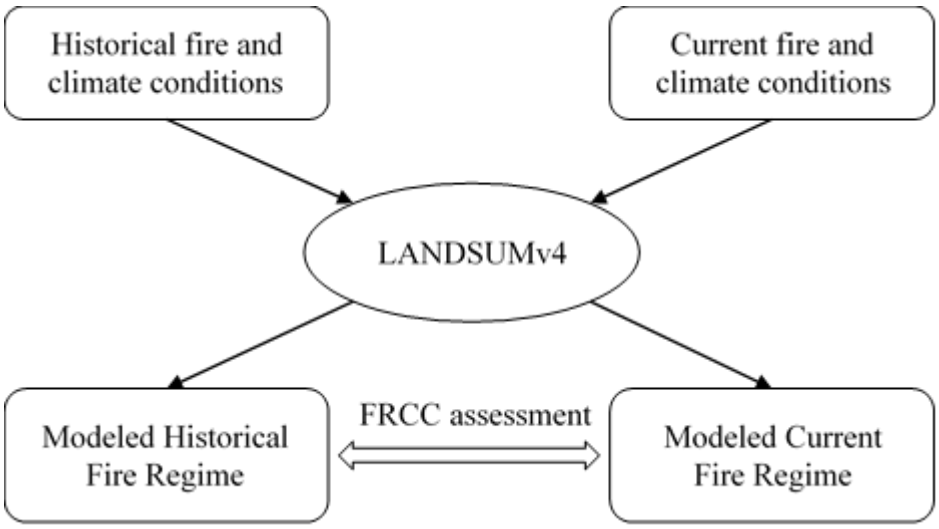

Figure 2- 2 Flow diagram of simulating historical and current fire regimes using the LANDSUMv4 model.
MTBS stands for Monitoring Trends of Burn Severity data and MFRI stands for mean fire return interval. Historical and current fire and climate data were fed into the LANDSUMv4 model to simulate the historical and current fire regimes. In the Fire Regime Condition Class (FRCC) Guidebook, FRCC is defined as the average of vegetation and fire regime departures. Vegetation departures were calculated from LANDFIRE vegetation departure data and fire regime departures were calculated by comparing the modeled historical and current fire regimes (Hann et al. 2004).

Three steps were involved to develop the fire regime departure maps. Step one was to derive the historical and current fire probabilities; step two was to use LANDSUM model to simulate historical and current fire regimes using fire probabilities derived in step one as model inputs; and step three was to calculate the fire regime departure of the current landscape from the historical fire regime by comparing the modeled historical and current fire regimes.

This fire regime calculation and comparison were stratified by potential vegetation type categories in the LANDFIRE project biophysical setting map layer. Mapped biophysical settings classes were nested within each ecological subsection for a given LANDFIRE mapping zone (zone 10 in this case). Fire frequency departures and fire severity departures were then calculated and summarized for each

biophysical setting, describing the magnitude of differences between the simulated historical and current fire regimes. Maps of fire return intervals and fire severities were also created from the LANDSUM model.

Extensive sensitivity analysis has been conducted in previous studies and the results showed that average fire size, frequency scalar, wind speed and landscape size (Table 2-2) are important to historical and current fire regime simulation concerns. Based on these sensitivity analysis, our simulation landscape were large enough to realistically simulate fire pattern and 1500 years was also a reasonable simulation interval (Keane et al. 2006; Keane et al. 2002a). LANDSUMv4 model is also very sensitive to the distribution of normal, dry and wet years with the most fires happening when you have a dry year. Keane et al. (2006) and Holsinger et al. (2006) conducted informal sensitivity analyses on the effects of weather years on annual burned area and found that, overall, each dry year increased area burned by 2-6 times and that if dry years are not balanced by wet years then around 4 times more area burns over a century. These increases are mostly from increases in fire ignitions. For more information on the sensitivity analysis of this model, please see Keane et al. (2002a), Keane et al. (2004) and Keane et al. (2006).

To estimate the impacts of random error, both historical and current fire regime simulations were repeated for five times, with different random number seeds. Comparison between the simulated results with the MTBS data were evaluated and reported. Since we used MTBS burned area data to calculate the fire frequency and the MTBS burned area data are highly accurate (98%), we did not assess the error propagation from MTBS burned area data to the final fire frequency simulation

results. We iteratively adjusted fire probabilities as well we average fire size coefficient and summarized annual burned area from the LANDSUMv4 output, until the annual burned area approximated the observations from MTBS. This process ensured that fire frequency would be accurately simulated by the stochastic LANDSUMv4 fire module.

2.2.3 Contemporary fires

Information for current fires was obtained from the MTBS dataset for the study area, which contained data for the years 1984 to 2010 on fire location, burned area, fire severity and fire start date. The MTBS project mapped fires from time series Landsat images using the pre- and post-fire differenced normalized burn ratio (dNBR) and relativized differenced normalized burn ratio (RdNBR) (Eidenshink et al. 2007b; Zhu et al. 2006). MTBS characterizes severity in five discrete classes: unburned/unchanged, low severity, moderate severity, high severity and increased post-fire response (Eidenshink et al. 2007b). Independent remote sensing based validations of fire occurrences show 98% agreement with MTBS on large fire events (Cohen et al. 2010; Eidenshink et al. 2007b), but overall accuracies of the NBR-derived maps of fire severity ranged from 53-81% (Cocke et al. 2005; Miller et al. 2009; Roy et al. 2006; Zhu et al. 2006). Fires less than 1,000 acres were excluded in this study, but this did not significantly bias our analysis because fires with sizes less than 1,000 acres represented a small portion of total burned area (less than 5%) (Eidenshink et al. 2007b).

Annual burned areas of each MTBS burn severity were summarized for the study region by summing up area of all MTBS low, moderate and high severity fire

pixels. As forests take up the majority of the land cover in the study region (over 70% of total study area), detailed trend analyses were conducted for annual burned area and the percentage of high severity fires of forest ecosystems. Instead of dividing the 27 years into arbitrary sub-periods, linear trends were examined using the entire time series (Dennison et al. 2014). Non-parametric Theil-Sen estimators were used to calculate slope over time for annual burned area and the percentage of high severity fires for forest ecosystems (Wilcox 2012). The Theil-Sen slope estimator is the median value of all pairwise differences between two time steps and is robust to outliers while still approaching an ordinary least squares estimate of slope when the distribution of values is close to normal (Wilcox 2012). A one-sided Mann-Kendall trend test was used to assess the significance of monotonic trends of the above fire variables in the time periods (Salmi 2002).

2.2.4 Current fire probabilities

One of the differences between traditional fire surveys and remote sensing techniques when related to frequency of wildfires is that current remote sensing maps of burned areas can only be used to estimate landscape fire rotations instead of point based fire return intervals. This is because most ecosystems have mean fire return intervals longer than the observation period of the remote sensing data. Therefore a large portion of remote sensing pixels would have no fire occurrences. Most traditional fire survey methods quantify point based fire return intervals instead of area frequencies (although this might not be true for some of the newer fire history methods such as Westerling *et al*. 2011). As discussed in the introduction, point based fire frequencies and area based fire frequencies are applied at different measurement

scales. Consequently, a method is needed to convert the landscape fire rotations to fire return intervals to apply remote sensing results to fire ecology studies.

The FRCC Guidebook v3.0 provided a method for estimating current fire frequency (the inverse of fire probability) using fire atlas records, which were similar to the contemporary remote sensing images. The FRCC Guidebook method has three steps for estimating current fire frequency. Step one and two is to estimate mean annual burned area of historical and current conditions, respectively. Step three is to compute the current fire frequency by comparing step one and two results (Hann et al. 2004). We adapted the Guidebook method to estimate current fire probabilities for each biophysical setting in five steps:

Step 1: For the historical period, we estimated the mean annual burned area by dividing the biophysical settings area by its associated fire frequency (inverse of fire probability). Fire probabilities for each biophysical setting were found in LANDFIRE biophysical settings documentation for each mapping zone. Information about the historical fire probabilities for each biophysical settings was collected from fire scars, lake charcoal sediments, bogs, or soils, or post-fire tree establishment dates from tree ring analysis (Keane et al. 2004; Pratt et al. 2006).

Step 2: We calculated the current mean annual burned area for this biophysical settings by analyzing the MTBS data. We first summarized the MTBS data into one fire map, with each pixel counting the number of fires occurred during the 27-year period. Then, we overlaid the biophysical setting map with the summarized fire map to compute the annual burned area for each biophysical setting.

Step 3: We computed the ratio between the historical and current mean annual burned area for this biophysical settings.

Step 4: We estimated current fire frequencies for each biophysical settings by multiplying historical fire frequency with the ratio between historical and current mean annual burned area; the current fire probability was the inverse of the current fire frequency or mean fire return interval (MFRI).

Step 5: Current fire probabilities derived from step two were divided into low, moderate, and high severity fire probabilities for each biophysical setting in LANDSUMv4. The ratio between low, moderate and high severities fire area for each biophysical setting was based on the ratio calculated from MTBS burn severity data.

One issue with the MTBS data, in addition to the moderate accuracy of burn severity data, was that 27 years were relatively short compared to the long fire return intervals in some biophysical settings. To solve this issue, we followed the FRCC Guidebookv3.0 approach and used the historical probability values of the biophysical settings if there were no records of fire occurring during the current time period.

2.2.5 Historical and current fire regimes

Using historical and current fire probabilities as model inputs, we simulated historical and current fire regimes using LANDSUMv4 model. For historical fire regime simulation, we used the same parameterization as the LANFIRE historical fire regime simulation. For current fire regime simulation, most model successional and simulation parameters remained the same as historical values, except for contemporary fire and climate parameters such as average fire size and ratio between dry, normal and wet years in a decade were calculated from contemporary fire and

climate data. Both historical and current time periods were simulated for 1,500 years using the LANDSUMv4 model. The current fire regime maps were calibrated against the MTBS data to make sure the simulated current fire regime maps represented the observed fire conditions. Major model parameters used are shown in Table 2.

2.2.6 FRCC calculation

FRCC is calculated as the average of the fire regime departure and the vegetation departure (Hann et al., 2004), whereas the fire regime departure is the average of the fire frequency departure and fire severity departure (Hann et al. 2004). In this study, fire regime departure was calculated using the simulated historical and current fire regimes as described previously. The vegetation departure map was developed by the LANDFIRE group and used values from 0 to 100 to represent the level of current vegetation departure from the historical vegetation condition (Rollins 2009). This data was calculated by considering the changes to species composition, structural stage and canopy closure. The regime departure map produced in this study used values from 0 to 100 to reflect the deviation of the current fire regimes to historical fire conditions.

The final FRCC classification was based on the FRCC Guidebook definition, which was 0-33 for FRCC group 1, 34-66 for FRCC group 2 and 67-100 for FRCC 3 (Hann et al. 2004). Since our study focused on natural vegetated ecosystems, water, snow/ice, barren land, urban, and agriculture pixels were masked out from all the departure and conditions class maps.

2.3 Results

2.3.1 Contemporary fire patterns from MTBS

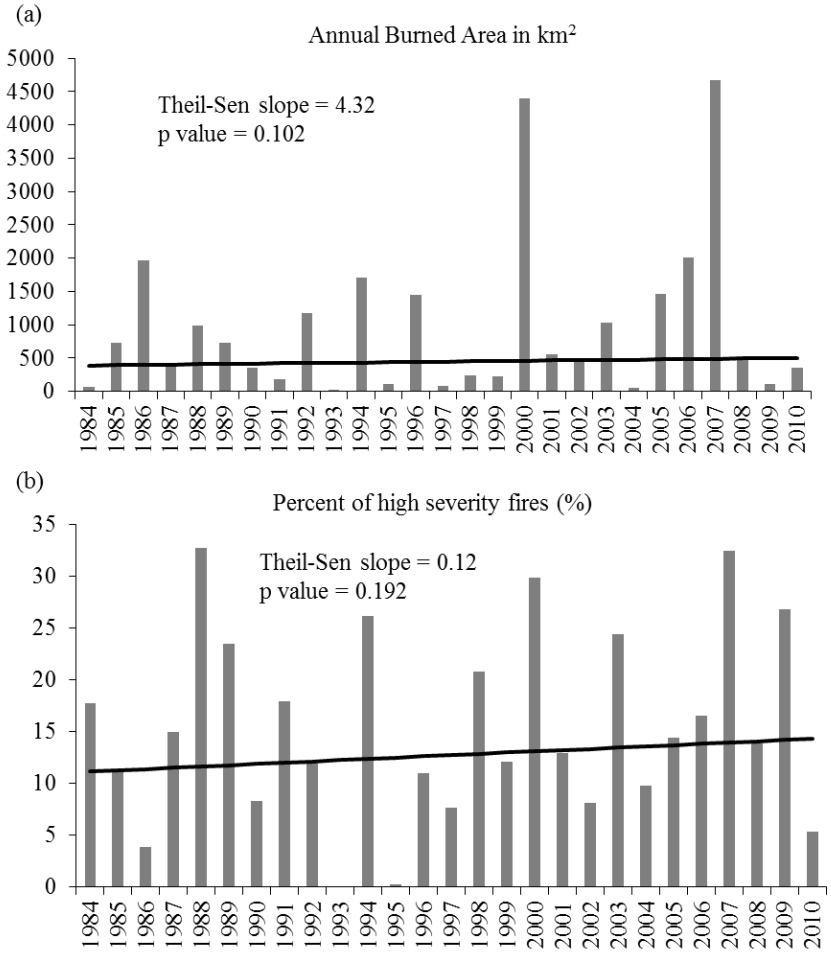

Figure 2- 3 (a) Annual burned area of the study region from 1984 to 2010; (b) Percent of high severity fires in the study region from 1984 to 2010; the black line on each plot indicates the Theil-Sen estimated slope, with slope values and Mann-Kendall significance test p values also shown in the figure.

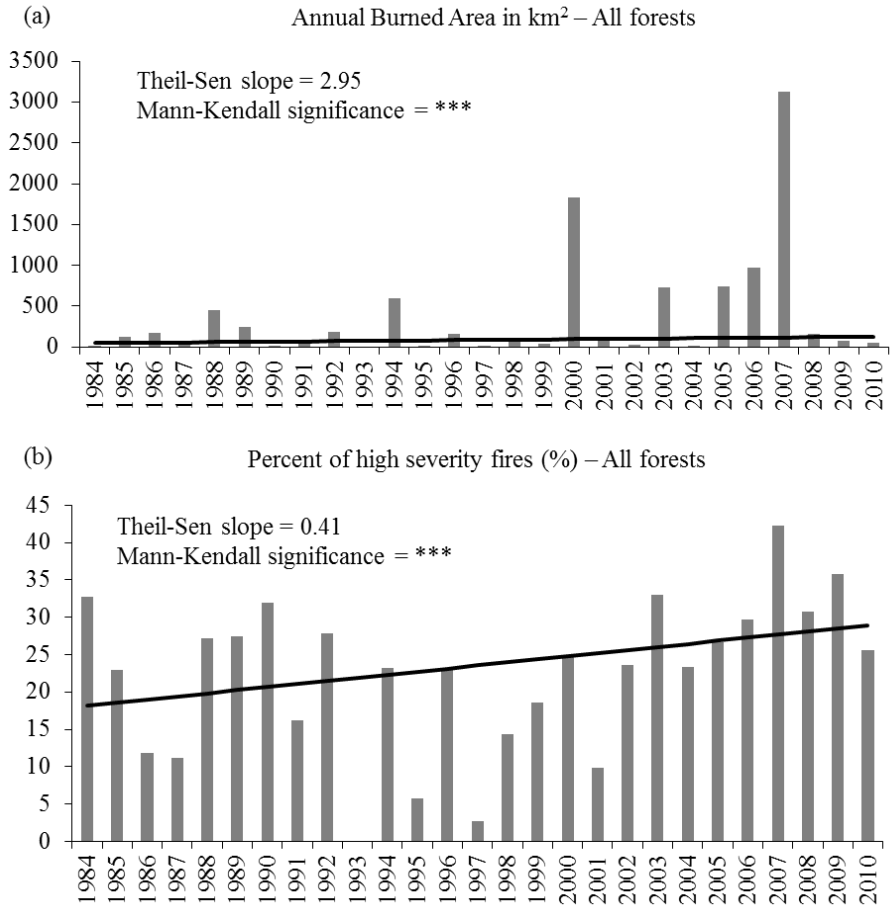

Figure 2- 4 (a) Trends for annual burned area of all forests ecosystems in the study region from 1984 to 2010; (b) Trends for average percent of fires that were high severity for all forest ecosystems in the study region from 1984 to 2010. The black line on each plot indicates the Theil-Sen estimated slope, with slope values and Mann-Kendall significance level also shown in the figure. Three asterisk Significance (p) of slopes assessed using the Mann-Kendall test represent $p < 0.001$.

There were increasing, though non-significant trends in annual burned area and average percentage of fires that were high severity in the study area (Figure 2-3). The results indicate annual burned area and percentage of high burn severity all increased in the Northern Rocky Mountain over the past 27 years. A close look at the forest ecosystems (Figure 2-4), taking up over 70% of total study region, reveals that the increasing trend in annual burned area and high severity fires of forest ecosystems was much greater than the whole region. Increasing trends in both annual burned area

and percentage of high severity fires were statistically significant (Theil-Sen slope >0 and $p<0.001$).

2.3.2 Historical and current fire frequencies

Table 2- 3 Summary of biophysical settings (BpS) ID, elevation, historical and current annual burned area and the current to historical annual burned area ratio of major forest biophysical settings (in the order of decrease elevation) in the study region.

BpS ID	Elevation (m)	Historical Mean Annual Burned Area ($km^2 yr^{-1}$)	Current Mean Annual Burned Area ($km^2 yr^{-1}$)	Current to Historical Mean Annual Burned Area Ratio
10460	1829-2743m	57.1	73.0	1.28
10550	1372-2438m	56.8	66.2	1.17
10560	W: 884-1981 E:1585-2682m	186.3	121.3	0.65
11660	NW: 0-1980m S: 0-2286m	133.5	79.9	0.60
10453	1372-1676m	249.9	58.0	0.23
10451	N: 762-1676m S: 1219-2286m	727.2	91.8	0.13
10452	N: 915-1828m	147.8	14.2	0.10
10471	609-1585m	243.6	12.2	0.05

Ratios of current to historical mean annual burned area for forest biophysical settings correlated well with the change of elevation and increased with the rise of elevation for each biophysical settings (Table 2-3). Most of subalpine forests ecosystems such as 10460 Northern Rocky Mountain Subalpine Woodland and Parkland and 10550 Rocky Mountain Subalpine Dry-Mesic Spruce-Fir Forest and Woodland had a ratio value larger than 1, suggesting that more forests are burned by fire each year in the subalpine forest than in historical records.

2.3.3 Simulated fire frequency and severity

Table 2- 4 Summary of biophysical settings (BpS) ID, simulated historical and current mean fire return interval (MFRI) and percent of high burn severity averaged for each biophysical settings, the current to historical average fire probability ratio and average percent of high severity fire ratio of major forest biophysical settings (in the order of decrease elevation) in the study region.

Bps ID	Simulated average historical MFRI (years)	Simulated average current MFRI (years)	Current to historical average fire probability ratio	Simulated average historical percent of high burned severity (%)	Simulated average current percent of high burned severity (%)	Current to historical average percent of high severity fire ratio
10460	167	335	0.50	43	67	1.56
10550	148	405	0.37	63	71	1.13
10560	173	647	0.27	89	95	1.07
11660	61	308	0.20	22	48	2.18
10453	84	594	0.14	43	60	1.40
10451	49	622	0.08	22	41	1.86
10452	60	723	0.08	26	46	1.77
10471	106	195	0.54	49	51	1.04

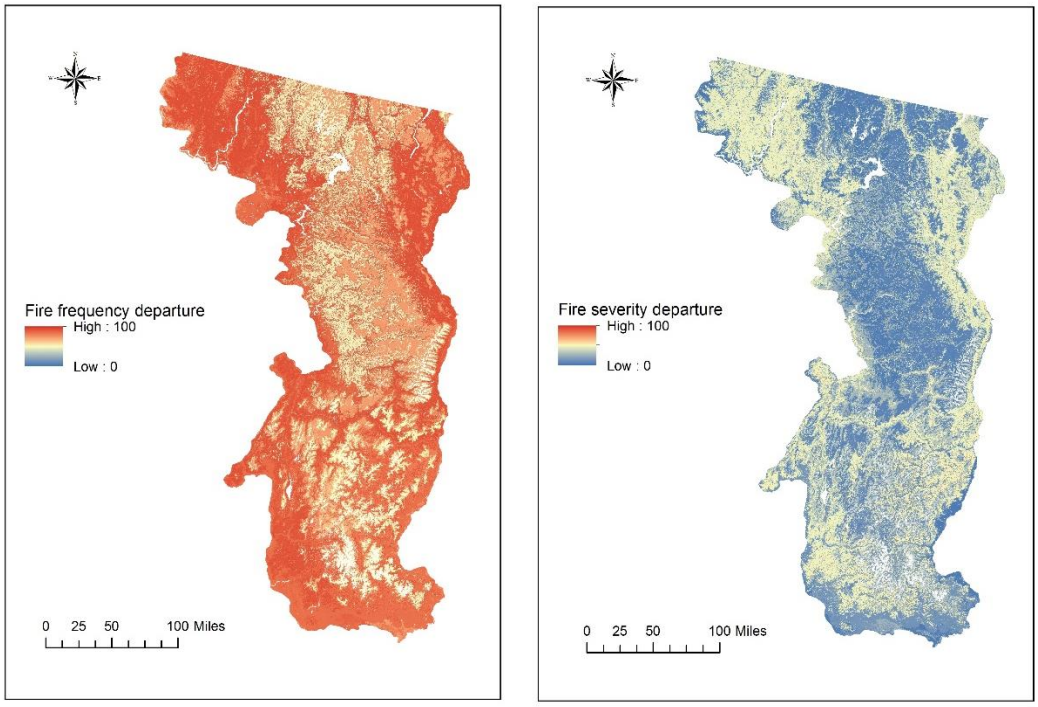

Figure 2- 5 Simulated mean fire frequency departure and severity departure maps for the study region. Fire frequency and severity departures represent the percentage change of current fire frequency and severity to the historical values. Values of fire frequency and severity departure equal to 0 mean no change between historical and current values and values of fire frequency and severity departures close to 100 mean maximum departures between historical and current values.

Simulated frequencies of forest biophysical settings show similar trends with the annual burn area derived from MTBS and LANDFIRE. In general, the ratio between simulated current to historical fire probability increase with the rise of elevation (Table 2-4). Current fire occurrences in high elevation subalpine ecosystems (mostly > 2,000 meters, see table 1 and 2 for more information) are more similar to historical conditions than low to middle elevation montane forests (ranging from 0 to 2000 meters). All forest ecosystems experienced less frequent but more severe current fires compared to historical conditions. Spatial map of fire frequency departure and fire severity departure maps are shown in Figure 2-5.

2.3.4 Vegetation departures and regime departures

Table 2- 5 Summary of biophysical settings (BpS) ID, dominant species, historical fire frequency and severity, current fire frequency and severity, mean vegetation departure (vegetation condition class) and mean fire regime departure (combined fire frequency and severity departures) of major forest biophysical settings (in the order of decrease elevations) in the study region.

Bps ID	Dominant Species	Historical fire regime	Current fire regime	Mean vegetation departure (vegetation condition class) from LADNFIRE	Mean regime departure (regime condition class) from this study
10460	Subalpine fir, Whitebark pine	Infrequent/high	Infrequent/high	52 (2)	42 (2)
10550	Engelmann spruce, subalpine fir	Infrequent/high	Infrequent/high	30 (1)	40 (2)
10560	Engelmann spruce, subalpine fir	Infrequent/high	Infrequent/high	39 (2)	41 (2)
11660	Douglas-fir	Frequent/low	Infrequent/moderate	51 (2)	64 (2)
10453	Grand fir	Frequent/moderate	Infrequent/moderate to high	44 (2)	55 (2)
10451	Ponderosa pine	Frequent/low	Infrequent/moderate	33 (1)	66 (2)
10452	Larch	Frequent/low	Infrequent/moderate	60 (2)	66 (2)
10471	Western hemlock, western red cedar	Infrequent/moderate to high	Infrequent/moderate to high	56 (2)	28 (1)

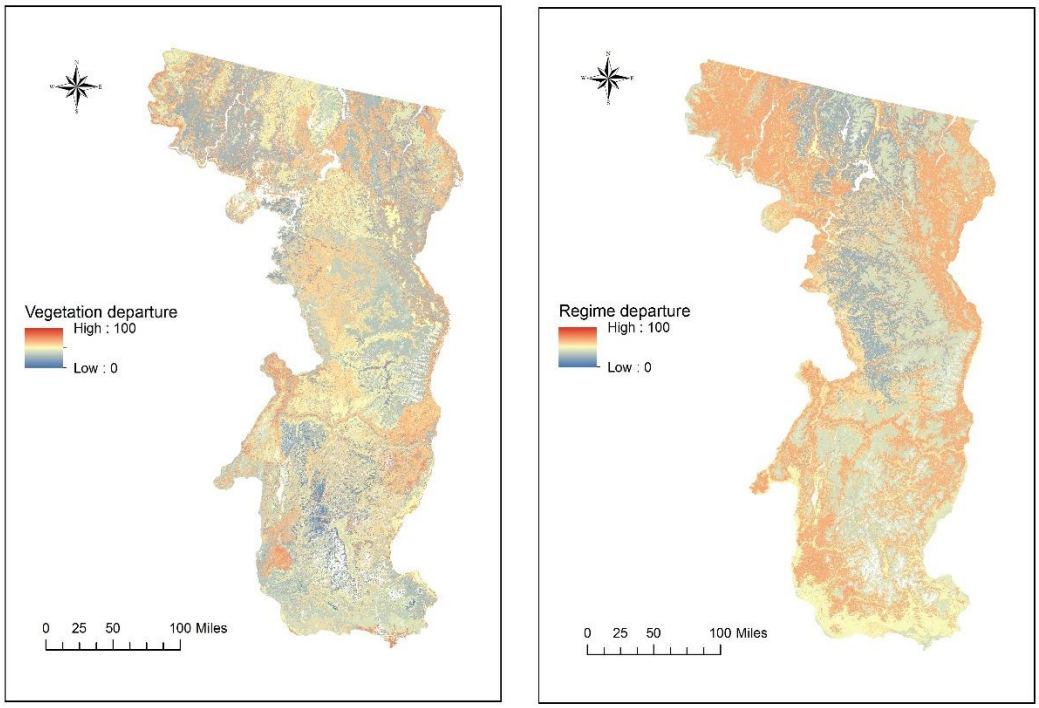

Figure 2- 6 Vegetation departure map and regime departure map. Vegetation and regime departures represent the percentage change of current vegetation condition and fire regime conditions to the historical values. Values of vegetation and regime departure equal to 0 mean no change between historical and current values and values of vegetation and regime departure close to 100 mean maximum departures between historical and current values.

The vegetation departure map and regime departure map are shown in Figure 2-6. Comparison of the vegetation departure map from LANDFIRE and the regime departure map from this study shows that fire regimes have changed the most for montane forests which historically were dominated by frequent and nonlethal fires (Table 2-5). Forest ecosystems characterized by infrequent stand replacement fires also experienced moderate departure from historical fire regimes.

2.3.5 Fire regime condition class

Table 2- 6 Summary of biophysical settings (BpS) ID, BpS name, percent of area and final FRCC group of the study region. Only vegetation types that cover above 1% in area are shown for simplicity.

BpS ID	BpS Name	Percent of Area	FRCC
10451	Northern Rocky Mountain Dry-Mesic Montane Mixed Conifer Forest - Ponderosa Pine-Douglas-fir	17.3	2
10452	Northern Rocky Mountain Dry-Mesic Montane Mixed Conifer Forest - Larch	4.5	2
10453	Northern Rocky Mountain Dry-Mesic Montane Mixed Conifer Forest - Grand Fir	9.8	2
10460	Northern Rocky Mountain Subalpine Woodland and Parkland	4.4	2
10471	Northern Rocky Mountain Mesic Montane Mixed Conifer Forest	12.6	2
10550	Rocky Mountain Subalpine Dry-Mesic Spruce-Fir Forest and Woodland	3.6	2
10560	Rocky Mountain Subalpine Mesic-Wet Spruce-Fir Forest and Woodland	13.3	2
11660	Middle Rocky Mountain Montane Douglas-fir Forest and Woodland	3.8	2
10800	Inter-Mountain Basins Big Sagebrush Shrub land	1.2	2
11240	Columbia Plateau Low Sagebrush Steppe	1.0	2
11250	Inter-Mountain Basins Big Sagebrush Steppe	2.0	2
11260	Inter-Mountain Basins Montane Sagebrush Steppe	5.9	2
11390	Northern Rocky Mountain Lower Montane-Foothill-Valley Grassland	2.8	2
11590	Rocky Mountain Montane Riparian Systems	5.2	2

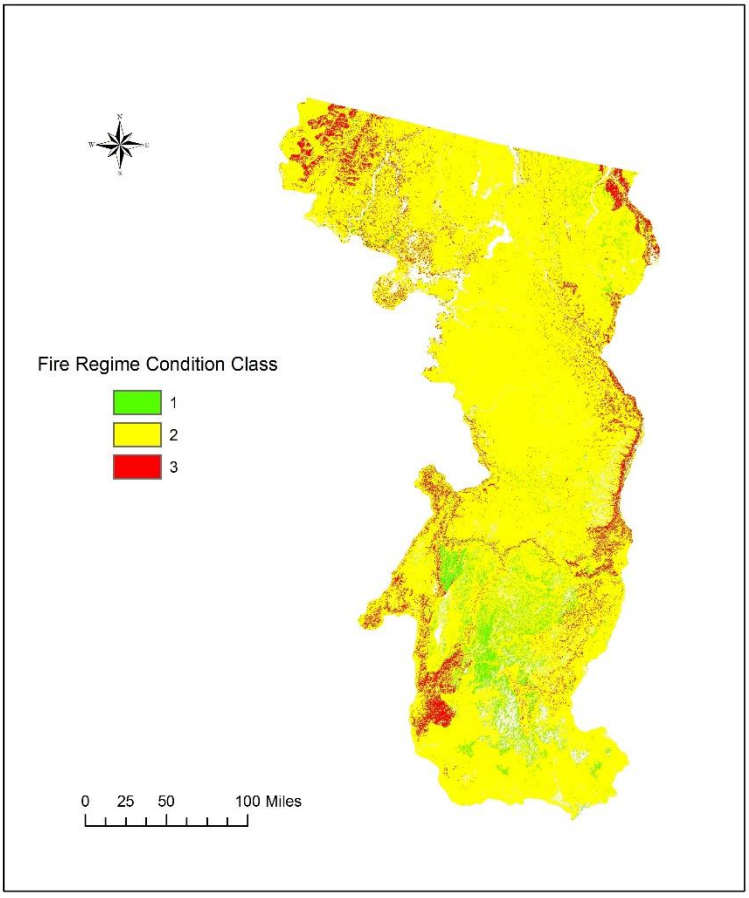

Figure 2- 7 Fire regime condition class map. Fire regime condition class shows the combined change between current vegetation and fire regimes to the historical conditions. Fire regime condition class 1 means that current vegetation and fire regimes are similar to historical conditions and are within the HRV(Historical Range and Variation); fire regime conditions class 2 means current vegetation and fire regimes have moderately departed from historical conditions; fire regime conditions class 3 means current vegetation and fire regimes have high departures from historical conditions.

The Fire Regime Condition Map of the study region is shown in Figure 2-7. About 88% of the total study region is FRCC 2, meaning moderate departure from historical conditions (Table 2-8). The rest of the study region is dominated by FRCC 3 and FRCC 1, taking up about 7% and 4% of total forested area, respectively. Almost all the major forest ecosystems are FRCC 2 (Table 2-6).

2.4 Discussions

2.4.1 Simulation modeling approach

Our results indicated that the LANDSUMv4 model can be applied to simulate the current fire regimes with inputs derived from remote sensing data. We can compare this current fire regime data with the simulated historical fire regime data for national consistent and local relevant FRCC assessment. Since historical fire regime and contemporary fire mapping are available for the whole U.S., from LANDFIRE and MTBS respectively, this approach can be applied at the national scale. This is helpful for complementing consistent and comparable large scale FRCC assessment for large scale forest management policy making (Keane et al. 2007). Forest managers can also use the produced fire regime departure and condition class maps to prioritize fuel treatment and fire monitoring efforts (Hann et al. 2004; Hardy et al. 2001). Knowing the differences between historical and current fire regime conditions, following the methods developed in this paper, can establish a good foundation for scientific research in many fields, including but not limited to landscape ecology, climate change, and carbon dynamics (Agee 1998; Liu et al. 2011; Spittlehouse and Stewart 2004; Westerling et al. 2011; Whitlock et al. 2003).

Table 2- 7 (a) Comparison between the fire or fire regime products from LANDFIRE, MTBS and this study; (b) Comparison between LANDFIRE vegetation condition class, regime condition class from this study and the final FRCC (Fire Regime Condition Class) from this study.

(a)

	LANDFIRE historical fire regime data	MTBS	Fire regime simulation from this study
Data source	Model simulation	Remote sensing	Model simulation
Time frame	Historical (pre-EuroAmerican settlement)	1984-current	Historical and contemporary
Development methods	Use historic fire records as model inputs, simulate historic fire regimes (frequency and severity) with the LANDSUMv4 model	Map fire perimeters and severities from time series Landsat images using the dNBR and RdNBR indices	Simulate historic and current fire regimes with LANDSUMv4 model using historic fire probabilities (from LANDFIRE) and current fire probabilities (mainly derived from MTBS) as inputs

(b)

	LANDFIRE Vegetation Departure map	Regime Departure map from this study	Fire Regime Condition Class (FRCC) from this study
Description	Use 0 -100 to quantify the amount current vegetation (succession classes) has departed from historical vegetation conditions.	Use 0 -100 to to reflect the deviation of the current fire frequency-severity combined value from historical fire regime conditions	Three condition classes to signify the amount of departure of current conditions from historical conditions, including both the vegetation departure and the regime departure
Development methods	Calculate changes to species composition, structural stage and canopy closure following the FRCC Guidebook method	Estimate changes to fire frequency and fire severity following the FRCC Guidebook method	Estimate the combined changes of fire regime and vegetation conditions following the FRCC Guidebook method, which is the final FRCC.

The historical and current fire products from LANDFIRE and MTBS were developed from different data sources. LANDFIRE used the LANDSUMv4 model to simulate the point based historical fire frequency (mean fire return interval) with different kinds of historical fire records as inputs while the MTBS data was derived from time series remote sensing data (similar to fire atlas records) and represents area based fire frequency (landscape fire rotation). These two terms cannot be compared

directly without a conversion scheme between the mean fire return interval and fire rotation period. The FRCC Guidebook v3.0 provides a standard methodology to estimate current fire frequency from fire atlas records and historical fire frequency at stands to landscape level (Hann et al. 2004). The modeled fire regimes created in this study estimated current fire frequency from the MTBS and LANDFIRE historical fire regime data following the FRCC Guidebook v3.0 method. With these probabilities as input parameters to the LANDSUMv4 model, we produced simulated current fire regime data sets that are comparable to the LANDFIRE historical fire regime data. This new simulation approach addresses the data comparability issue between model results and remote sensing products and also has the potential to be applied to the entire U.S. A detailed comparison between the LANDFIRE, MTBS and the simulated fire regime and condition class data is shown in Table 2-7.

There are some uncertainties and limitations in the study. Insufficient data, limits in modeling capabilities and the inadequate scientific understanding of these complex interactions between natural phenomena can lead to uncertainties in this study. With proper calibration with remote sensing observations, uncertainties in this assessment are limited to input data and methods related to fire regime characterization and simulation. The known limitations of this approach include the following: (1) The MTBS data time span is relatively short compared to the long fire return interval in the study region. The common fire return interval in the study region is between 50 -500 years while we only have less than 30 years of remote sensing data. However, with the continuation of the Landsat mission (Williams et al. 2006; Wulder et al. 2008), improvement to the accuracy of the current fire frequency

estimation is promising. (2) Impacts of changing climate were simplified to ratios of dry, normal and wet years in a decade. These ratios might not capture the temporal change of climate conditions and could be improved by using time series climate data in future studies.

2.4.2 Simulated fire regimes, departures and condition classes

Results of this study indicate that most forest ecosystems in the study region experienced less frequent but more severe current fires during the contemporary period compared to historical conditions (Table 2-3). High-elevation subalpine forest ecosystems tend to have more frequent current fires than mid-elevation montane forests, consistent with the observation offered in Running *et al.* (2006) about increased fire activities in the snow-dominated forests of 2,100 m or above in the western U.S. The findings also correlate with previous studies suggested by Kilgore and Heinselman (1990) and Keane *et al.* (2002b). Forest ecosystems characterized by infrequent stand replacement fires do not depart from historical fire regimes as much as ecosystems characterized by frequent low severity fires, probably for two reasons: 1) these forest ecosystems have long mean fire return intervals (>100 years) and may not have been greatly altered by 60 to 90 years of fire exclusion (Arno et al. 2000); 2) these forest ecosystems are dominated by stand replacement fires which is often not easy to suppress (Agee 1998; Arno et al. 2000).

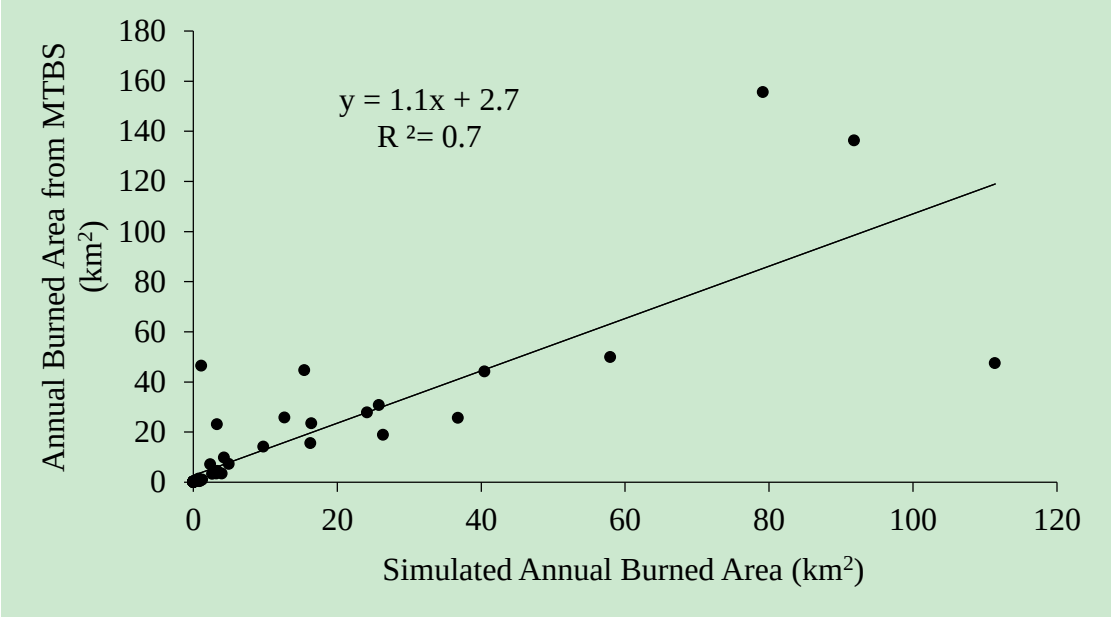

Figure 2- 8 Comparison of the simulated annual burned area with the annual burned area calculated from the MTBS data. Each point represents the mean value for a biophysical setting.

The simulated current annual burned area was compared with the annual burned area calculated from MTBS data, stratified by each biophysical settings (Figure 2-8). The simulated annual burned area for each biophysical settings agrees well with those calculated from the MTBS data, indicating that LANDSUM model is a viable vehicle for simulating current fire regimes. The scatter at the high end of annual burned area was mainly due to the spatial adjacency of a few biophysical settings and the design of the fire spread model. Fire was initiated in one biophysical settings and spread uphill and down-wind to the neighboring biophysical settings (Keane et al. 2006), causing the underestimation of annual burned area in the first biophysical settings and the overestimation of annual burned area of the second biophysical settings. As Keane and colleagues (2006) pointed out, it is difficult, at this time, to fully integrate fire spread with ignition and get realistic results because

fire probabilities are estimated from studies that do not quantify landscape relationships.

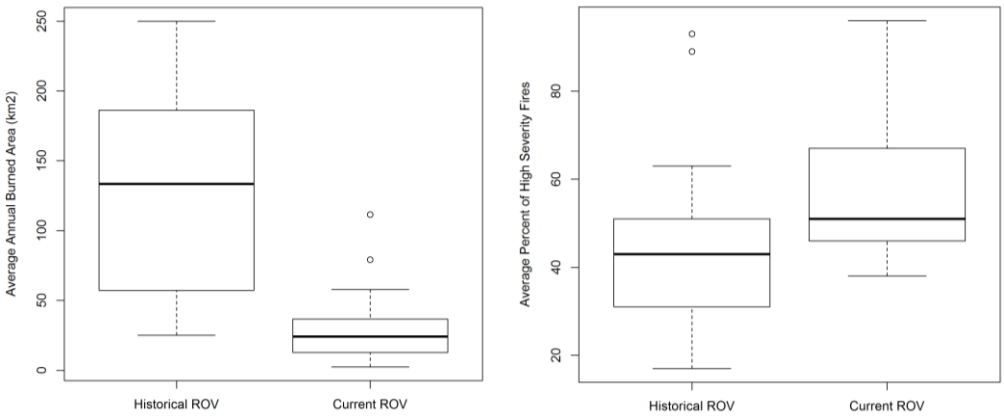

Figure 2- 9 Comparisons of simulated Historical Range and Variation (HRV) and current Range and Variation of annual burned area (left, km^2) and average percent of high severity fires (right) for all biophysical settings in the study area

By comparing the simulated historical and current range and variation of annual burned area, it is shown that on average the study region used to experience more than five times in fire area historically than the current years, with the historical period experiencing a higher variability in areas burned than the current years (Figure 2-9). For fire severity, average current percent of high severity fires would be higher than the historical mean percent. The upper and lower bounds of current range and variation of percent high severity fires are estimated to be over 25% higher than the historical upper and lower bound values, respectively. These results are in accordance with previous findings (e.g. *Keane et al*., 2002b) that long term fire exclusions have led to moderate or high fire regime departures in the Northern Rocky Mountains, which is characterized with less areas burned but higher percentage of severe current fires.

Table 2- 8 Percentages of vegetation condition classes derived from LANDFIRE, fire regime condition map from this study and the final FRCC (Fire Regime Condition Class) map from this study.

FRCC class	LANDFIRE vegetation condition class (%)	Regime condition class from this study (%)	FRCC from this study (%)
1	28.7	12.4	4.2
2	61.5	53.9	88.8
3	9.8	33.7	7.0

The final FRCC map, produced as a composite score of fire regime departure and vegetation departure, shows over 80% FRCC 2 ecosystems (moderate departure) in the study region (Table 4-8). The rest of the forests are small areas of FRCC 3 (high departure) and FRCC 1 (low departure). Ecosystems with the same FRCC group can have quite different vegetation and fire regime change patterns, partly due to the methodology used to calculate FRCC. The final FRCC is a combination of LANDFIRE vegetation departure data, fire frequency departure, and fire severity departure data derived from this study (Table 2-8). For example, Montane forests, dominated by Ponderosa Pine and Douglas Fir, were historically shaped by frequent low severity fires, can have very high fire frequency departures, and low vegetation departures from the different data sources (Table 2-4), possibly leading to a final combined FRCC of 2 (Table 2-6). Aside from these frequent low severity fire regime forests, a large portion of the study region is dominated by forests which were historically characterized by infrequent high severity fires. Fire occurrences in these forests were relatively low to have been significantly altered by the relatively short period of fire suppression (Keane et al. 2002b). Other studies show that increased fire activities in the western U.S. were mostly affected by recent climate change rather

than human management and coincided with increase spring temperature and drought severity (Brown et al. 2004; Westerling et al. 2011; Westerling et al. 2006). In addition, the 27-year Landsat record is inadequate to characterize most of the long fire return interval ecosystems in the study region and might reduce the accuracy of fire regime estimation.

High elevation forest biophysical settings areas, taking up over 20% of the total study region, experienced more frequent current fires comparing to the other lower elevation forest biophysical settings (Table 2-4). This seems to indicate that lower elevation forests might have been affected more heavily by current fire management activities, comparing to the high elevation ecosystems. Or it may be reasoned that higher elevation forests are more susceptible to change in the climate conditions and would thus experience more frequent and more severe current fires (Running 2006; Westerling et al. 2006). Fire frequency in lower elevation forest ecosystems in the contemporary time period in the study area were reduced due to various management actions or land use patterns, but the fuel accumulations from the fire exclusion induced more severe fires (Keane et al. 2002b).

4.4.3 Management implications

Fire management will confront many challenges in the future from global climate change to protecting people, communities, and values at risk (Brown et al. 2004; Spittlehouse and Stewart 2004). The current advances of landscape simulation models and the remote sensing technology provide means to characterize both historical and current fire regime characteristics in a more consistent and comprehensive manner. Therefore, the integration of simulation model and remote

sensing data will be vital for addressing these challenges, especially in prioritizing, planning, and implementing fuel treatments (Hardy et al. 2001; Keane et al. 2003).

To apply HRV and FRCC in forest management activities, however, it must be assumed that the record of historical conditions to some degree reflects the range of possible conditions for future landscapes, which we now know is overly simplistic (Keane et al. 2009). Documented climate change, exotic species and human land use can all alter the landscape conditions. While managers need to acknowledge the importance of using historical landscape dynamics as HRV reference conditions to minimize the loss of important landscape elements and maintain key ecosystem service functions.

In the study area, about half of the forest ecosystems are characterized by infrequent and stand replacement fires such as the subalpine forest ecosystems. Although current fire frequencies in these regions have not exceeded historical fire occurrences rate, current fire severities have increased for all forest ecosystems and fire regimes have already moderately departed from historical conditions (Table 2-4). This increase in current fire severity can have negative feedback on the landscape such as reduced shading, increased erosion and increased stream water temperature (Amaranthus et al. 1989). The change in high elevation fire regimes might also become a threat to ecosystem biodiversity and sustainability. For example, these high elevation ecosystems are home to many keystone species (such as Whitebark Pine) that are critical for survival of many other animals in these ecosystems (Kendall and Keane 2001). Without proper fuel monitoring and reduction, these ecosystems might

have increased departures from the historical conditions and cause biodiversity loss, as well as harm to fire fighters and properties.

Besides these high elevation ecosystems, the simulated results also show that a large part of the Northern Rocky Mountain region has moderate departure to historical conditions, such as the montane forest ecosystems. Historically, these montane ecosystems used to have much more frequent surface fires. With long term fire exclusion, these forests have high departure (over 66%) from historical conditions both in terms of vegetation composition and fire regimes. Keane and colleagues (2002b) pointed out that long term consequences of fire exclusion in the middle and high elevation ecosystems include the conversion of a mixed-severity fire regime to a stand-replacement fire regime. And the restoration of some semblance of native fire regimes seems a critical step toward improving the health of many Rocky Mountain ecosystems (Keane et al. 2002b).

Chapter 3: Characterizing Forest Disturbance History in the Past Three Decades in Greater Yellowstone Ecosystems

3.1 Introduction

Forests of the Greater Yellowstone Ecosystems (GYE) undergo frequent natural (e.g. wildfires, insect and disease outbreaks, snow and wind damages) and anthropogenic (e.g. land use change and timber harvesting) disturbance events, and these changes lead to feedback effects on patterns and trends of carbon and nutrient cycling (Liu et al. 2011; Marks and Bormann 1972). Therefore, developing methods to document the disturbance records is important to studying and managing long term health of GYE forests (Turner 2010).

Time series remote sensing data are useful for tracking ecosystem disturbances in a variety of studies (Huang et al. 2010; Kennedy et al. 2010a). However, efficiently identifying and separating disturbance types such as wildfire and harvest still remain a technical challenge. Recently, new attribution techniques have been introduced for use with time series Landsat and other satellite images (Loboda et al. 2012; Neigh et al. 2014; Schroeder et al. 2011). However, few efforts have gone into separating disturbance types from time series disturbance pools using machine learning algorithms. Technically, machine learning algorithms (such as support vector machine (SVM)) are well suited for applications of detecting and differentiating disturbances (Huang et al. 2002; Pal and Mather 2005), but few success stories have been reported.

Although GYE have been a focal point for many studies (Hatala et al. 2010; Parmenter et al. 2003; Turner et al. 2003), a consistent annualized record of forest disturbances from 1980s to current is not available. Such a comprehensive and consistent record would be very useful for informed forest management and policy making, ecosystem conservation and restoration, biodiversity protection and carbon assessment in the region.

Table 3- 1 Types and definitions of forest disturbances mapped in this study

Mapped Forest Disturbances	Wildfires	Harvests	Other disturbances
Definitions	All fires in the forest ecosystem	Clearing or patch cut of forests	A generalized disturbance class with mostly insects and diseases, also include tornado, wind, snow damage and stress related mortality etc.

The main goal of this paper was to evaluate the usefulness of the support vector machines (SVM) algorithm for separating forest disturbance types mapped using the vegetation change tracker (VCT) algorithm and time series Landsat data (Huang et al. 2010; Huang et al. 2009b). Specifically, we used VCT to map forest disturbances annually and then used SVM to separate wildfire, harvest and other forest change types (Table 2-1). For fire activities, only forest wildfires were included in this study. Harvest in this study referred to clear and patch cuts. All forest disturbances caused by agents other than wildfire or harvest, such as insects, diseases, tornado, wind, snow damage and stress related mortality, were grouped and reported as other forest disturbances in this study.

Since VCT has been used extensively to map forest disturbances in previous studies (Huang et al. 2009b; Li et al. 2009a; Li et al. 2009b; Masek et al. 2013), this

paper focuses on the SVM part of the analysis. The derived disturbance products were validated and used to summarize disturbance patterns for different land ownerships. With the free public access of the Landsat data, the VCT-SVM approach demonstrated in this study may allow annual mapping of different disturbance types in other areas where time series Landsat data exist.

3.2 Methods

3.2.1 Study area and input data

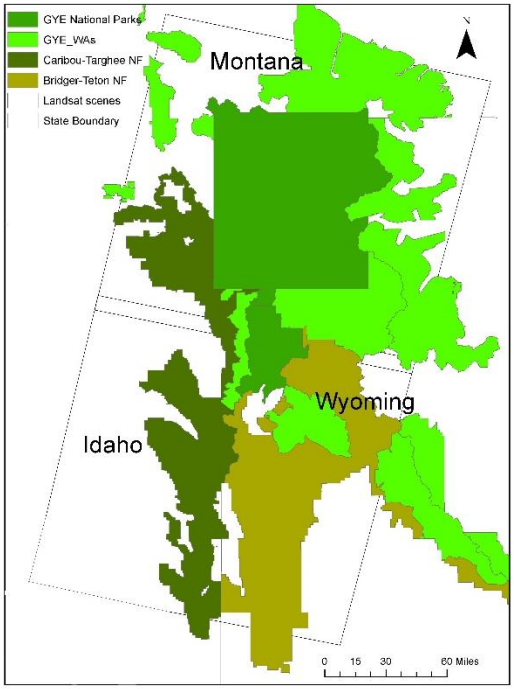

Figure 3- 1 Geographical boundary of the study region. Only area within the Landsat p38r29 and p38r30 were mapped (grey squared polygons).
Leaf green: Yellowstone National Park and Grand Teton National Park; light green: area designated under the Wilderness Act; dark spruce green and olivenite green colors: non-wilderness area within the Caribou-Targhee and Bridger-Teton National Forest, respectively.

The study area of the GYE region includes the Yellowstone and Grand Teton National Parks (NPs), Bridger-Teton National Forest (NF) and Caribou-Targhee NF that were adjacent to the NPs (Figure 3-1). Wilderness area (WAs) in this study refers

to the area under the National Wilderness Preservation System, designated in or after the original 1964 Wilderness Act. WAs within the NFs were examined separately since WAs have different management policies than NFs (Landres et al. 2008). Therefore in the following descriptions, NFs refer to the non-wilderness areas within the NF boundary. Climate in this area is characterized by cold continental climate and varies predictably with elevation (Hansen 2006), with ranges from 1500 to 3400 meters.

The study area was covered by two Landsat time series stacks (LTS) (WRS-2, path 38 row 29 and path 38 row 30). Imagery data of the LTS were ortho-rectified and converted to surface reflectance using the Landsat Ecosystem Disturbance Adaptive processing System (LEDAPS, (Masek et al. 2006b)). Total forested area mask was derived from VCT product, where, in order to be considered forested, a pixel must have been labeled as forest at least once over the 26 years. Masks of cloud and cloud shadow were derived with the algorithm developed by Huang and colleagues (Huang et al. 2008a). The identified cloud and shadow pixels were then filled using a temporal interpolation approach which estimated spectral values using temporally nearest pixel observations acquired before and after the cloudy observations (Huang et al. 2008a).

3.2.2 Overall approach

In this section, we outline a new method to address the gap and test the feasibility that different types of disturbances can be identified and characterized. The following steps were involved to develop and validate the forest disturbance maps. First, VCT algorithm (Huang et al. 2010) was applied to the LTS to produce time

series VCT disturbance maps in the study region. Second, Support Vector Machine (SVM) algorithm was used to split annual wildfires, timber harvest and other forest disturbances from the VCT forest change pools. The classification was conducted separately for each year. Third, post-classification processing was applied to reduce the "pepper and salt effect" and other obvious errors. Fourth, independent, design-based accuracy assessment using TimeSync Tool (Cohen et al. 2010) validation was used to determine the accuracy of both VCT disturbance polygons and the differentiated fire, harvests and other disturbance maps. After validation, rates of different forest disturbances were summarized for the study area for the past three decades. Details of the method are described in the following sections.

3.2.3 Initial disturbance mapping using VCT

Initial disturbance maps (disturbed vs. undisturbed) were produced using VCT and LTS. The VCT algorithm was designed for analyzing LTS to create spatially comprehensive and temporally continuous records of general forest change history (Huang et al. 2010; Huang et al. 2009b). For GYE forests, we used the VCT forest threshold for sparse forest and classified each pixel as forest or non-forest. A disturbance event can only occur if the pixel remained as forest for consecutive two years before the disturbance and the pixel remained as non-forest for at least two consecutive years after the disturbance. Therefore a second disturbance can only after at least four years after the first disturbance. VCT also produced temporally normalized Landsat images which were used for the final disturbance attribution.

3.2.4 Forest disturbance type mapping

Information for forest changes introduced by wildfires was mapped by separating fire disturbances from VCT disturbance pools using the SVM algorithm. SVM represents a group of theoretically superior machine learning algorithms, which was designed to locate optimal spectral boundaries between classes. It has been widely used in pattern recognition and land cover classifications (Chang and Lin

2011; Huang et al. 2002; Huang et al. 2008a). The algorithm has been shown to be more accurate in remote sensing land cover classifications than many other classifiers (Huang et al. 2002; Pal and Mather 2005).

In this study, we used the libsvm package for the R project for statistical computing (Chang and Lin 2011; Team 2012). Fire training samples for SVM classification were randomly selected from the MTBS (Monitoring Trends in Burn Severity) maps. The MTBS project mapped fires from time series Landsat images (1984-2010) using differenced normalized burn ratio (dNBR) and relativized dNBR (Eidenshink et al. 2007a). While fires less than 1,000 acres were generally excluded for the western U.S. in the MTBS data (Eidenshink et al. 2007a), this study mapped fires of all sizes in the study region. The selected training pixels were then visualized in n-dimensional space to locate, identify and cluster the purest fire pixels. Only the purest pixels were kept for SVM training. Non-fire training samples were randomly selected from VCT no disturbance masks. After applying the SVM algorithm to the VCT temporally normalized Landsat images, the mapped wildfire pixels were overlapped with the VCT disturbance mask and only pixels that were labeled by both SVM and VCT were kept as wildfire disturbances. Since we had higher confidence in mapping fire than other forest disturbance types, the mapped fire pixels were separated from the VCT disturbance maps and the remaining pixels were considered to be timber harvest as well as other forest disturbances.

Forest harvests were also mapped using the SVM algorithm with similar procedure. Since timber harvests usually have a uniform shape and were easy to capture, training samples for SVM classification were manually selected each year

from the VCT disturbance maps. For years without overlap between VCT, training data from adjacent years were combined and used as inputs for SVM classification. Then the mapped timber harvest pixels were overlapped with the remaining VCT disturbance pixels (after subtracting wildfire pixels) and only coinciding pixels were kept as timber harvests. The rest of the VCT disturbances (after subtracting wildfires and harvests pixels) all went to the other disturbance category.

Two types of post-classification processing were performed after the disturbance type mapping using SVM. First, fire patches with size less than 0.0036 km^2 (4 Landsat pixels) were removed. Most forest fires in this region are larger than this size, and therefore such small disturbances would be more likely noise instead of real changes. Second, we visually inspected the mapped disturbance types and checked against Google Earth images. For example, if there were disturbance patches with clear sharp boundaries in the wildfire maps, we would check Google Earth time series images to see if these pixels were harvests misclassified as fires.

3.2.5 Validation of forest disturbance maps

Pixel based stratified random sampling approach was used to validate VCT disturbance maps and the disturbance types (forest wildfire, harvest and other disturbances) in the TimeSync platform. TimeSync is a computer tool specifically designed to sync algorithm and human interpretations of LTS (Cohen et al. 2010). The tool has been applied to validate Landsat based time series disturbance mapping results (Kennedy et al. 2012; Thomas et al. 2011). We used the stratified random sampling approach to make sure that there were enough validation points for each class. For VCT disturbance map validation, we used 300 points and 100 points for

disturbed and no change classes, respectively. For the disturbance type mapping validation, 100 validation points were selected for each of wildfire, harvest, other forest change and no-change classes (400 validation points in total). To account for the fact that the class area proportions were unbalanced we used inclusion probability to calculate the design-based inference of map accuracy (Stehman 2000). For the samples in each forest disturbance stratum, the probability that a particular map pixel was included in the sample was calculated following the Stehman and Czaplewski method (Stehman et al. 2003). We then calculated the overall, user's and producer's accuracies and assessed the uncertainties of the commission and omission errors related to our reference validation (Olofsson et al. 2014; Olofsson et al. 2013; Pontius Jr and Millones 2011).

3.2.6 Forest disturbance rate calculation

The wall-to-wall forest disturbance type maps allowed a comprehensive assessment of the forest dynamics in GYE. As discussed previously, the study region included national parks, wilderness area and national forests. For ownership group types in the study region, total forested area, annual area and percent of forest disturbed by wildfires, harvests and other disturbances from 1985 to 2010 were summarized. Since 1984 data included all disturbances occurred in or before 1984 (age unknown), we did not include 1984 data in the summary. Total forested area was calculated from time series VCT disturbance maps.

3.3 Results

3.3.1 Validation of forest disturbance and disturbance types

Table 3- 2 (a) Accuracy values (%) for VCT Mapped Change Classes; (b) Accuracy Values (%) for Mapped wildfires, harvests, Other Disturbances and No Change Classes.
UA: User's Accuracy; PA: Producer's Accuracy; OA: Overall Accuracy
(a)

	Change	No Change	Row Total	UA (%)
Change	284	16	300	71.1
No Change	13	87	100	87.0
Column Total	297	103	400	
PA (%)	50.2	94.2		
OA (%)		88.0		

(b)

	Fires	Harvests	Others	No Change	Row Total	UA (%)
Fires	96	0	1	3	100	96.0
Harvests	0	91	4	5	100	91.0
Other	17	2	73	8	100	73.0
No Change	2	0	11	87	100	87.0
Column Total	115	93	89	103	400	
PA (%)	73.2	88.6	24.4	99.2		
OA (%)				87.1		

Evaluations for both the VCT disturbance maps and the disturbance type maps with the TimeSync tool revealed that the method and the resulting maps were robust with satisfactory accuracy (Table 3-2). Overall accuracy of VCT disturbance maps and the mapped forest disturbance type maps were roughly 88% and 87%, respectively. Except for the other forest disturbance class, most other accuracy values listed in Table II were above 70%. Wildfire and harvests classes had the highest accuracies, with the user's accuracies for the two classes above 90%. The "other" disturbance category had the lowest producer's accuracy, because VCT algorithm were not very sensitive to partial disturbance events (such as low severity insect and disease outbreaks and thinning) at 30 meter resolution, especially when these pixels

returned to forested signal in a few years (Thomas et al. 2011).

For the geolocation error, since we were using the original Landsat images in the TimeSync tool, there were no mis-registration between the classification results and the reference images; for the interpreter uncertainty, the validation work was conducted by the same interpreter therefore interpreter variability was prevented.

3.3.2 Forest disturbance status by land ownership in the study region

During the post-classification processing, about 1.1% of mapped fire pixels were removed to reduce the 'pepper and salt effects'. 0.5% and 1.5% of mapped fire pixels were changed to harvests and other disturbance categories during the second step of post-classification processing. This process helps to reduce the obvious errors from the final disturbance type maps.

Summary statistics derived from the forest change maps show that about 6651 km^2 of forest area were affected by disturbances in the study region from year 1985 to 2010. This equals a cumulative 31.2% of the forested area in the study region, of which 18.4% was attributed to wildfire, 1.4% to timber harvests and 11.4% to other forest disturbances.

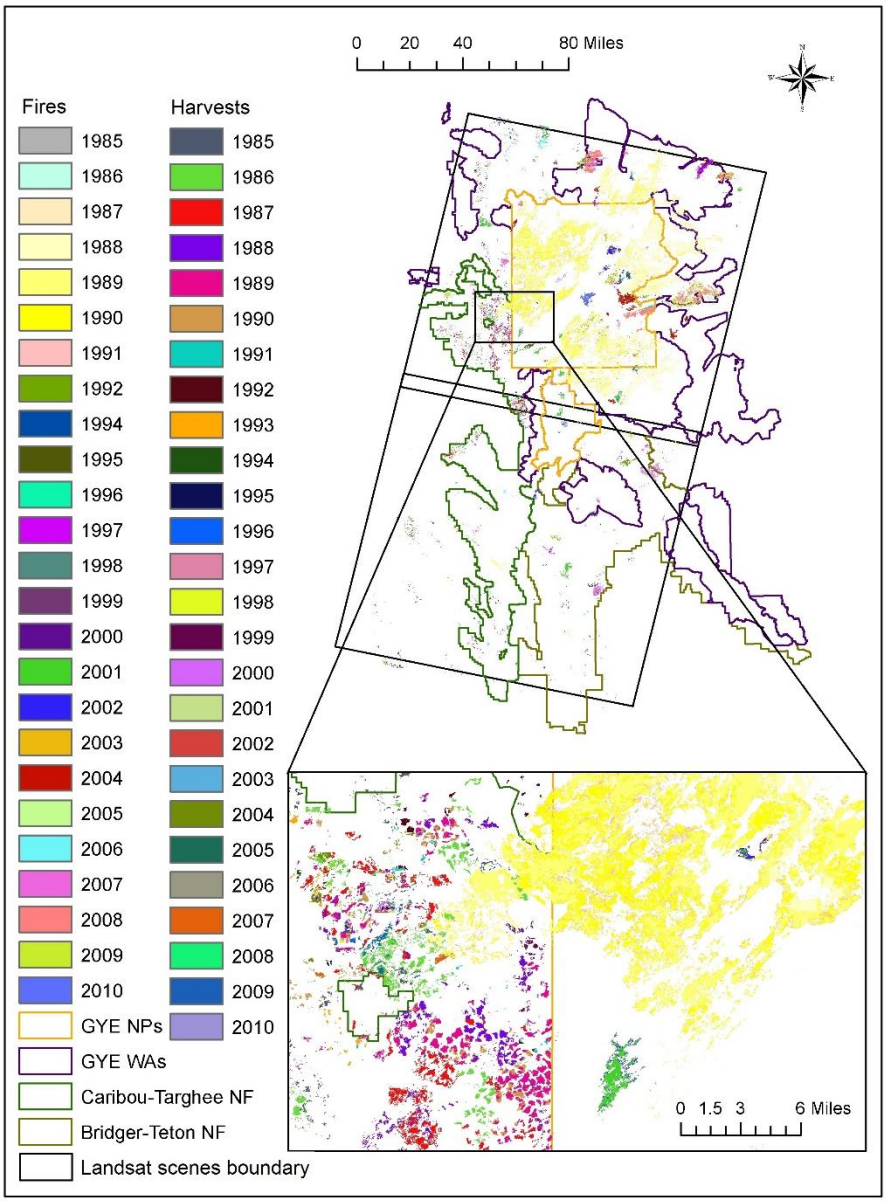

Figure 3- 2 Final classification results for mapping wildfires and harvests in the study region and a zoom-in view at the boundary between the Yellowstone National Park and Caribou-Targhee National Forest

Analysis of forest disturbances by landownership in GYE, as tracked in this study, suggests that NPs and WAs had different distributions of disturbance types (Figure 3-2). In the study region, NPs have the highest forested area compared to WAs and NFs. Fire was the dominant forest disturbance in the GYE NPs and WAs, affecting cumulatively about 37% and 20% of forests in NPs and WAs, respectively,

during the study period. While in Caribou-Targhee and Bridger-Teton NFs, where fires would be closely monitored and managed, the accumulative percentages of forests affected by fires were 1.5% to 3.7%, respectively. In the Caribou-Targhee NF, area of forests harvest were four times of area of forest fires. Despite the impact of harvests, the other forest disturbances such as insect and disease were the major forces shaping the forests within the NFs. Although the SVM model did not distinguish between other types of disturbances, according to our validation results (e.g., from TimeSync tool and Google Earth high resolution images), over 50% of the other-type forest disturbance class were insects and disease outbreaks. The results indicate that the two NFs had higher percentage of insect and disease outbreaks than those in the NPs.

3.4 Discussion and conclusions

Using Landsat time series observations, we mapped annual rates of different forest disturbance types in the GYE region by combining the VCT and SVM algorithms. This VCT-SVM approach was found effective for mapping wildfires and harvest/logging. But it missed most disturbances in the "other disturbance" class, which were mostly minor disturbances due to insect/disease as well as snow and wind damages. This was mainly due to the limited capability of the current version of the VCT to detect those disturbances, which was also observed in previous studies (Thomas et al. 2011).

Our results revealed that forest fire was the most dominant forest change agent in GYE NPs and WAs during the study interval. However, harvest was significant in the NFs. In particular, harvested areas in the CTNF were four times of burned areas

during the 26-year observing period. The validation results derived using the TimeSync tool revealed that damages from Mountain Pine Beetle (MPB) infestations, which accounted about half of the other disturbance class, were widespread across the entire study area, confirming observations from other studies that MPB outbreak had been a severe issue in GYE in recent decades (Hatala et al. 2010; Logan et al. 2010). Although these disturbance types were typically characterized by low disturbance intensity in each individual year, given the large areas affected by them and their cumulative effect over multiple years, it is important that they be mapped accurately. Further improvement to the VCT algorithm is needed in order to better detect these disturbance types. In addition, the other disturbance type class can be further classified in the future by incorporating more training data for each specific disturbance categories.

The disturbance products derived through this study will be used in a carbon modeling study to quantify the carbon fluxes from the mapped disturbance events and their impacts on future carbon sequestration potential in the GYE region. By providing details on both the timing and causal agents of the mapped disturbances over nearly three decades, these products likely will be valuable for many other applications, including forest management, biological conservation, and ecosystem restoration. SVM appeared to be an effective tool for separating different forest disturbance types after those disturbances have been detected. While it was used together with VCT in this study, it can be used with other change detection algorithms designed for detecting changes but not for separating different change types. Now that Landsat data are publically available at no data cost to users, this

algorithm can be used together with VCT or other change detection algorithms to achieve annual mapping of different disturbance types for areas that have time series Landsat data.

Chapter 4: Assessing Post-disturbance Forest Recovery in Greater Yellowstone Ecosystems

4.1 Introduction

Forests in the Greater Yellowstone Ecosystem (GYE) experience frequent natural (e.g., wildfires, insect and disease outbreaks, snow and wind damage) and anthropogenic (land use changes and timber harvesting) disturbance events (Parmenter et al. 2003; Zhao et al. 2015a). Recovery from past disturbances is an integral process in the carbon and nutrient cycles (Houghton et al. 1999; Pan et al. 2011). Inclusion of the forest recovery process following disturbances is critical to calculating regional C fluxes and can better inform policy makers on both the importance and uncertainty of disturbances in the regulation of the regional and global carbon cycle (Goetz et al. 2012).

Remote sensing techniques provide an effective tool for examining forest disturbance and recovery over large areas. In particular, a series of Landsat systems have been imaging the Earth's surface since 1972, creating a time series of Landsat observations that is highly valuable for tracking land change history for over four decades. Although numerous change detection algorithms have been developed (Lu et al. 2004; Singh 1989), with some having succeeded in mapping forest disturbances over large areas (e.g. Huang et al. 2007; Masek et al. 2008; Potapov et al. 2009), characterizing post-disturbance forest recovery remains challenging. Depending on local environmental conditions and post-disturbance management practices, it often takes years to decades for trees to grow back, following a stand-clearing disturbance

event. It is difficult to determine at any point in time during this process whether young trees have started to grow back and whether their height and density exceeds the threshold values of a forest according to a particular definition.

With the opening of the Landsat archive to free access in 2008 (Woodcock et al. 2008), many algorithms have been developed to monitor vegetation dynamics using dense Landsat time series observations (Huang et al. 2010; Kennedy et al. 2010a; Zhu et al. 2012). One of the algorithms, the Vegetation Change Tracker (VCT), was designed to both detect forest disturbance and track post-disturbance recovery (Huang et al. 2010) using annual or biennial Landsat time series stacks (LTSSs) (Huang et al. 2009a). Although the disturbance products derived using this LTSS-VCT approach have been validated extensively across the United States (Huang et al. 2015; Huang et al. 2011; Thomas et al. 2011), the ability of this approach to characterize post-disturbance recovery has yet to be assessed. One of the main goals of this study was to evaluate the effectiveness of this approach in mapping post-disturbance recovery in the GYE region.

Although the GYE has been a focal point for many post-disturbance vegetation recovery studies (Harvey et al. 2014; Turner et al. 1997), most previous studies relied on plot-level data and were limited in their ability to sample in the remote, high-elevation areas of the Yellowstone Caldera. No systematic assessment of forest recovery following disturbances has been conducted across the whole region in recent decades (1980s to the present). The results from such an assessment will be highly valuable for many ecological studies and can be used to inform management decision making regarding ecosystem conservation and restoration, biodiversity

protection, and carbon management. Previously, we annually mapped different forest disturbance types in the GYE using the LTSS-VCT approach and support vector machines (Zhao et al. 2015a). In this study, we used the LTSS-VCT approach to map post-disturbance forest recovery and conducted a comprehensive assessment of the derived recovery products. The validated recovery products were then used to quantify patterns and rates of forest recovery following major fires and logging activities and to assess the impact of the disturbance type, management approach, and environmental factors on forest recovery. The latter part focused on disturbances that occurred in the 1980s and 1990s. Because recovery is generally slow in the GYE region and can take more than 10 years to occur in areas with unfavorable conditions, the LTSSs used in this study (1984-2011) did not allow accurate mapping of forest recovery for disturbances that occurred after 2000.

The specific goals of our study, as described in this paper, were as follows: 1) to validate a VCT map product focused on tracking post-fire and post-harvest forest recovery in GYE, using year 2010 as a reference year for the recovery; 2) to use the validated recovery product to analyze the recovery rates for all major fires and harvests that occurred in the 1980s (to allow adequate time for recovery to occur). The analysis examines spatial patterns of forest recovery and the differences between fires and harvests, and the impact of post-disturbance management approaches; 3) to understand how environmental factors such as climate and topography can affect forest recovery vs no-recovery in GYE.

4.2 Study Area

The 91,758-km^2 study area of the GYE region includes Yellowstone National Park (YNP) and Grand Teton National Park in the center, seven surrounding national forests (Bridger-Teton, Caribou-Targhee, Gallatin, Shoshone, Custer, Helena, and Beaverhead-DeerLodge), 21 other federal and state jurisdictions areas, and relatively few private lands (Figure 4-1(a)).

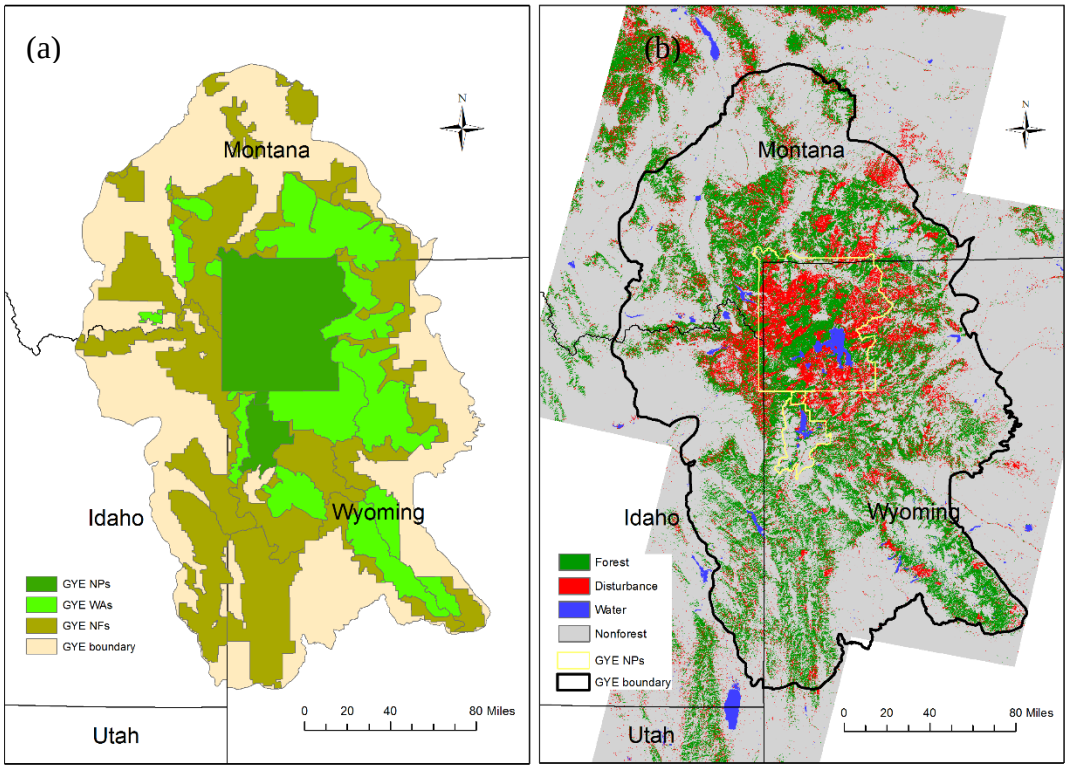

Figure 4- 1 (a) Boundary and ownership of the study area; (b) forest disturbances mapped by Vegetation Change Tracker (VCT) between 1985 and 2011. Landsat scenes for the study region include: WRS-2, p37r29, p37r30, p38r28, p38r29, p38r30, p38r31, p39r28, and p39r29.

The GYE features distinct gradients in elevation, climate and soil. Elevation played the key role in affecting the vegetation distribution in the GYE, but its effects

are manifested through its influences on temperature and moisture availability (Martson and Anderson 1991). Mean annual temperature varies from 7.6 ℃ at lower elevations (< 1400 m) to 0.13 ℃ at higher elevations (> 2300 m) (Hansen 2000). Precipitation mostly falls as snow and generally increases with elevation; mean annual precipitation ranges from 1368 mm to 2414 mm (Martson and Anderson 1991). The growing season varies from two to three months at higher elevations to five to six months at lower elevations. A large portion of the national parks (NPs), including the Yellowstone Plateau and surrounding mountain ranges, lies at relatively high elevations. The national forest (NF) lands are mostly at moderate and low elevations on the flanks of the plateau. The soils at higher elevations are largely composed of nutrient poor rhyolites and andesites with low water-holding capacities (Marston and Anderson 1991). The valley bottoms and floodplains contain glacial outwash and alluvium soils that generally feature higher nutrients and water-holding capacities in relative terms (Hansen 2000).

Natural forest vegetation in the study area is a mosaic of major coniferous species. Lodgepole Pine was widespread in YNP before year 1988 and dominated over 70% of the forested NP area (approximately 5295 out of 7355 km^2), followed by Whitebark Pine, Engelmann Spruce/Subalpine Fir and Douglas-fir. Whitebark Pine occupies approximately 15% of the YNP forested area, especially at the higher elevations. Engelmann Spruce and Subalpine Fir often co-exist below the elevation zone of Whitebark Pine, with Douglas-fir dominating the lowest elevations. Upland rhyolite soils support Lodgepole Pine (*Pinus contorta*) forests between 2000 m and 2600 m (Schoennagel et al. 2003), and Douglas-fir (*Pseudotsuga menziesii*) is

common up to 2300 m on andesitic soils and in warmer microclimates. Above these elevations in both soil types, subalpine fir (*Abies lasiocarpa*), Engelmann spruce (*Picea engelmannii*), and whitebark pine (*Pinus albicaulis*) dominate. The majority of the forested area of the GYE is located in national forests (~80% of the GYE forested area), which contain a wilderness area designated by the Wilderness Act of 1964 (~22% of the GYE forested area) and areas managed for timber production (~47.7% of GYE forested area). National parks occupy approximately one-fifth of the GYE forested area and the remaining forested areas are under other ownership, such as state or private forests.

The recent history and composition of disturbance events during the study interval (1984-2011, Figure 4-1(b)) also show an ownership pattern. In the GYE national parks and wilderness area, fire was the most dominant disturbance agent, affecting over 37% of the forested area in the GYE national parks. However, active harvest events occurred in the national forests. In particular, the harvested area in the Caribou-Targhee National Forest was four times larger than the burned areas during the study period (Zhao et al. 2015a).

4.3 Methods

4.3.1 LTSS assembling

LTSSs were assembled for the 8 Landsat World Reference System-2 (WRS-2) tiles required to cover the GYE (Figure 1). Each LTSS consisted of one image per year for the years between 1984 and 2011 that had at least one cloud-free or nearly cloud-free (< 5% cloud cover) image acquired during the summer growing season. If no such image was available in a particular year, multiple partly cloudy images

acquired during the growing season of that year were used to produce a composite using a best observation method. Here, best observation was defined based on criteria designed to enhance forest disturbance mapping. Specifically, if no more than 1 clear-view observation was available in a year at a given pixel location, the pixel with the maximum NDVI value was selected. If more than 1 clear-view observation was available, the clear-view observation that had the highest brightness temperature was selected. Here, clear-view observations refer to those that were not contaminated by clouds or shadows and did not have other data quality problems.

These images were downloaded from the U.S. Geological Survey (USGS) at the 30-m resolution. They were first converted to surface reflectance using the Landsat Ecosystem Disturbance Adaptive Processing System (LEDAPS) atmospheric correction algorithm (Masek et al. 2006a). Geometrically, no additional correction was performed on these images because they had already been ortho-rectified by the USGS to achieve subpixel geolocation accuracy. A detailed description of the procedures involved in assembling LTSSs has been provided in a previous study (Huang et al. 2009a).

4.3.2 Forest disturbance and recovery mapping

The LTSS assembled in section 3.1 were analyzed using the VCT algorithm to map forest disturbance and recovery. VCT used an integrated forest z-score (IFZ) index to track forest change at each pixel location:

$$IFZ = \sqrt{\frac{1\sum_{band3,5,7}(\frac{bi-\overline{bi}}{SDi})^2}{3}} \qquad \text{Equation 4-1}$$

where bi is the spectral value of a pixel in band i, and $\overline{bi}$ and SD_i are the mean and standard deviation of the forest samples in that band, which were identified automatically using a dark object approach (Huang et al. 2008b). The IFZ is a non-negative, inverse indicator of forest likelihood. The closer to 0 this value is, the more likely the pixel is a forest pixel. The higher this value is, the more likely this pixel is a non-forest pixel. Thus, a forest pixel typically maintains low IFZ values when undisturbed. When a disturbance occurs, that pixel loses part or all of its forest cover, often resulting in a sharp increase in the IFZ value. Thus, the year of disturbance is defined as the year when the IFZ increases sharply (Figure 3). The IFZ then decreases gradually if trees grow back after that disturbance event. If the IFZ drops below a predefined forest threshold value and remains below that value for two consecutive years, post-disturbance recovery is considered to have occurred, and the disturbed pixel is reclassified as having forest cover after that point (Figures 3(a) and (b)). Otherwise, the VCT concludes that post-disturbance forest recovery did not occur during the years covered by the LTSS (Fig. 3(c)). Thus, the VCT produces two types of recovery products. The first indicates whether there is recovery or no- recovery (RNR) of forest cover for each disturbance mapped by VCT. If recovery did occur at a disturbance location, the number of years it took for that pixel to regain forest cover, defined as years-until-recovery in this study, is recorded as the second product type. Detailed descriptions of the VCT algorithm and its disturbance products have been provided in previous publications (Huang et al. 2010; Huang et al. 2009b; Huang et al. 2011).

(a)

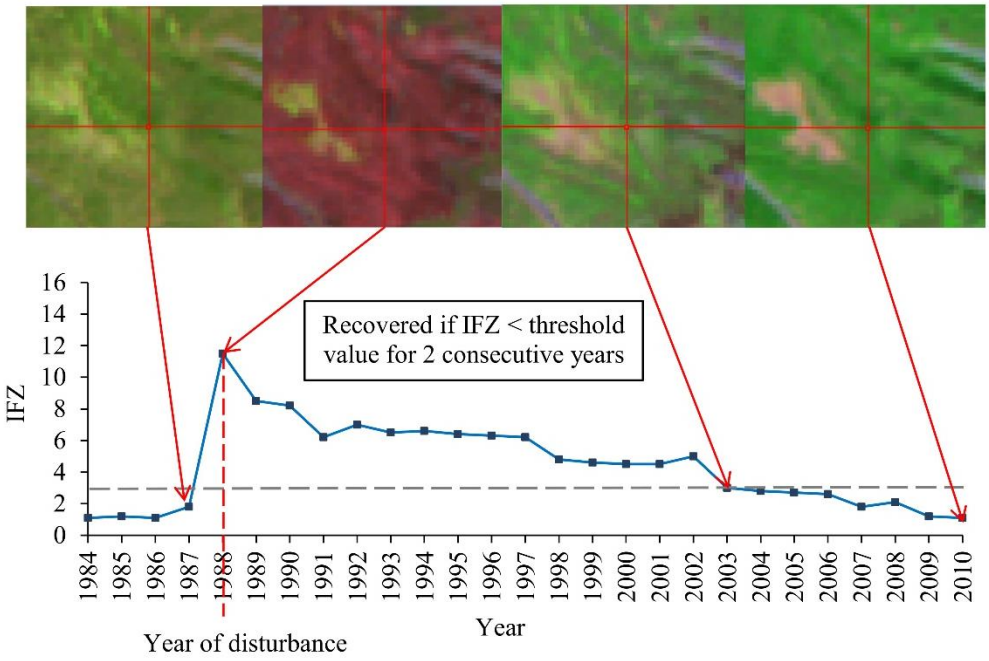
Recovered if IFZ < threshold value for 2 consecutive years
IFZ
Year
Year of disturbance

(b)

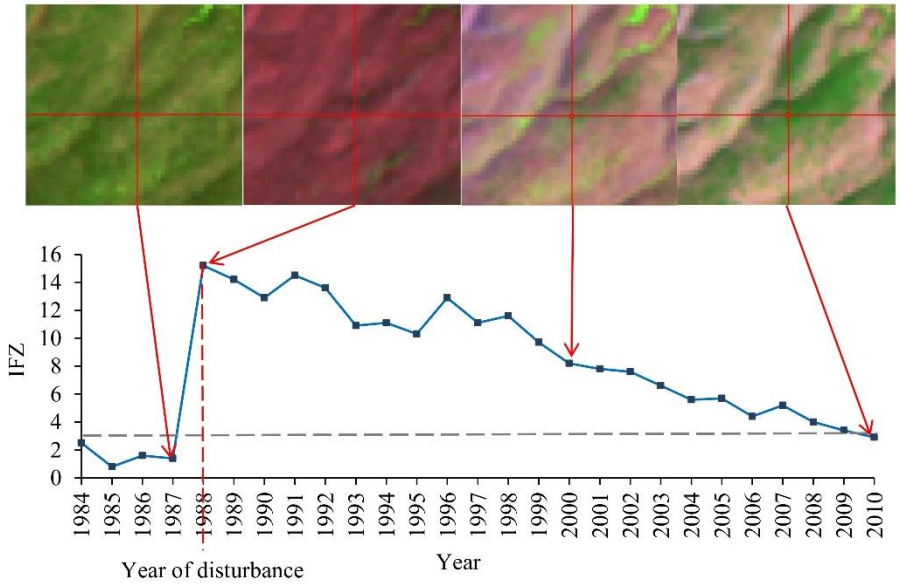
IFZ
Year
Year of disturbance

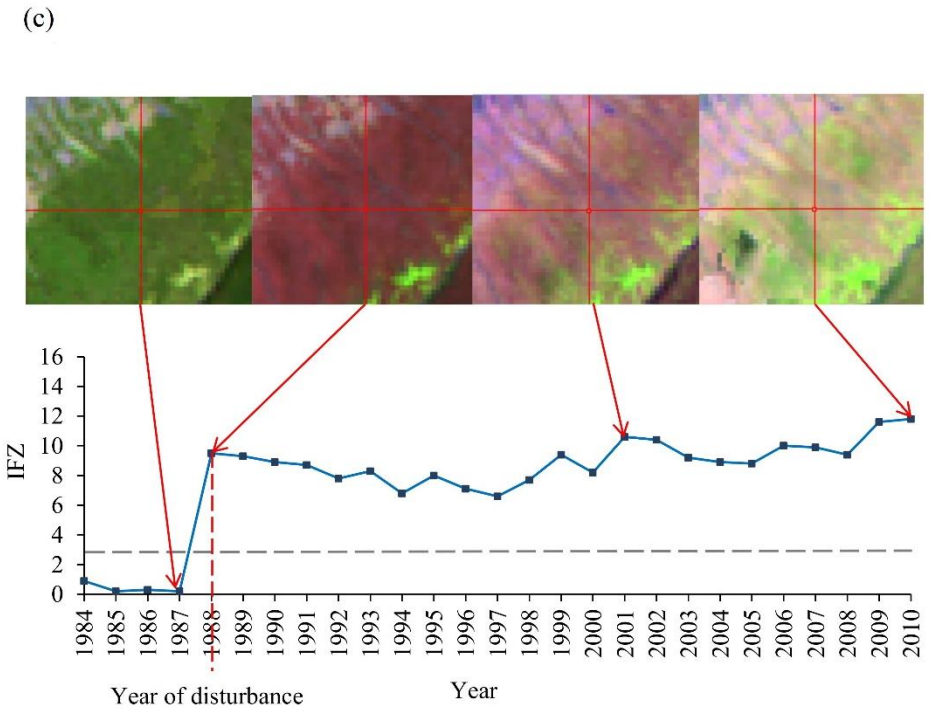

Figure 4- 2 Examples showing where forest recovery occurred (a) and (b) and did not occur (c) following the 1988 Yellowstone fire as determined by tracking the IFZ. In (a) and (b), the disturbed pixels were reclassified as having forest cover by around 2003 and 2009, respectively. Each IFZ plot is for the center pixel, shown as the intersection of the two red lines in the images above it. The images are shown with bands 5, 4, and 3 displayed in red, green, and blue.

The disturbances mapped by VCT were classified into fire, harvest, and other disturbances using the support Vector Machine (SVM), which has been described in a previous study (Zhao et al. 2015a). The fire disturbances were further divided into low-, medium-, and high-intensity fires using the Relative difference Normalized Burn Ratio (RdNBR) using threshold values developed by Miller et al. (2009).

4.3.3 Validation of recovery product

In this study, we define forest following the definition of the Food and Agriculture Organization (FAO) of the United Nations, i.e., greater than 10% tree

cover at the Landsat pixel scale (30 meters by 30 meters). Forest recovery was then defined as the spectral IFZ value exceeding the pre-determined threshold by year 2011, approximating the regrowth of forest cover to more than 10% of the area. Notably, a spectral recovery is not synonymous with ecological definitions of forest recovery (Huang et al. 2010). In addition, recovery does not mean that the pixel is occupied by the original species. For example, a post-fire Whitebark Pine forest might grow back as birch forest in the first few decades after the fire.

We used the high-resolution images available from Google Earth to validate the RNR products. By the time this study was conducted, Google Earth had acquired a comprehensive set of high-resolution images covering the study area in approximately 2011. With spatial resolutions of 1 m or better, these images allowed reliable determination of whether an area had tree cover through visual analysis. If at any specific validation point the available Google Earth images did not allow reliable visual analysis, ortho-photos acquired through the National Agricultural Imagery Program (NAIP) program were used to assist with the visual analysis. Three steps were involved in the validation. First, based on forest type maps and burn severity maps, we randomly selected 100 pixels from each of the four major forest types (Lodgepole Pine, Whitebark Pine, Douglas-fir, and the combination of Engelmann Spruce and Subalpine Fir) and burn severities (low-, medium-, and high-severity fires) in the study region (1,200 points in total). The forest type map[5] was drafted before the 1988 fires and represented the forest conditions that were burned in 1988. Second, for each selected validation point, we divided the 30-m pixel equally with a

[5] https://irma.nps.gov/App/Reference/Profile/1045509

6m by 6m grid (25 cells in one 30-m pixel) and overlaid the grids onto the high-resolution images (Figure 3). Then, we counted the number of grids that was covered by trees and summed the percent tree cover by multiplying the number of forested grids by 4%, which is the area in percent of each grid (i.e., 1/25). Following the FAO forest definition (i.e., ≥10% tree cover), a disturbed pixel was considered to have recovered if the tree cover was at least 10% or more by 2011. Otherwise, that pixel was classified as having no recovery. Third, we summarized the validation results to calculate the User's, Producer's and Overall Accuracies of the RNR products for fire and harvest and for each of the four forest types.

Figure 4- 3 Examples of Google Earth validation of recovered and non-recovered pixels in 5 by 5 grids

No design-based accuracy assessment was conducted for the years-until-recovery products because such an assessment would require annual high-resolution images at each selected validation location, which do not exist. Instead, we did a qualitative assessment of this product using the Landsat images and the IFZ profiles, as shown in Figure 2, to verify that the VCT algorithm worked as designed in determining the years-until-recovery value.

4.3.4 Recovery pattern analysis

4.3.4.1 Spatial and Temporal Patterns of Forest Recovery in GYE

The maps made using the methods described in Section 3.2 provided the raw material used to evaluate the spatial and temporal patterns of forest recovery in the GYE. Global Moran's I values were calculated to determine whether any spatial clustering is present in the post-disturbance forest recovery in the GYE. Global Moran's I is a measure of spatial autocorrelation and is characterized by a correlation in a signal among nearby locations in space (Li et al. 2007; Moran 1950). To examine the spatial patterns of forest recovery in the GYE, the fires, harvests and their associated recovery maps were overlaid with ownership boundary maps. For each disturbed pixel, we derived the annual forest recovery status by the end of the study interval. Then, we summarized the yearly percent forest recovery in the study area within the geographic area stratified by forest type and disturbance magnitude. Yearly percent forest recovery was calculated by dividing the number of recovered forest pixels by the number of total disturbed pixels.

We examined the spatial patterns of post-disturbance forest recovery in the GYE by calculating the number of years until a disturbed pixel recovered to forest. Lower numbers of years required for a pixel to recover indicate faster recoveries, and higher numbers indicate slower recoveries. For temporal analysis, we used the annual fire and harvest data from 1985 to 2011 to track long-term post-disturbance forest recovery in the GYE. We summarized the yearly percent forest recovery in the burned and harvested areas and compared the percent forest recovery following these two disturbance types. More in-depth descriptions and modeling of the impact of

environmental factors on forest regrowth in the GYE will be presented in the following sections.

4.3.4.2 Relationship between recovery pattern and environmental factors

Environmental conditions and management activities are the two major determinants of forest recovery following a disturbance (Kane et al. 2015b). Management variables in the GYE were strongly related to policy and socioeconomic factors that are difficult to characterize as environmental variables. In YNP, forests were left "unimpaired", making it an ideal place to study the impact of environmental variables on natural forest recovery following fires. Therefore, we took the major forest species' recovery conditions in the YNP as dependent variables and only modeled the impact of environmental factors on forest recovery in the YNP after the 1988 fires.

After analyzing the spatial and temporal pattern of forest recovery in the GYE, we took a four-step approach to further model the impact of environmental factors on forest recovery following the 1988 fires in the YNP. First, we randomly selected sample points to represent the population traits. Due to the large number of qualified burned pixels (Figure 1), random sampling was necessary to increase computational efficiency for random forest modeling. The minimum sample size was estimated using Equation 1 (Kotrlik and Higgins 2001).

$$n = \left[\frac{z_{\frac{\alpha}{2}}\,\delta}{E}\right]^2 \qquad \text{Equation 4-2}$$

where α is the confidence level, $z_{\frac{\alpha}{2}}$ is the corresponding critical value, δ is the population standard deviation, and E is the margin value. Here, we defined α as 5%, δ as 350, and E as 30 based on the time series Forest Index values of recovered and non-recovered pixels. As a result, the sample size needed to be larger than 522 to represent population traits.

Second, we extracted all environmental characteristics of these sample points from our reference datasets (Table 2). Third, a random forest (RF) decision tree algorithm was used to predict the regeneration status of these points based on their environmental conditions. Fourth, the importance of the environmental variables was also produced by following the stepwise elimination approach (Díaz-Uriarte and De Andres 2006). The top ten variables with the highest RF importance were selected and used to construct the nested collection of RF models. We then constructed an ascending sequence of RF models by invoking and testing the variables stepwise. The variables of the last model were selected and used to interpret the factors that had the highest impact on post-disturbance forest recovery.

To examine the effects of environmental factors on the rate of forest recovery from the 1988 fires, we used the RF algorithm to model the forest regrowth following the 1988 Yellowstone fires. The RF algorithm is a machine learning algorithm based on traditional decision tree classification, and it has been widely applied in ecological studies (Breiman 2001; Kane et al. 2015a; Kane et al. 2015b; Prasad et al. 2006). It randomly selects input variables from a large number of available variables and generates a large ensemble of independent tree classifiers that vote for class membership (Breiman 2001). The RF algorithm provides an internal unbiased

estimate of the training set error called the out-of-bag (OOB) error (Breiman 2001). During the process of RF classification, each tree classifier was constructed from bootstrapped samples comparing approximately two-thirds of the original dataset. Samples not used in the tree construction were put into the tree classifier to obtain a classification. In the end, a class is assigned to the largest number of votes from the OOB sample. The ratio of the times that a class is not the true class across all bootstrap iterations is called the OOB error estimate (Breiman 2001). In addition, standard methods for evaluating classification accuracies, such as confusion matrices and the kappa coefficient, were calculated to compare the RF classification of regenerated and non-regenerated forests for major species in the GYE following the 1988 fires.

Table 4- 1 List of dependent and predictor variables in random forests modeling for major species in YNP

Category	Variables	Units	Resolution
1. Dependent Variable	Forest regrowth status (recovered vs. non-recovered) from 1988 fires by year 2011	Unitless	30 m
2.Topography	Elevation	m	30 m
	Slope	degrees	30 m
	Eastness		30 m
	Northness		30m
3.Climate	Spring precipitation in 1989, 1990, 1991 and 1992	mm	1 km
	Summer precipitation in 1989, 1990, 1991 and 1992	mm	1 km
	Maximum July temperature in 1989, 1990, 1991 and 1992	℃	1 km
	Minimum January temperature in 1989, 1990, 1991 and 1992	℃	1 km
	Mean spring precipitation during the 1980-2013 period	mm	1 km
	Mean summer precipitation during the 1980-2013 period	mm	1 km
	Mean maximum July temperature during the 1980-2013 period	℃	1 km
	Mean minimum January temperature during the 1980-2013 period	℃	1 km
4.Climate Anomaly	Spring precipitation anomaly in 1989, 1990, 1991 and 1992	Unitless	1 km
	Summer precipitation anomaly in 1989, 1990, 1991 and 1992	Unitless	1 km
	Maximum July temperature anomaly in 1989, 1990, 1991 and 1992	Unitless	1 km
	Minimum January temperature anomaly in 1989, 1990, 1991 and 1992	Unitless	1 km
5.Water Availability	Spring water balance in 1989, 1990, 1991 and 1992	mm	1 km
	Summer water balance in 1989, 1990, 1991 and 1992	mm	1 km
	Spring moisture index in 1989, 1990, 1991 and 1992	Unitless	1 km
	Summer moisture index in 1989, 1990, 1991 and 1992	Unitless	1 km
6. Soil	Soil type	Unitless	30 m
7. Fire attribute	Fire severity	Unitless	30 m

It can be difficult to understand the functional relationship between predictors and an outcome when using ensemble-based prediction methods such as random forests. In this study, we use partial dependence plots to describe a predictor's contribution to the fitted model. The partial dependence plots are graphical visualizations of the marginal effect of a given variable on the response variable (Friedman et al. 2001). We used the partialPlot function in R package randomForest (Liaw and Wiener 2002) to produce partial dependence plots for most important predictor variables and further discussed the influences of these variables on post-disturbance forest recovery in the YNP.

4.4 Results

4.4.1 Accuracies of the Forest Recovery (RNR) maps

The VCT RNR maps had overall accuracies of ~80% for different disturbance and forest types. In general, these accuracies were consistent among different disturbance types (Table 2) and forest types (Table 3), although recovery detection over harvested areas was slightly more accurate than over burned areas. Errors were mainly associated with pixels that were classified as non-recovered by VCT but had tree cover > 10% by 2011 (0.13 for fire disturbances and 0.12 for harvests).

Table 4- 2 Validation accuracy of VCT (a) post-fire and (b) post-harvest regeneration product for all forest species in GYE

(a) Post-fire recovery validation results

		Reference			
		Recovered (tree cover>10%)	Non-recovered (tree cover <= 10%)	Row total	User's Accuracy
Map	Recovered	0.19	0.07	0.26	0.75
	Non-recovered	0.13	0.61	0.74	0.82
	Column total	0.32	0.68	1.00	

	Producer's Accuracy	0.59	0.90		
	Overall Accuracy			0.80	

(b) Post-harvest recovery validation results

		Reference			
		cover>10%	cover <= 10%	Row total	User's Accuracy
Map	Recovered	0.69	0.02	0.71	0.97
	Non-recovered	0.12	0.17	0.29	0.58
	Column total	0.81	0.19	1.00	
	Producer's Accuracy	0.85	0.89		
	Overall Accuracy			0.86	

The species-level post-forest recovery validation reveals more information regarding the algorithm performance under different site and vegetation conditions. Based on the forest types before the 1988 fires, we validated the VCT post-fire forest recovery product for the GYE following the 1988 fires. Because there were insufficient samples for species-level harvesting, we did not analyze post-harvests for the GYE by forest type. Error matrices at the species level (Table 3) for the post-fire forest recovery reveal that the VCT has the highest producer's accuracies for the non-recovered class, ranging from 92% to 98% across all forest types. For the dominant Lodgepole Pine forests in YNP, the user's accuracy and overall accuracy of the VCT recovery product by year 2011 varies from 78% to 94%. Although the User's accuracy for the recovered class is less than 20%, the overall accuracy for Whitebark Pine forests remains over 85%, suggesting (1) that the majority of burned Whitebark Pine pixels have not recovered from the fires and the overall accuracy of Whitebark Pine forest recovery product relies heavily on the classification accuracy of the non-recovered class, and (2) that improvements are needed for the VCT algorithm to accurately track sparse and bright forest ecosystems at high elevations, such as the Whitebark Pine ecosystem.

For less common forest types, such as Douglas-fir, Engelmann Spruce and Subalpine Fir, the VCT also shows consistent accuracies for the rest of the YNP forests. The overall and user's accuracies for both forest types fluctuate by approximately 80%, with the main source of error stemming from omission errors for the recovered class. These results show that the VCT has high accuracy for the 'non-recovered' class but omits certain pixels that have already recovered from the fires, based on our forest definition discussed above.

Table 4- 3 Validation accuracy of VCT post-fire forest regrowth product for four major forest species in YNP

(a) Lodgepole Pine (72% in area)

		Reference			
		cover>10 %	cover <= 10%	Row total	User's Accuracy (%)
Map	Recovered	0.28	0.02	0.30	0.94
	non-recovered	0.15	0.55	0.70	0.78
	Column total	0.43	0.57	1.00	
	Producer's Accuracy	0.65	0.97		
	Overall Accuracy			0.83	

(b) Whitebark Pine (15% in area)

		Reference			
		cover>10 %	cover <= 10%	Row total	User's Accuracy (%)
Map	Recovered	0.01	0.04	0.05	0.18
	non-recovered	0.08	0.87	0.95	0.92
	Column total	0.09	0.91	1.00	
	Producer's Accuracy	0.11	0.95		
	Overall Accuracy			0.88	

(c) Douglas-fir (7.1% in area)

		Reference			
		cover>10 %	cover <= 10%	Row total	User's Accuracy (%)
Map	Recovered	0.17	0.04	0.22	0.80
	non-recovered	0.19	0.59	0.78	0.75
	Column total	0.37	0.63	1.00	
	Producer's Accuracy	0.47	0.93		
	Overall Accuracy			0.76	

(d) Engelmann spruce and subalpine fir (5.9% in area)

		Reference			
		cover>10 %	cover <= 10%	Row total	User's Accuracy (%)
Map	Recovered	0.03	0.02	0.05	0.68
	non-recovered	0.15	0.80	0.95	0.84
	Column total	0.18	0.82	1.00	
	Producer's Accuracy	0.18	0.98		
	Overall Accuracy			0.84	

4.4.2 Recovery patterns across ownership, disturbance type, and forest types in GYE

Spatial patterns of forest recovery were summarized and analyzed following all disturbances occurring in the GYE before 2000 to allow enough time for forest recover to occur (Figure 5). The Global Moran's I value of the forest recovery map by year 2011 was 0.55, indicating that the forest recovery was highly clustered across the GYE. The main cluster of forest recovery in the GYE is distributed centrally around the boundary of Yellowstone National Park and Caribou-Targhee National Forest, where both large fires and intensive harvests occurred in the 1980s. For the 1988 Yellowstone Fire, this recovered clustering is largely located at lower elevations (<2300 m) where the growing season is longer and productivity is higher. Over 80% of the higher-elevation (>2300 m) burned area in Yellowstone National Park has not recovered from the 1988 fire. Post-fire forests in the national forests appear to have grown back faster than those in the national parks and wilderness area.

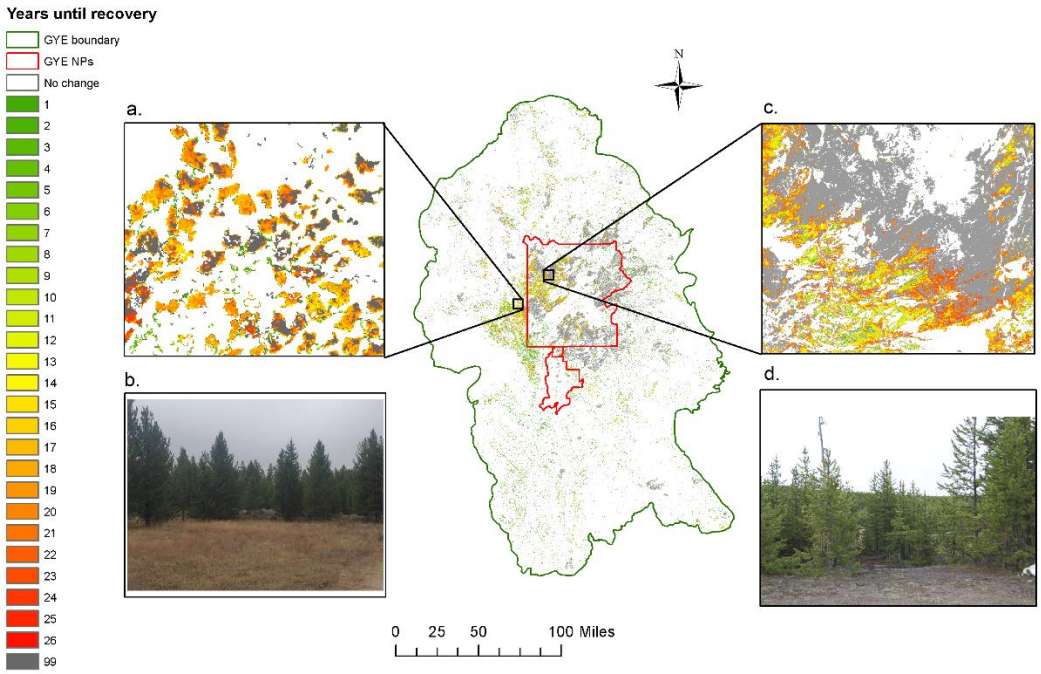

Figure 4- 4 GYE forest recovery maps and field photos. Time for recovery shows the number of years it takes for a pixel identified as forests after disturbance events by VCT time series recovery product. Grey color is the non-recovered area by 2011. Map a. and photo b. show an example of forest recovery which followed harvesting events in the Caribou-Targhee National Forests (near the boundary of YNP) in the 1980s. Map c and photo d show an example of forest recovery from YNP 1988 fires. Photo b and d show the current forest condition in the post-harvest and post fire site, and were taken on September 22, 2013 and May 17, 2014, respectively

Temporal patterns of forest recovery in the GYE were computed and summarized by disturbance type (Figure 6). Fires in the GYE are primarily infrequent high-severity fires with fire intervals ranging from 50 to 300 years (Turner et al. 2003; Westerling et al. 2011). We summarized the percent of forest recovery following two major fire years (year 1988 and year 1997) by land ownership in the GYE. The year 1988 represents a catastrophic fire year, whereas the year 1997 represents a relatively small fire year in the 1990s era. Although many fire years occurred in the 2000s, the recovery times following these fires were too short to show a forest recovery trend. The long-term forest recoveries following the fires by

ownership (Figures 6a and 6b) reveal that the post-fire forest recovery differed between the two fires years, and a longer recovery period did not necessarily result in higher recovery rates. After more than two decades of recovery, the percent of forest burned in 1988 that returned to forest by the year 2011 is quite low, even lower than the forest recovery rates by 2011 following the 1997 fires (Figures 6a and 6b).

The long-term GYE forest recovery trend also differs by ownership. Given the inherent differences in natural environmental conditions, forests on national forest land generally have longer growing season and grow back faster than forests in national parks and wilderness areas. During the two decades following the catastrophic fires in 1988, national forests consistently had higher values of forest recovery than national parks and wilderness areas. Despite the short-term similarity to the wilderness areas in the first few years after the 1997 fires, forest recovery in the GYE national forests rapidly outpaced the rest of the GYE forests.

(a)

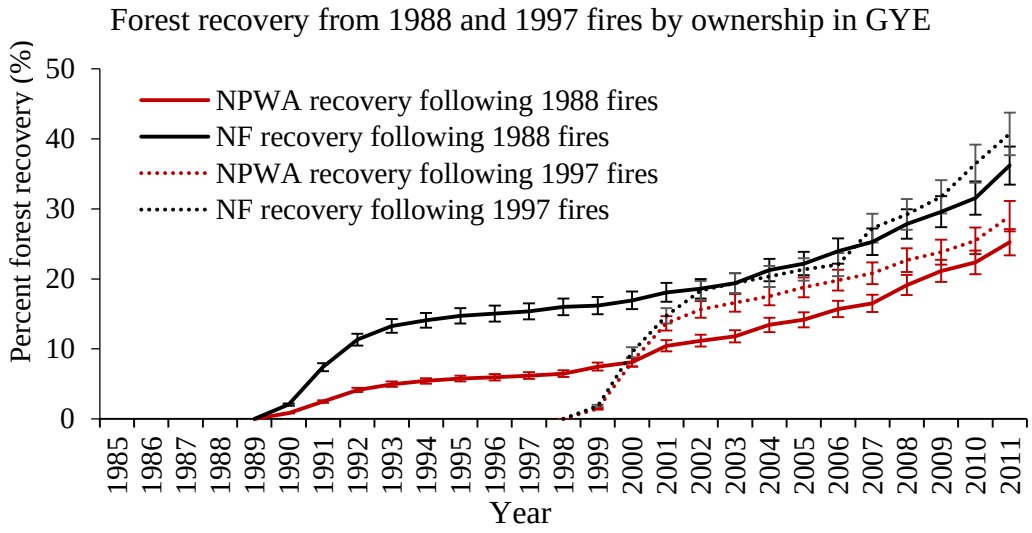

(b)

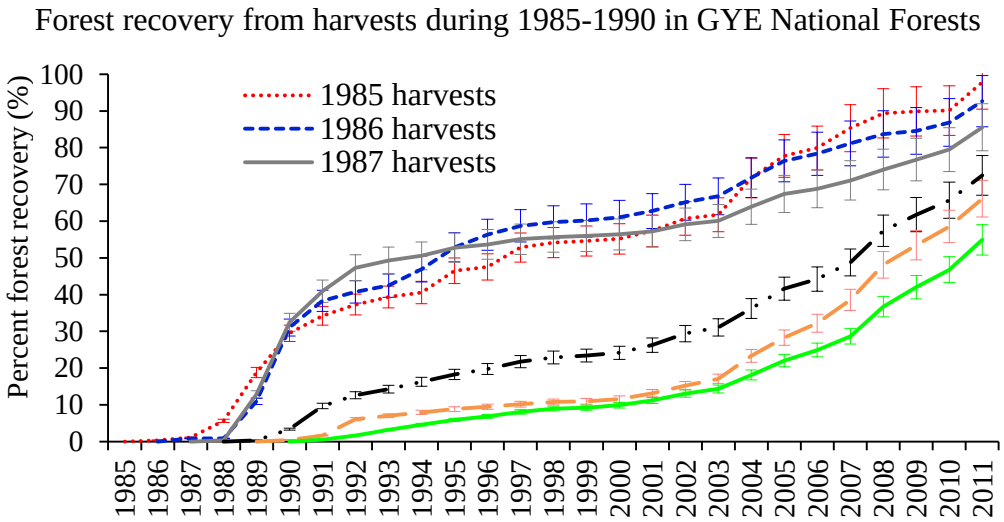

Figure 4- 5 Temporal patterns of forest recovery in GYE by disturbance type. (a) Percentages of forest recovery by ownership following fires in 1988 in GYE. Long term (>10 years) forest recovery rates were highest on National Forests lands, followed by National Parks and Wilderness Area. (b) Percentages of forest recovery by ownership following fires in 1997 in GYE. (c) Percentages of forest recovery following major harvesting years (1985 to 1990) in GYE National Forests (Wilderness Area excluded). The slope of the cumulative proportion charts indicates rates of recovery. Percentage of forest recovery was calculated by dividing the number of recovered pixels in the year 2011 (numerator) by the total number of disturbed pixels (denominator). Error bars are 1 standard error.

The recovery of the forests following major harvesting years in the GYE NFs (1985-1990, Figure 6c) exhibits the following trends. (1) The percentage of forest that recovered from a harvest in the GYE by year 2011 generally depends on the year of the harvest, and the recovery trajectory can be grouped into two recovery periods, before the late 1980s (the earlier years) and the late 1980s. (2) For harvests in the earlier years (1985 to 1987), over 85% of the harvested area has returned to forest by 2011. Harvests that occurred in late 1980s (1988 to 1990) have lower percentages of forest recovery than the early years, and the recovery trajectories differ between the

two time periods. (3) For the earlier harvest period, two rapid recovery intervals occurred in the early 1990s and mid-2000s. In contrast, for the late 1980s harvesting period, the average recovery speed was slow for the first 15 years after the harvest, followed by rapid regrowth over the last decade.

Among different disturbance types, post-harvest forest recovery rates are consistently higher than post-fire forest recovery rates in the GYE. The percentages of forest recovery reach 50-90% following the 1980s' harvests, whereas the highest percent of forest recovery following the 1988 fires is less than 40% by the year of 2011. Even only considering the national forest land, post-harvest forest recovery rates (72% for harvests that occurred in 1988) are still much higher than the post-fire forest recovery rates (36% for fires that occurred in 1988) by year 2011. Further investigation into the potential causes of different forest recovery rates among different ownership and disturbance types is discussed in the following sections.

4.4.3 Recovery patterns along environmental gradients in Yellowstone National Park

An examination of the recovery percentages of major forest types in YNP following the 1988 fires (Figure 7b) shows that Whitebark Pine, Engelmann Spruce and Subalpine Fir at higher elevations have very low recovery percentages (less than 10%). Lodgepole Pine has the highest percent of forest recovery by 2011 (more than 30%), followed by Douglas-fir with more than 25% of the forest having recovered from the 1988 fires.

(a) (b)

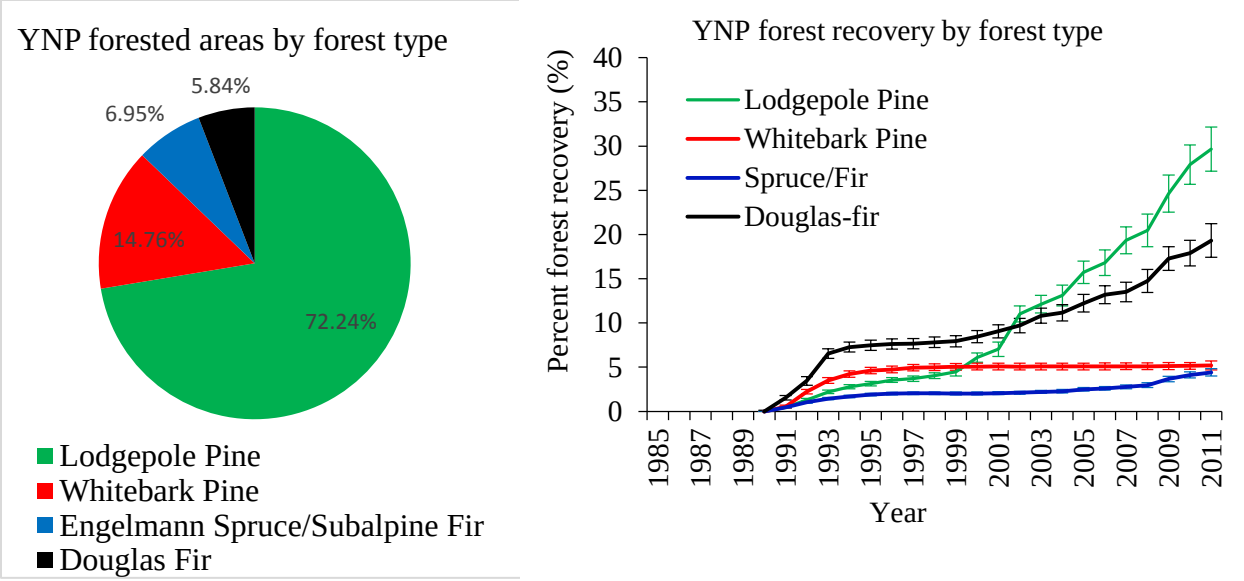

Figure 4- 6 Forest species and recovery in Yellowstone National Park (a) Forested area by forest type in Yellowstone National Park (before the 1988 fires); (b) YNP forest regrowth after the 1988 fires stratified by major forest types. Forest type map was developed before the 1988 fires. Error bars are 1 standard error.

The Random Forest OOB error rates for all major species range from 4.5% to 18.2%, revealing a high prediction accuracy for modeling the impact of environmental variables on forest recovery conditions for the major forest types following the 1988 fires in YNP (Table 4). High-elevation Whitebark Pine and Spruce/Fir forests have the lowest OOB rates, i.e., 4.5% to 5.4%, whereas Lodgepole Pine and Douglas-fir have higher OOB rates, i.e., 13.4% to 18.2%.

Forest distributions in YNP generally are generally related to elevation and soil gradients, which also play important roles in predicting YNP forest recovery rates following the 1988 fires (Table 4). Using the stepwise ascending variable selection method, the most important variables have been selected to demonstrate the effects of environmental parameters on the binary forest regrowth conditions. The results suggest that topography (elevation and aspect) and post-disturbance climate play critical roles in the recovery of all four major forest species by 2011 in YNP.

Table 4- 4 Random Forest (RF) modeling results for major forest types in YNP. The out of bag error rate was derived from RF modeling with Response Variable: Recovered or non-recovered by year 2011.

Forest Type	Out of Bag Error Rate (%) for Response Variable	Most important predictor variables
Lodgepole Pine	18.2%	Soil type, post-fire spring precipitation anomaly, Slope, Elevation, Northness
Whitebark Pine	5.4%	Northness, Elevation, Slope, Eastness, Soil type
Douglas-Fir	13.4%	Northness, Slope, Eastness, Elevation, Soil type
Engelmann Spruce /Subalpine Fir	4.5%	Soil type, Northness, Eastness, Slope, Elevation

(a)

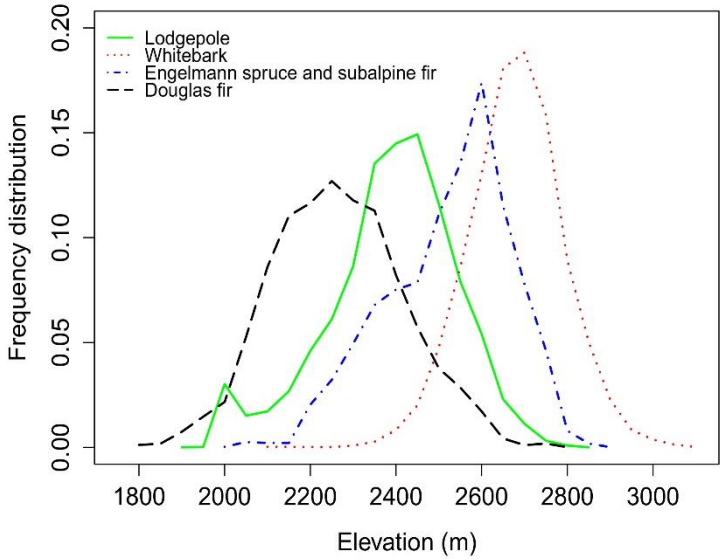

(b)

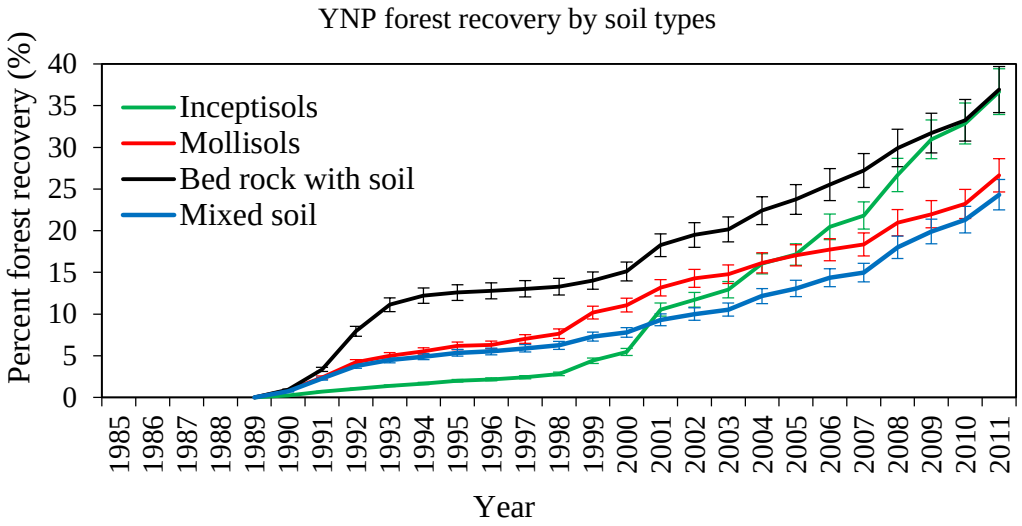

Figure 4- 7 Distributions of common tree species with the elevation gradient before 1988 fires and percentages of forest recovery with soil types after 1988 fires in YNP. (a) Elevation. Engelmann spruce and subalpine fir is found in the subalpine zone, but at the upper end of this zone, Whitebark pine is dominant. Below the subalpine zone lies the montane zone, co-dominated by Douglas-fir (*Pseudotsuga menziesii*) at the lowest elevation zone, and Lodgepole Pine (*Pinus contorta*). Lodgepole Pine occurs over a broad range of elevations and survives on drier, more exposed slopes with relatively poor substrates; (b) Soil type. Inceptisols and bed rock with soil are the main substrates that support the Lodgepole Pine stands; while the other forest types such as Whitebark Pine, Engelmann Spruce and Subalpine Fir, and Douglas-fir mostly grow on nutrient rich Mollisols and mixed soils. Error bars are 1 standard error.

We further examined the most important predictors for forest recovery between the 1988 fires and 2011 in YNP (Figures 8 and 9). Due to its spatial predominance in YNP (over 72% of YNP's forested area), the Lodgepole Pine forest was selected for additional analysis. The five most important predictor variables were identified via the stepwise elimination approach: soil type, post-fire spring precipitation anomaly, slope, elevation, and northness. The impact of elevation on forest recovery in YNP (Figure 8a) is evident in the significantly lower recovery rates of Whitebark Pine, Engelmann Spruce and Subalpine Fir, which are located at higher elevations than Lodgepole Pine and Douglas-fir. The percentages of forest recovery

for these higher-elevation forest types are approximately one-third those of the lower-elevation species. Soil also plays an important role in post-fire forest recovery, mainly because of the unique biophysical environment in YNP. The shallow and nutrient-poor Inceptisol and bedrock soils can only support Lodgepole Pine forests, a fire-dependent and fast-growing species, and these soils were associated with the highest percentages of forest recovery by 2011. The other forest types, especially Engelmann Spruce and Subalpine Fir, usually grow in relatively deep and nutrient-rich Mollisol soils.

After the most relevant variables were identified, partial dependence plots of the four continuous variables (Figure 9) were used to determine the relationships between these environmental conditions and the post-fire recovery of the Lodgepole Pine forest in YNP. The post-fire spring precipitation anomaly and northness factors generally had a positive impact on Lodgepole recovery after the 1988 fires, meaning sites with higher post-fire spring precipitation anomalies and sites that faced true north tended to recover faster. The number of years needed for Lodgepole Pine recovery exhibits more non-linear piecewise dependencies on slope and elevation. From 15 to 25 degrees, the number of years until recovery is strongly dependent on the slope and decreases with increasing slope. In the elevation range of 2200 to 2500 meters, the time required for recovery is strongly dependent on elevation and increases with increasing elevation.

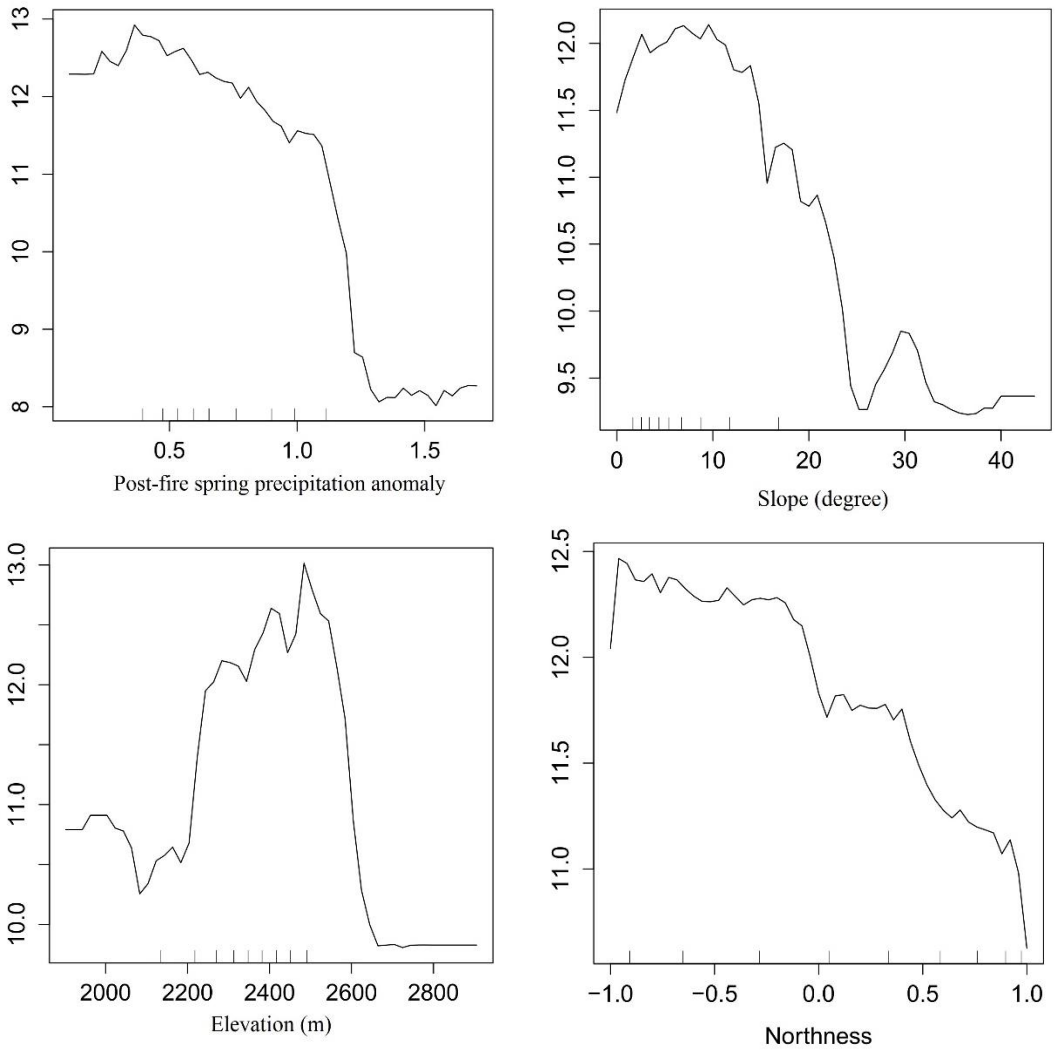

Figure 4- 8 Partial dependence analyses for variables affecting post-fire recovery of Lodgepole Pine forests. X axis shows the variable analyzed and the corresponding unit. Y axis show the number of years for the disturbed area to recover to forests. Post-fire spring precipitation anomaly shows the departure of precipitation in the spring following the fire from the 30-year mean spring precipitation values. Northness equals sin (aspect), a unitless value to show if the aspect is north-facing, value of 1 is true north and -1 is true south.

4.5 Discussions and Conclusions

Studies of disturbance events in the GYE forest catalyzed recognition of the importance of large-scale disturbances and regrowth as key drivers of carbon fluxes in terrestrial ecosystems. The disturbance and regrowth patterns in the GYE underscored the importance of environmental variables (such as substrate and

topography) in ecosystem responses to disturbance. This study assessed the usefulness of time series composed of Landsat images and the VCT in tracking post-fire and post-harvest forest regrowth in the GYE. The VCT algorithm was found to be effective in tracking forest recovery through time in the GYE.

4.5.1 Challenges in time series forest recovery mapping

The VCT algorithm recorded a total of 5,341 km^2 of fire disturbances and 953 km^2 of harvesting in the GYE forests from 1985 to 2011 (Figure 4-2). A comparison with point-based interpretations from TimeSync showed that the VCT fire detection was highly reliable, with a user's accuracy of 96% and a producer's accuracy of 73% (Zhao et al. 2015a). The VCT's detection of high- and moderate-severity fires is highly successful, and most of the omission errors were from low-severity fires. The accuracy of the estimated forest loss due to harvesting was also high, with a user's accuracy of 91% and a producer's accuracy of 89% (Zhao et al. 2015a).

Certain uncertainties and limitations are present in the study. Insufficient data, limited mapping capabilities and inadequate scientific understanding of the complex interactions between natural phenomena may have generated uncertainty in this study. With proper quality control in the validation process, the uncertainties in this assessment are limited to the biophysical map input and the methods related to forest regrowth modeling. The known limitations of this approach include the following: 1) the VCT algorithm is not sensitive to low-severity disturbances and may miss some low-intensity forest loss (Thomas et al. 2011; Zhao et al. 2015a) and 2) the coarse spatial resolution of the climate and topographic data limited our ability to link forest regrowth with finer environmental gradients.

The VCT algorithm was able to accurately capture forest recovery at the regional level, but there are still certain issues to solve at the species level. For dominant species at moderate elevations, such as Lodgepole Pine and Douglas-fir, the performance of the algorithm is consistent and reliable. However, the algorithm might need to be adjusted for high-elevation forest types, such as Whitebark Pine, Engelmann Spruce and Subalpine Fir, because of the different forest structure and spectral characteristics of the high-elevation forest ecosystems.

4.5.2 Spatial and temporal pattern analysis of forest recovery in GYE

In the GYE, forest recovery trends vary from one forest type to another. This mainly has to do with species-specific regrowth attributes. Lodgepole Pine and Aspen are fast-growing species that usually occupy lower elevations and may grow back in 5 - 20 years after a stand-clearing disturbance (Alexander 1974; Alexander and Edminster 1980). Forests that grow at higher elevations, such as Whitebark Pine, Engelmann Spruce and Subalpine Fir, usually take longer to recover (Alexander 1974).

Forest recovery trends in the GYE also differ between various land ownership and disturbance types. The post-harvest forest recovery in national forest land is generally faster than the post-fire forest recovery in both national parks and national forests, likely due to the following reasons. 1) Land productivity in national forests is generally higher than that of the national parks and wilderness area (Hansen et al. 2000). Most fires occur at high-elevation low-productivity sites with shorter growing seasons, whereas harvested sites generally have longer growing seasons and higher site productivity. 2) Post-harvest forest management activities helped increase forest

recovery rates in the national forests. In addition to other forest management techniques used to aid forest grow, planting is a common practice in GYE national forests, especially for harvested forests after natural regeneration fails. 3) The post-disturbance forest recovery in national parks and wilderness areas is subject to threats from various wild animals, insects and diseases, and national forests usually have higher levels of protection against these factors.

Forest recovery rates following fires in different years can vary based on different regeneration conditions, such as seed availability and post-disturbance climate conditions (Savage et al. 1996; Wijdeven and Kuzee 2000). By 2011, the forest recovery rates following the 1988 fires were lower than those of the 1997 for national parks, wilderness areas and national forests. Several potential contributing factors include the following. 1) Seed bank availability is lower for mega fires; therefore, the large burned areas in 1988 required a longer time to recover than the smaller fires in 1997. 2) The three-year mean annual precipitation following the 1988 fires (205 mm) was much lower than that following the 1997 fires (249 mm), producing less ideal conditions for forest regeneration.

Spectral recovery tends to occur fairly quickly (within 5-15 years depending on the forest type), and even low biomass levels may lead to IFZ values comparable to those of mature forests (Huang et al. 2010). For both post-fire and post-harvest forest recovery, we see gentle spikes of forest recovery in the first decade following the disturbance. This immediate increase in forest recovery could be caused by the following reasons: 1) the quick recovery of understory grass and shrubs that increases forest indices to levels close to the forest level and/or 2) the failure of low- and

moderate-severity fires to kill all the trees; the survivors then green up in the following years, saturate the spectral information, and trick the algorithm into labeling the pixel as recovered. However, during the validation process, we noticed that over 80% of the validated 'no-recovery' plots have sparse saplings growing back, but not to the level that can be detected at a resolution of 30 meters. The saplings within 1 Landsat pixel are either too small or too sparse to be detected at the pixel level. The density of small saplings also decreased with decreasing growing season and water availability and also varied with elevation and slope aspect.

Although the spatial and temporal patterns of forest recovery in the GYE vary by forest types, the dominant variables are similar across the study region: topography and post-disturbance climate. The effects of topography on forest distribution and forest recovery are manifested by changes in temperature and water availability (Marston and Anderson 1991). Previous studies demonstrate that the climate conditions in the first few years following the disturbances are critical for forest regrowth patterns in future decades. This theory might help explain the different temporal trajectories of forest regrowth following the harvests in 1985-1987 and 1988-1990.

Fire severity has been suggested to have substantial effects on early post-fire plant cover and species richness in Yellowstone National Parks (Turner et al. 1999; Turner et al. 1997). Our results reveal that fire severity did not show significant impact on long-term forest recovery by the year 2011, whereas the effects of environmental variations were more pronounced (Franks et al. 2013; Turner et al. 2003). Earlier field-based studies in Yellowstone National Park suggested that the

abundance and spatial distributions of surviving trees and seedlings may be the pivotal factors determining early forest regrowth following disturbances (Turner et al. 1998). Our results show that abiotic factors, such as topography and post-fire climate conditions, have a dominant effect on the long-term post-fire forest recovery in the GYE.

4.5.3 Conclusions

In summary, the results from this study underscore the ability of the VCT algorithm to monitor large-scale time series data on forest recovery associated with multiple disturbance types. Based on the temporal and spatial consistency, we characterized the temporal forest recovery history in the GYE using the VCT forest recovery data. We analyzed the spatial and temporal forest recovery trends in the GYE with respect to different land ownership (management regimes), disturbance types, and forest types. We also assessed the impact of environmental conditions, such as topography and climate, on post-disturbance forest recovery using a machine learning modeling approach. With the public availability of VCT disturbance and recovery products nationwide, this approach can be applied to other regions of the U.S. for many other monitoring and management purposes.

Chapter 5: Quantifying the Impact of Forest Management and Disturbances on carbon Dynamics in Greater Yellowstone Ecosystems

5.1 Introduction

Forest carbon stocks and fluxes are important components of the global carbon cycle, and estimating the variables provides for accounting of land sink of the atmospheric CO_2 (Canadell and Raupach 2008; Pan et al. 2011). With increasing interests in quantifying greenhouse gas emissions and potentially managing forests to increase the rate of CO2 sequestration, there are urgent needs to quantify current patterns of forest carbon stocks and fluxes, especially as they relate to forest management and natural disturbances(Magnani et al. 2007). Forest carbon sequestration is increasingly recognized as an ecosystem service and has been included among indices of sustainability and in modeling studies that seek to examine interactions among multiple ecosystem services.

US's national park system began over 140 years ago (Everhart 1972). Several national parks and wilderness were established in the Greater Yellowstone Ecosystem (GYE) between 1872 and 1976 (Clark et al. 1991). As mandated by the U.S. National Parks Act in 1872, maintenance of ecological integrity has become the first priority of the U.S. National Park Service (Everhart 1972). More recently, the potential contribution of these parks to climate change mitigation has become a question of policy and management interest. Protected areas are recognized worldwide as being important components of climate change mitigation and adaptation strategies because

of their governance structures, permanence, and management effectiveness (Soares-Filho et al. 2010). It is not clear, however, how forest C dynamics differ between forests managed for sustainable timber harvest versus those protected for conservation, particularly when both are subject to natural disturbances.

Numerous modeling efforts have been made to quantify the impact of forest fire and harvest on plot-, regional-, national- and global-scale C dynamics (Bond et al. 2005; Caspersen et al. 2000; Girod et al. 2007; Hurtt et al. 2002; Liu et al. 2011; Turner et al. 2015). Many modeling tools use either hypothetical landscapes or generalized conditions on real landscapes to infer carbon dynamics in forested ecosystems (Chen et al. 2000; McGuire et al. 2001; Running and Hunt 1993). Recent advances in remote sensing of vegetation condition and change (Huang et al. 2010; Kennedy et al. 2010b; Zhu et al. 2012), along with new techniques linking remote sensing with inventory records, have allowed investigations that are much more tightly constrained to actual landscape conditions. For example, these new capabilities are built into the Forest carbon Management Framework (ForCaMF), which is being used by the National Forest System to not only model, but to monitor across very specific management units, the impact of different kinds of disturbance on carbon storage.

The objective of this study is to quantify the effects of forest disturbances (natural and anthropogenic) on carbon dynamics in GYE. A Landsat based automated time series analysis of forest disturbances (Vegetation Change Tracker, VCT) and a forest inventory based C modeling approach (ForCaMF) were used to explore temporal patterns of ecosystem C dynamics in different ownerships in GYE. The

simulation approach incorporates spatial information on forest type, initial forest C condition, disturbance type and magnitudes, and forest C responses to management and disturbances were modeled from forest inventory and a growth and yield model (Forest Vegetation Simulator). We also provided detailed uncertainty assessment including both population level sampling error and pixel level map accuracies.

5.2 Study Area

The 91758 km^2 study area of the GYE region includes the Yellowstone (YNP) and Grand Teton National Parks in the center, seven surrounding National Forests, 21 other federal and state jurisdictions areas, and relatively few private lands (Figure 5-1). The national parks are at relatively high elevations, centered on the Yellowstone Plateau and surrounding mountain ranges. National Forests lands are largely at mid-elevations on the flanks of the plateau.

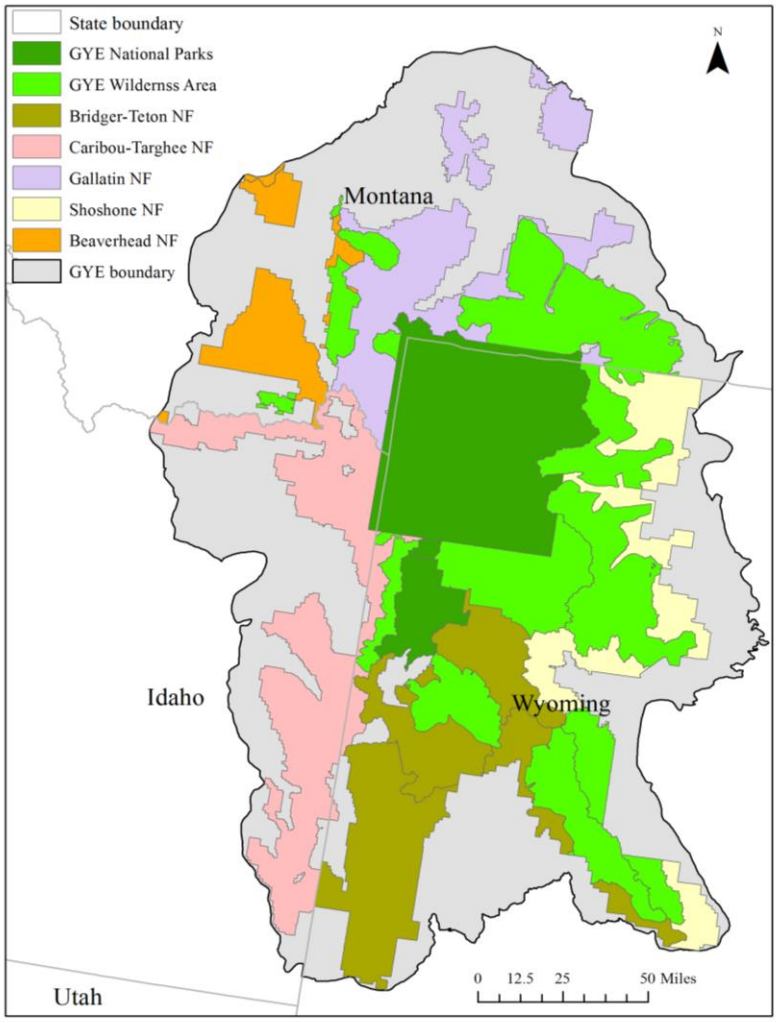

Figure 5- 1 Forest ownership over the GYE study area. National Parks locate in the center with dark leaf green color; Wilderness area are light green color area surrounding the National Parks. The rest colors are National Forest area excluding Wilderness Area, with the Bridger-Teton National Forest in Olivine green, Caribou-Targhee National Forest in soft pink, Gallatin National Forest in light purple, Shoshone National Forest in light yellow and Beaverhead-Deerlodge National Forest in orange color.

The GYE features distinct gradients in elevation, climate and soil. Elevation played a key role in affecting the vegetation distribution in GYE, but its effects are manifested by influences on temperature and moisture availability (Martson and Anderson 1991). Mean annual temperature varies from 7.6 ℃ at lower elevations (< 1400m) to 0.13 ℃ at higher elevations (> 2300m) (Hansen 2000). Much of the

precipitation falls as snow and generally increases with elevation, and mean annual precipitation ranges from 1368mm to 2414mm (Martson and Anderson 1991). The growing season varies from two to three months at higher elevations to five to six months at lower elevations. A large portion of National Parks is distributed in relatively high elevations, centered on the Yellowstone Plateau and surrounding mountain ranges. National Forests' lands are mostly at mid- and low-elevations on the flanks of the plateau. Soils at higher elevations are largely nutrient poor rhyolites and andesite with low water-holding capacity (Marston and Anderson 1991). Valley bottoms and floodplains contain glacial outwash and alluvium soils that are generally higher in nutrients and water-holding capacity in relative terms (Hansen 2000).

Natural forest vegetation in the study area is a mosaic of major coniferous species. Lodgepole Pine was wide spread in YNP before year 1988 and dominated over 70% of the forested NP area (about 5295 out of 7355 km^2), followed by Whitebark Pine, Engelmann Spruce/Subalpine Fir and Douglas-fir. Whitebark Pine occupies about 15% of the YNP forested area, especially at the higher elevations. Engelmann Spruce and Subalpine Fir often co-exist below the elevation zone of Whitebark Pine, with Douglas-fir dominate the lowest elevations. Upland rhyolite soils support lodgepole pine (*Pinus contorta*) forests between 2000 and 2600m; Douglas-fir (*Pseudotsuga menziesii*) is common up to 2300m on andesitic soils and in warmer microclimates. Above these elevations on both of the soil types, subalpine fir (*Abies lasiocarpa*), Engelmann spruce (*Picea engelmannii*), and whitebark pine (*Pinus albicaulis*) dominate. The majority of the GYE forested area located in National Forests (~80% of GYE forested area), which contains Wilderness Area

designated by Wilderness Act of 1964 (~22% of GYE forested area) and the rest is managed for timber production (~47.7% of GYE forested area). National Parks occupy about one-fifth of GYE forested area and the rest forests are under other ownership such as State forest or private forest.

The recent history and composition of disturbance events also show an ownership pattern during the study interval (1984-2011, Figure 5-1(b)). In GYE National Parks and Wilderness Area, fire was the most dominant disturbance agent, affecting over 37% of the forested area in GYE National Parks. However, active harvest events occur in the National Forests. In particular, harvested area in the Caribou-Targhee National Forest was four times of burned areas during the study period (Zhao et al. 2015a).

5.3 Methods

5.3.1 Overview

This paper aims to model forest carbon dynamics by integrating forest inventory, time series satellite images and carbon modeling in the Greater Yellowstone Ecosystems (Figure 5-2). Baseline C condition starts from year 1984 and we tracked the effects of major management and disturbances (such as timber harvests and wildland fires) on C dynamics in GYE. Our carbon dynamic analysis focused on three terms: (1) total forest carbon storage excluding soil carbon, (2) carbon removal by forest fires, harvests and insects, and (3) total forest carbon fluxes (carbon flux in year y = carbon storage in year y– carbon storage in year y-1). Estimates for each of these three terms were made for each year of the 1985-2011 time periods.

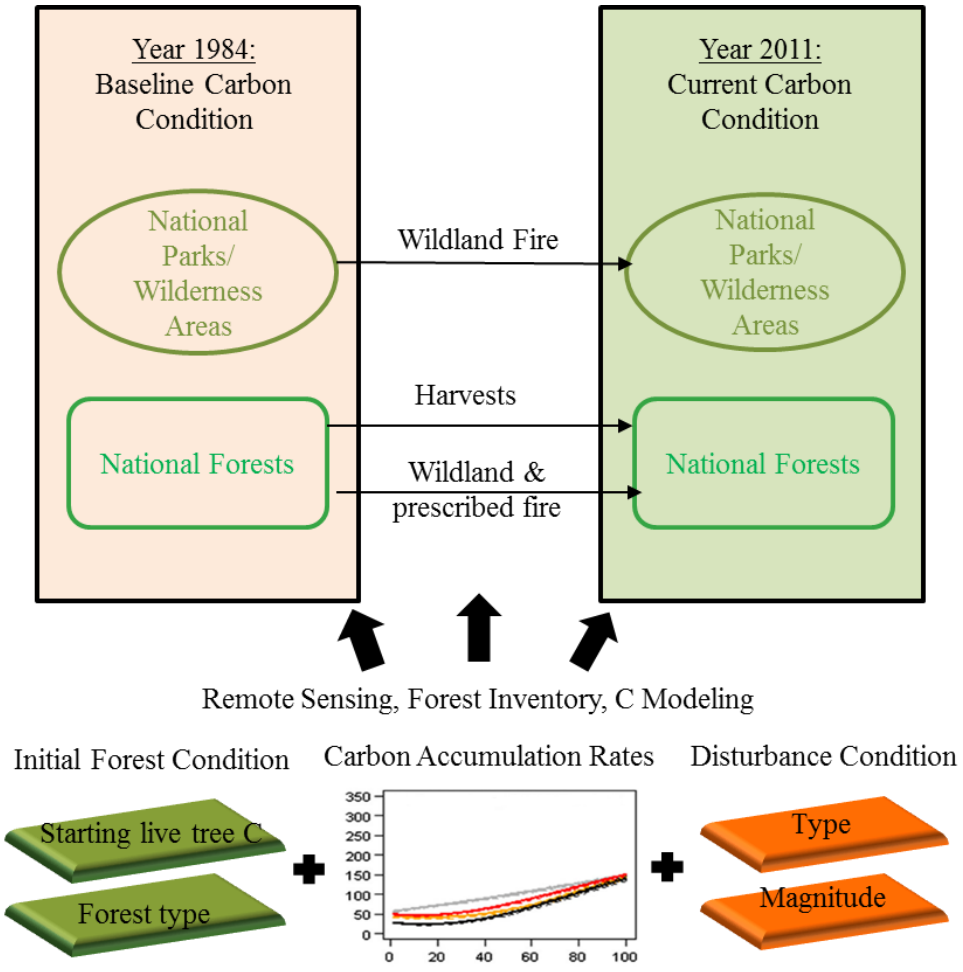

Figure 5- 2 Conceptual model for analyzing impact of management and disturbances on C dynamics in GYE.

We took five steps to model the carbon dynamics in the study region: (1) mapping initial forest carbon condition and forest change history in GYE using time series remote sensing data, including disturbance types and magnitudes. We conducted robust validation and calculated the map accuracies; (2) calculating average carbon accumulation rates from forest inventory data for major forest type groups. We created difference carbon accumulation curves for each disturbance scenario and starting volume condition, and used standard error as the uncertainty of the data; (3) generating simulation units to increase computation efficiency. Pixels of

the same forest type, initial volume and disturbance scenarios were grouped together for simulation; (4) computing threshold values from forest inventory data. We queried forest type group composition, error and forest carbon bin error from all FIA plots within the study area; (5) simulating time series carbon storage change using the ForCaMF model and effects of management and disturbances. Average carbon accumulation curves, simulation units, input data uncertainties and threshold value from the forest inventory data.

5.3.2 ForCaMF carbon model

ForCaMF was designed for use in the US to determine the relative impact of disturbance, growth, and management upon the amount of carbon stored in forested landscapes over time (Healey et al. 2014). ForCaMF may be described as an accounting system which, given categorical Landsat based maps of starting vegetation conditions and subsequent disturbances, applies regionally average carbon dynamics to track carbon storage or release at the pixel level. As pixel level carbon stores are summarized to the landscape level to provide landscape level insights, ForCaMF uses a Monte Carlo framework to vary the input map class values used to associate each pixel with particular carbon storage trajectories. Resulting variance in carbon storage model outputs provides an integrated, empirical measure of uncertainty.

ForCaMF tracks carbon accumulation for an individual map unit based upon mapped starting conditions and subsequent disturbances. Landsat-based maps of historical volume (binned into 4 classes) and forest type are used to assign each pixel to an appropriate initial carbon “trajectory”. This trajectory indicates the regionally

average annual change in the sum of major non-soil forest carbon pools: above- and below-ground live and standing dead trees; down dead wood; shrubs; herbs; litter and duff. Production and validation of vegetation and disturbance maps are discussed in the following sections. Trajectories are specific to mapped forest type and binned starting volume classes within different disturbance scenarios. In GYE, there were 7 major forest type groups: Lodgepole Pine, Whitebark Pine, Douglas-fir, Engelmann Spruce, Subalpine Fir, Aspen/Birch, and Other Western Softwoods.

5.3.3 Mapping forest ecosystem change dynamics

A series of pixel-based map is developed to identify areas where trajectories of undisturbed growth are interrupted by events such as fires, harvests and pests. We mapped initial carbon condition and forest ecosystem change dynamics, including disturbance types and magnitudes, with both Forest Inventory Analysis data (FIA) and Landsat Time Series Stack (LTSS) from 1984 to 2011. For Landsat image pre-processing, we applied the Landsat Ecosystem Disturbance Adaptive Processing System (LEDAPS) (Masek et al. 2006b) to ortho-rectify the images and convert pixel digital numbers to surface reflectance. To map initial carbon condition for GYE, we modeled the relationship between FIA based aboveground carbon values with environmental predictor variables following Powell et al. (2010) method.

We used Vegetation Change Tracker (VCT) algorithm (Huang et al. 2010) to track forest changes in LTSS and produce annual forest disturbance maps for GYE. Then we used Support Vector Machine (SVM) algorithm (Cortes and Vapnik 1995; Huang et al. 2002) to separate forest disturbance types such as fires and harvests following Zhao et al. (2015) approach.

In this study, we defined disturbance magnitude as changes in percent canopy cover. Four levels of disturbance magnitudes represent canopy cover changes from 0-25%, 25-50%, 50-75% and 75-100%. Percent canopy cover per hectare was calculated from FIA data and used as the response variable for modeling canopy cover change. Random Forest algorithm was used to model the canopy cover change over GYE, and predictor variables include Landsat spectral bands, vegetation indices, shortwave radiation and topography (Powell et al. 2010).

We validated forest disturbance and disturbance type maps using TimeSync platform (Cohen et al. 2010; Thomas et al. 2011; Zhao et al. 2015a). Forest disturbance magnitudes were validated in three steps: (1) we stratified random sampled 100 pixels from the magnitude map and created 5 by 5 grid lines within each sample pixel; (2) overlaid the 5 by 5 sampling grid with Google Earth high resolution images; (3) we counted the changes in pre and post-disturbance high resolution satellite images and determined the changes in percent canopy cover after the disturbance. We classified the disturbance magnitudes into four groups based on thresholds of 0-25%, 25-50%, 50-75% and 75-100%.

5.3.4 Average carbon accumulation rates

Average C accumulation rates serves as a key inputs for our C modeling approach (Healey et al. 2014). We quantified average C accumulation rates after each disturbance scenarios (no change, fire, harvest, and insects) in GYE using a growth and yield model, Forest Vegetation Simulator (FVS) (Dixon 2002). FVS is an extensively calibrated growth model that is widely used for management and planning within the National Forest System and is corporately maintained by the US

Forest Service. It is an individual-tree based, distance independent forest growth model, and it allows simulation of a wide range of management and disturbance processes. FVS uses Forest Inventory as input data and simulates forest growth and yield under different forest change scenarios. Unlike most biogeochemical process models, FVS simulated mixed species and uneven-aged stands, enabling detailed simulation of disturbance effects specific to tree species and size. One of FVS's outputs is carbon storage, broken into the pools mentioned above (Reinhardt and Crookston 2003).

A regionally average carbon trajectory is derived for every species and starting volume bin by combining data from the FIA field sample and FVS. All regional FIA plots are submitted to FVS using the appropriate disturbance keywords, simulating carbon densities at 5-year intervals over 100 years for either undisturbed growth or different intensities of harvests and fires. A python program was developed to translate the FIA database into inputs data for FVS modeling, simulate the effects of different disturbance types and model average C accumulation curves. We used all forested single condition inventory in GYE and produced average C accumulation rates following three steps (Raymond et al. 2015): (1) translate FIA plots into FVS inputs. We initiated FVS with a large dataset drawn from FIA's spatially balanced simple random sample. Thus, the average functions for C accumulation were representative of a wide range of pre-disturbance conditions; (2) simulate total stand carbon over time after different management and disturbance scenarios for all suitable FIA plots. By simulating the effects of three disturbance types with two levels of severity, we captured a wide range of responses in total forest C in terms of

disturbance type, severity and pre-disturbance forest conditions; (3) within each starting condition and disturbance history bin, equations are fit to all available projections. Equations are taken to be representative because simulations are based on field-measured tree lists gathered as part of FIA's simple random sample.

For GYE forests, we summarized and fitted average C accumulation curves, including seven major forest types (Lodgepole Pine, Whitebark Pine, Douglas-fir, Engelmann Spruce, Subalpine Fir, Aspen and Birch, and Other Western Softwoods). For each major forest type groups, we computed average C accumulation rates following 4 disturbance scenarios (no disturbance, fire, harvests and pests) and 4 disturbance magnitudes (0-25%, 25-50%, 50-75% and 75-100%). Final C accumulation rate results included the estimated annual C values in 100 years and the standard error associated with the values. The two files were fed into the C accounting program to provide growth functions for all potential growth and disturbance scenarios.

5.3.5 Producing simulation units to improve computation efficiency

To reduce the computational load of C simulations, we aggregated pixels with same forest type, initial volume, change scenario, and disturbance magnitudes into 10-hectare simulation units (about 111 30-meter pixels). A python based ArcMap tool was developed to generate simulation units file from a series of inputs maps including disturbance map, disturbance magnitude maps, initial carbon condition map, and forest type group map.

5.3.6 Computing constrain values for model simulations from inventory

To force model simulation results match ground measurements, we used forest type group percentage, initial C values and the associated errors derived from FIA data to constrain model simulations and calculate population level uncertainties (Healey et al. 2014). Since GYE is a relatively small and unified ecosystem, we derived one set of population level uncertainty around the mapped estimates for the forest type and starting volume map from FIA plots for the whole GYE.

For forest type group, we used the Evalidator[6] online query tool to calculate the proportion of each forest type and the standard error associated with the proportions in our study region. We took three steps to calculate the above variables from the FIA data: (1) queried the forest type group (choose "Forest Type Group abbr" for the column value) for the study area, and pasted the results in an excel sheet; (2) calculated the percent area of each forest type in the study area by dividing the area of the forest type by the total area of forested area; (3) calculated the standard error around these percentages by integrating the sampling error of the plots. We divided the sampling error area of the forest type (area of the forest type multiply the sampling error for that forest type) by the total forested area to get the sampling error for the whole landscape.

Processes for calculating constraint values for initial C conditions were relatively complex compared to forest type groups. We used FIA COND and TREE tables to query desirable plots and calculate initial carbon values. The FIA COND table contains information regarding to the general attribute of the plot, such as

[6] http://apps.fs.fed.us/Evalidator/evalidator.jsp

inventory year, forest condition, ownership, etc. In this study, we used forested plots with single forest conditions in GYE, meaning forest type is pure in these plots. We only included recent inventory to make sure the sampling methods were consistent among all plots. To calculate total aboveground carbon for each plot, we multiplied TPA_UNADJ field by CARBON_AG field in TREE table for each tree, summed up the trees by plot CN, and converted the unit to million grams per hectare. Then we calculated the distribution of these selected plots by the bin breaks of 25%, 50%, 75% and 100% percentiles. These bin breaks were also used in calculating the carbon accumulation curves and mapping initial carbon maps. The final step computed the standard error (Equation 5-1) around the proportions of each bin breaks.

$$\mathrm{SE}(\hat{p}) \quad \sim = \quad \sigma(\hat{p}) = \sqrt{\frac{p(1-p)}{n}} \qquad \text{Equation 5-1}$$

We used both forest type and initial C constraint values in our C modeling process to link remote sensing with inventory records, and compute C dynamics that are much more tightly constrained to actual landscape conditions.

5.3.7 Simulating carbon balance and uncertainty using ForCaMF

The Forest carbon Management Framework (ForCaMF) model was designed to apply regionally representative carbon dynamics to remote sensed forest dynamics pathways to identify the relative impact of management activities and natural disturbances upon landscape level carbon stocks (Healey et al. 2014). Specifically, these pathways are determined across the landscape through categorical Landsat-based maps of starting volume and forest type, coupled with the Landsat historical record of subsequent disturbances of different types and magnitudes.

Uncertainties associated with both inputs maps and population level errors were quantified by Monte Carlo simulations. The range of variation in the simulated output distribution is primarily constrained using information from the FIA, which can be used to estimate forest conditions and uncertainties at a range of scales. The standard error reported for FIA population estimates covering the entire landscape are used to determine how much variation in class area is to be realized among simulations, which then constrain the probability density functions (PDFs) produced by the weaving process. The goal of PDF weaving is simply to create a framework where simulations involving these types of mapped inputs can accommodate PDFs which change across simulations and which, in aggregate, produce MC input variation that conforms to map validation results and FIA-derived assumptions about population parameters and uncertainties.

In this study, we applied ForCaMF to quantify the carbon impact of natural disturbances and land management in GYE from 1985 to 2011. Inputs for the model included disturbance type and magnitude maps from 1985 to 2011, forest type group map, initial carbon map, and carbon accumulation functions. Except for the forest type group map, which was extracted from national forest type group map produced by United States Forest Service (Ruefenacht et al. 2008), all other model inputs were produced in previous sections.

5.3.8 Analyzing impact of management and disturbances on carbon dynamics in GYE

After simulating the annual C stocks in GYE, we computed and compared the effects of management and disturbances on time series C distributions of GYE NPs,

WAs and NFs, stratified by forest type groups. We first compared the initial forest condition of these regions, such as initial C density and stand age class from the same forest types. Then we also plotted and overlaid frequency distribution for C densities to compare the general C density differences in the three ownership types. Thirdly, we compared time series C removal/emission from harvest/fires for different ownership. For GYE NPs and WAs, fire was the major disturbance type; while for GYE NFs, harvests were more pronounced than fires, especially in the 1980s. Uncertainties associated with the inputs maps and inventory data were quantified using Monte Carlo simulations (100 iterations in this study).

5.4 Results

5.4.1 Validation results

We assessed pixel-level accuracies for the 2 maps submitted to MC analysis (starting volume and forest type). Table 5-1 show error matrices comparing these 2 maps with FIA ground measurements and high resolution satellite images. The MC analysis we describe used the most basic accuracy parameter from these assessment:

Table 5- 1 Accuracy assessment of ForCaMF input maps, including (a) error matrix for GYE forest starting C map. Per-hectare volumes were grouped according to thresholds described in Section 3.3; (b) error matrix for GYE forest type group map, validated against 100 random sampled FIA plots in GYE. Forest type groups include: Lodgepole Pine (LP), Whitebark Pine (WP), Douglas-fir (DF) and Spruce/Fir/Other (SF). Observed forest type was from FIA plot observation;

(a)

		Observed volume class				
		Low	Medium low	Medium high	High	Producer's Accuracy
Predicted volume class	Low	5	2	0	0	71%
	Medium low	7	15	7	7	47%
	Medium high	4	7	19	13	48%
	High	0	0	2	12	86%
	User's Accuracy	31%	71%	75%	38%	
	Overall Accuracy			55%		

(b)

		Observed forest type				
		DF	SF	LP	OT	Producer's Accuracy
Predicted forest type	DF	8	2	0	0	80%
	SF	2	33	2	3	83%
	LP	1	2	25	1	86%
	OT	0	4	1	6	55%
	User's Accuracy	73%	80%	89%	60%	
	Overall Accuracy			80%		

5.4.2 Initial forest carbon condition in GYE

Forests cover over 38% of the GYE region and the ratio of forested area in National Parks, Wilderness Area and timber managed National Forests (Figure 5-1) is approximately 1: 1.2:2.5. Before the 1988 mega fires, the mean C density of the forests in 1984 to 1987 differed between ownership classes, with higher C density distributions in Wilderness Area and National Forests lands than in National Parks (Figure 5-3).

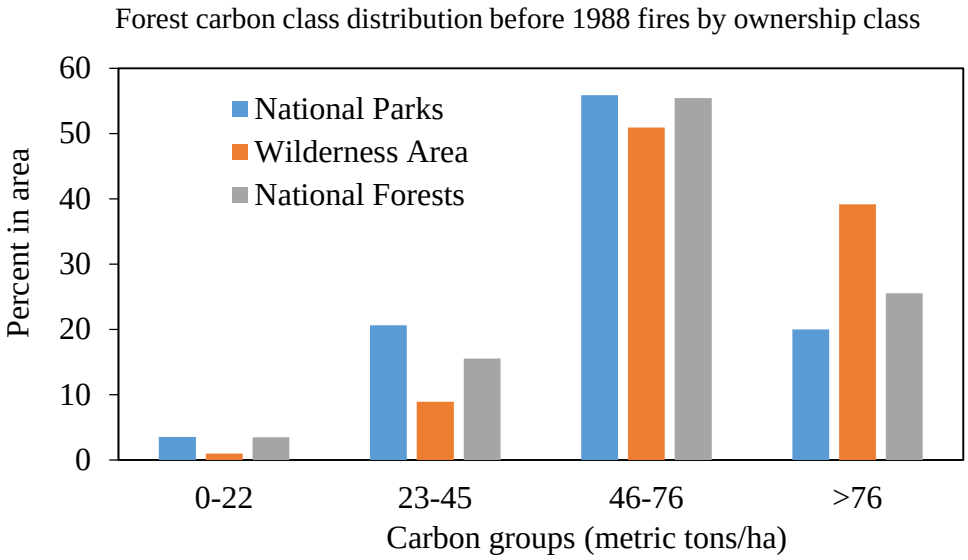

Figure 5- 3 Initial C condition class by ownership

5.4.3 C dynamics in the GYE region

The potential pixel- and population-level errors simulated in each realization of the MC analysis were parameterized by the validation activities above. Before presenting results of the simulations, it is important to consider how often a solution could actually be found for the linear systems we have described. Specifically, these solutions were required to present specific randomly drawn levels of population-level error as well as constraints related to overall accuracy and for ordinal maps, constraints requiring that big error be less common than small errors.

ForCaMF model simulation results (Figure 5-4) reveal that GYE regional C stocks have been increasing during the study interval, mainly due to forest recovery from the previous disturbances and background forest growth. As observed in Figure 5-3, GYE National Forests and Wilderness area have higher C densities at the beginning of the study period. The impact of the 1988 mega fires on regional C dynamics is striking. GYE National Parks, where most of the 1988 fires occurred,

experienced the most dramatic decrease in total forest C stocks (Figure 5-4) after the fires. Direct C removal from the fires are about 42 million metric tons for GYE National Parks. With the highest C density among all forested area in GYE before 1988, Wilderness Area also emit 17 million metric tons C due to the 1988 fires.

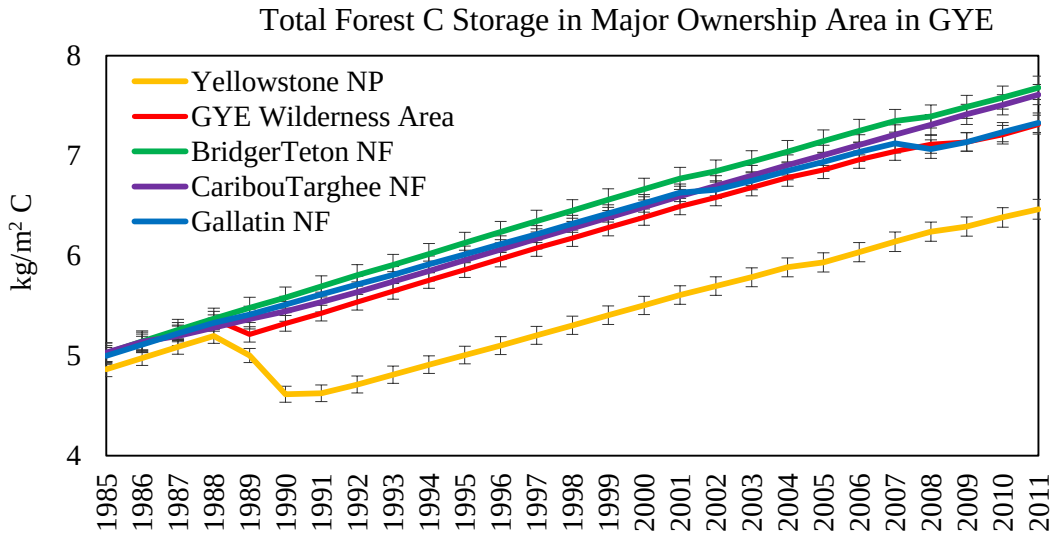

Figure 5- 4 Forest C density in major land ownership areas in GYE. Yellow line represents Yellowstone National Park, red line represents Wilderness Area in GYE, green, purple and blue lines represent Bridger-Teton, Caribou-Targhee, Gallatin National Forests, respectively.

5.4.4 Impact of different management approached on carbon dynamics in GYE

Differences in C storage for each land ownership shown in Figure 5-5 reveal the relative effects of fire and harvests on forest C dynamics in GYE. C storage in Yellowstone National Park and GYE Wilderness Area show similar temporal trend: 1988 fires have shown to be the major C source in the past few decades, with some additional C loss from fires after year 2000s. Temporal C trend in GYE National Forests, however, tells a different story. In Caribou-Targhee National Forest, which

has been heavily harvested in late 1980s to salvage trees from beetle kill, timber harvests account for more than four times C than released by fires (1.2 million metric tons vs. 0.28 million metric tons C). In Bridger-Teton and Gallatin National Forest, harvests are less pronounced in the 1980s but rather evenly distributed in the whole time series; while fires claim main changes of C storages in the 2000s, confirming the drastic increase in fire activities in Western United States after year 2000 (Westerling et al. 2006). Accumulative C loss due to fires from 1985 to 2011 are about 0.96 and 1.56 million metric tons in Bridger-Teton and Gallatin National Forests. Accumulative C loss due to harvests from 1985 to 2011 are about 0.12 and 0.85 million metric tons in Bridger-Teton and Gallatin National Forests.

(a)

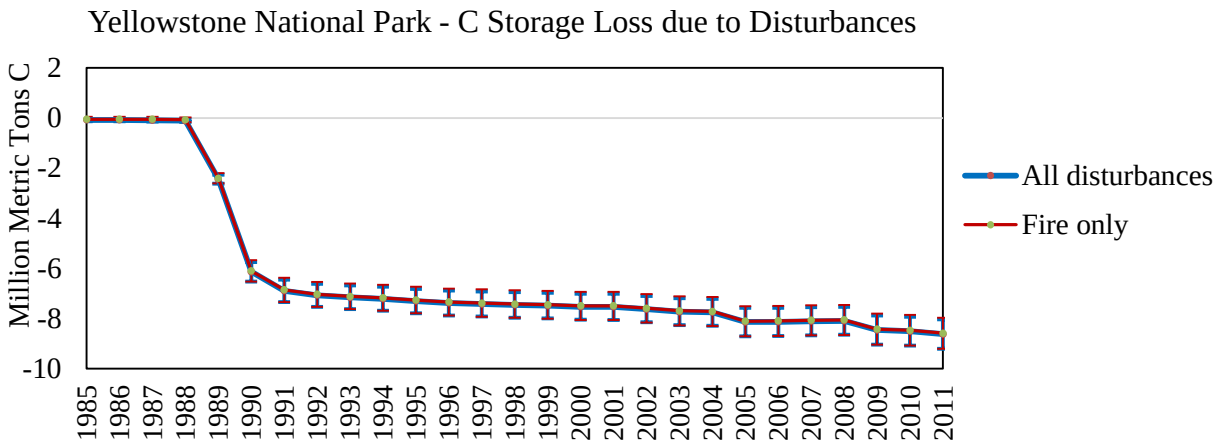

(b)

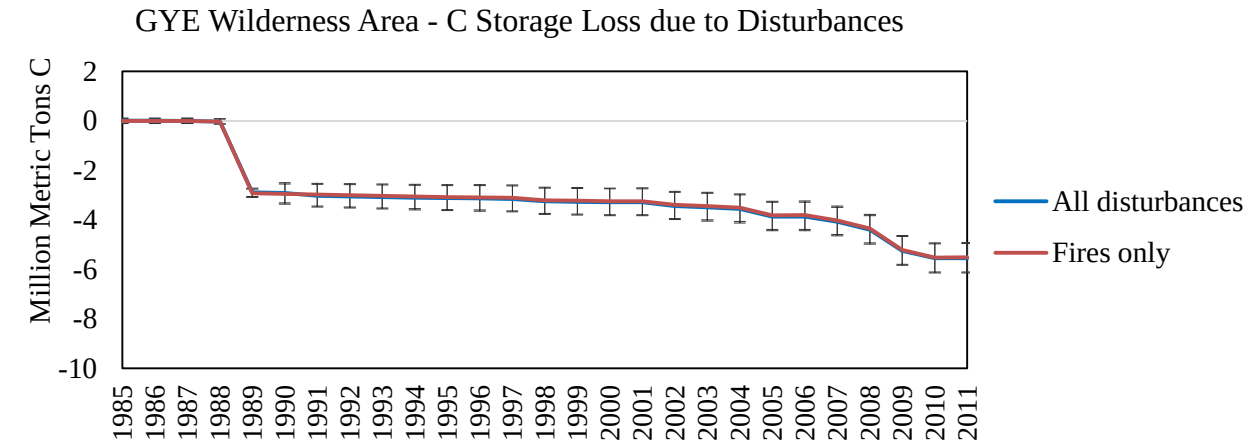
GYE Wilderness Area - C Storage Loss due to Disturbances
Million Metric Tons C
2
0
-2
-4
-6
-8
-10
1985 1986 1987 1988 1989 1990 1991 1992 1993 1994 1995 1996 1997 1998 1999 2000 2001 2002 2003 2004 2005 2006 2007 2008 2009 2010 2011
All disturbances
Fires only

(c)

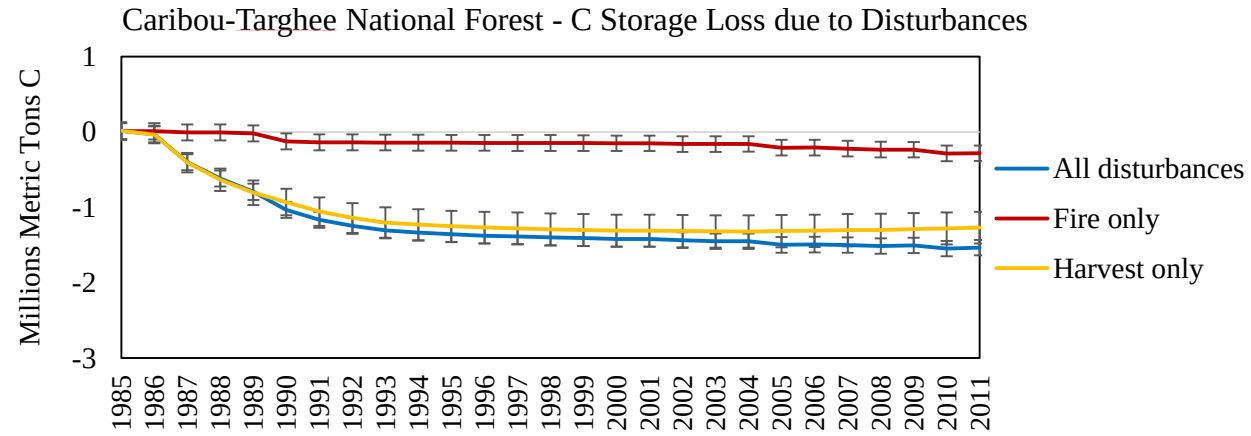
Caribou-Targhee National Forest - C Storage Loss due to Disturbances
Millions Metric Tons C
1
0
-1
-2
-3
1985 1986 1987 1988 1989 1990 1991 1992 1993 1994 1995 1996 1997 1998 1999 2000 2001 2002 2003 2004 2005 2006 2007 2008 2009 2010 2011
All disturbances
Fire only
Harvest only

(d)

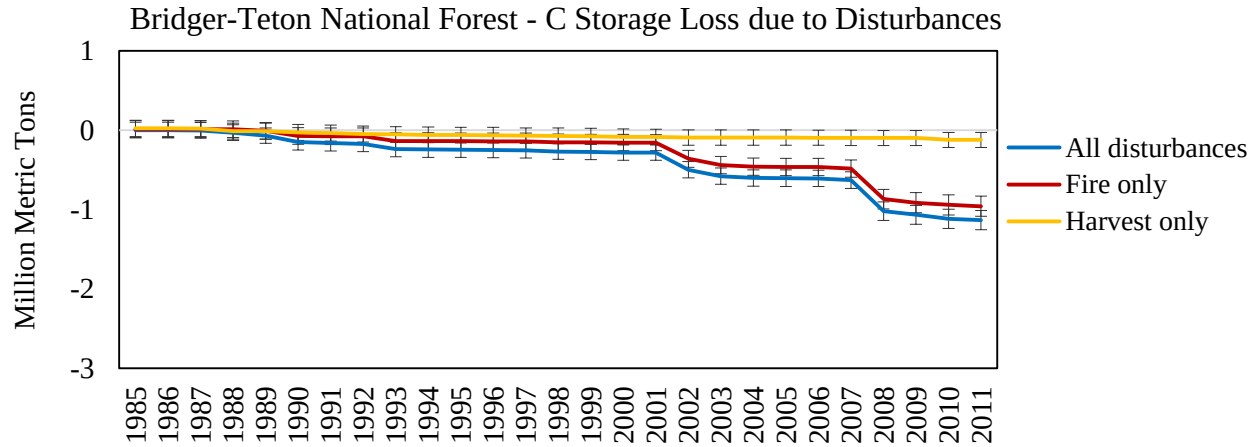
Bridger-Teton National Forest - C Storage Loss due to Disturbances
Million Metric Tons
1
0
-1
-2
-3
1985 1986 1987 1988 1989 1990 1991 1992 1993 1994 1995 1996 1997 1998 1999 2000 2001 2002 2003 2004 2005 2006 2007 2008 2009 2010 2011
All disturbances
Fire only
Harvest only

(e)

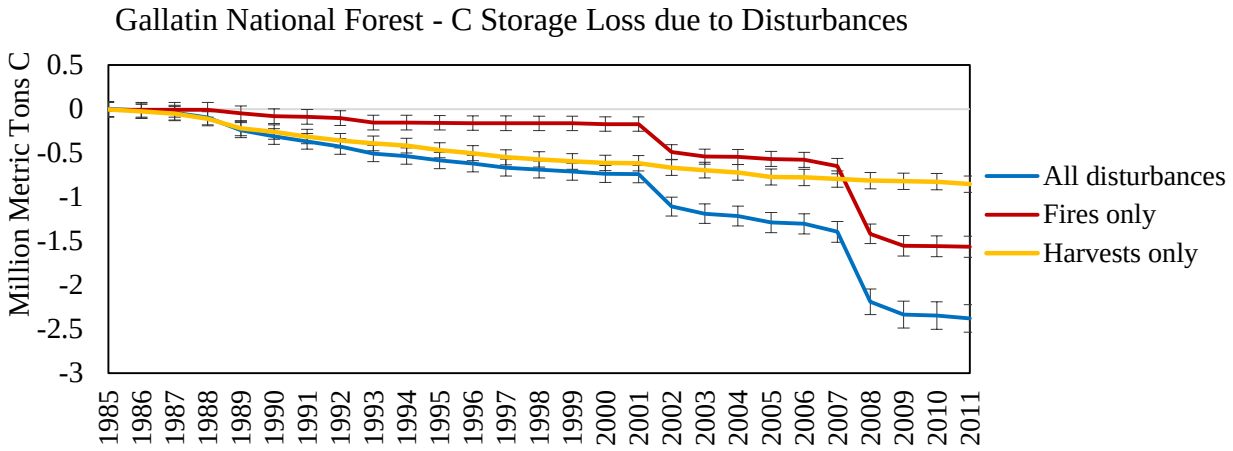

Figure 5- 5 Differences in C densities due to disturbances in (a) Yellowstone National Park (b) GYE Wilderness Area (c) Caribou-Targhee National Forest (d) Bridger-Teton National Forest (e) Gallatin National Forest

Total C stock at per unit area is a direct measure of C density and can be compared among different regions, especially C loss due to disturbances such as fire and harvests (Figure 5-6). In Yellowstone National Park, fire was the dominant disturbance agent for changing ecosystem C dynamics in recent decades. The mega fires in 1988 have caused the ecosystem C density to decrease about 900 g/m^2, emitting C equivalent to more than four, five and forty-seven times of all harvests occurred in Caribou-Targhee National Forests (199 g/m^2), Gallatin National Forests (171 g/m^2), Bridger-Teton National Forests (19 g/m^2), respectively, in the past few decades. Most burned area in 1988 located in National Parks, followed by Wilderness Areas. The effects of 1988 fires on GYE Wilderness Area (276 g/m^2) are about one third of the same fires on National Parks. While for C loss from post-2000 fires in GYE Wilderness Areas (210 g/m^2) and Gallatin (280 g/m^2) National Forests exceeded the effects of those fires on National Parks (140 g/m^2). Bridger-Teton (132 g/m^2).

(a)

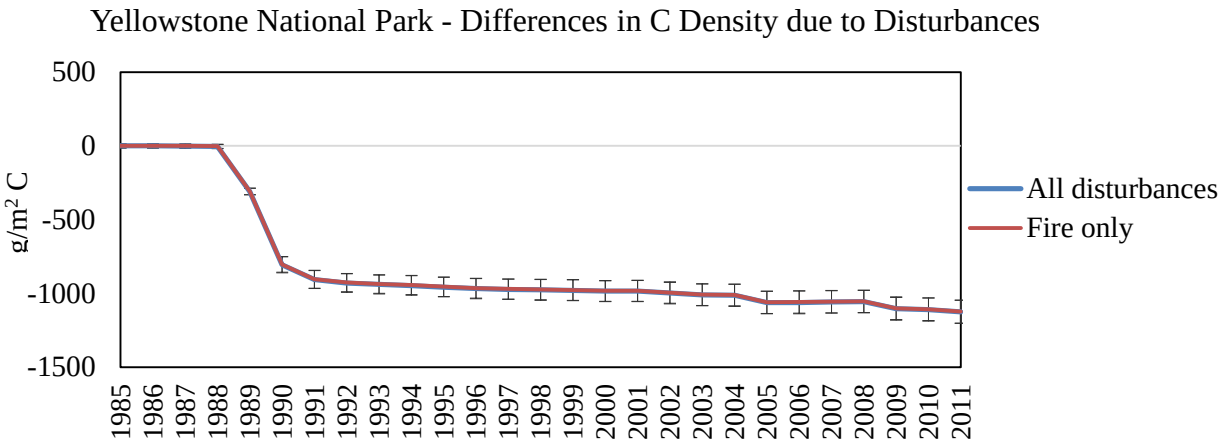
Yellowstone National Park - Differences in C Density due to Disturbances
500
0
-500
-1000
-1500
g/m2 C
1985 1986 1987 1988 1989 1990 1991 1992 1993 1994 1995 1996 1997 1998 1999 2000 2001 2002 2003 2004 2005 2006 2007 2008 2009 2010 2011
All disturbances
Fire only

(b)

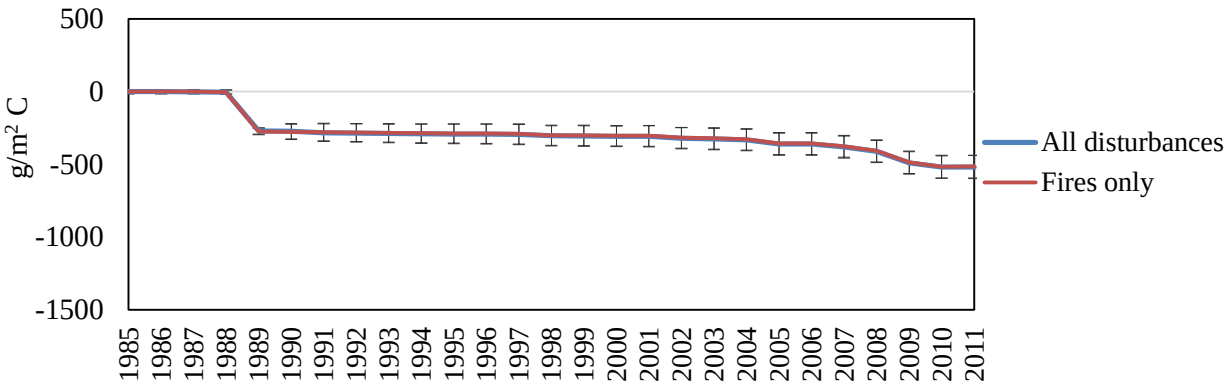
GYE Wilderness Area - Differences in C Density due to Disturbances
500
0
-500
-1000
-1500
g/m2 C
1985 1986 1987 1988 1989 1990 1991 1992 1993 1994 1995 1996 1997 1998 1999 2000 2001 2002 2003 2004 2005 2006 2007 2008 2009 2010 2011
All disturbances
Fires only

(c)

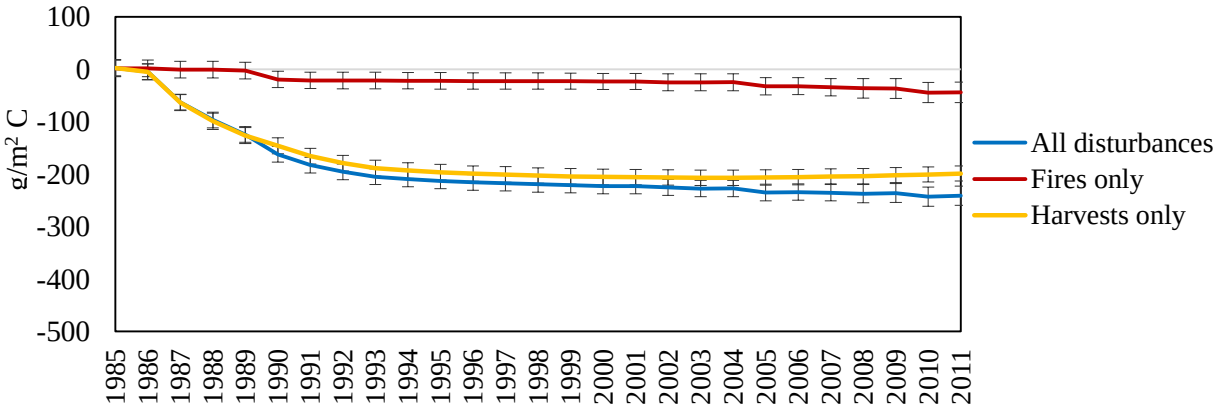
Caribou-Targhee National Forest – Differences in C Density due to Disturbances
100
0
-100
-200
-300
-400
-500
g/m2 C
1985 1986 1987 1988 1989 1990 1991 1992 1993 1994 1995 1996 1997 1998 1999 2000 2001 2002 2003 2004 2005 2006 2007 2008 2009 2010 2011
All disturbances
Fires only
Harvests only

(d)

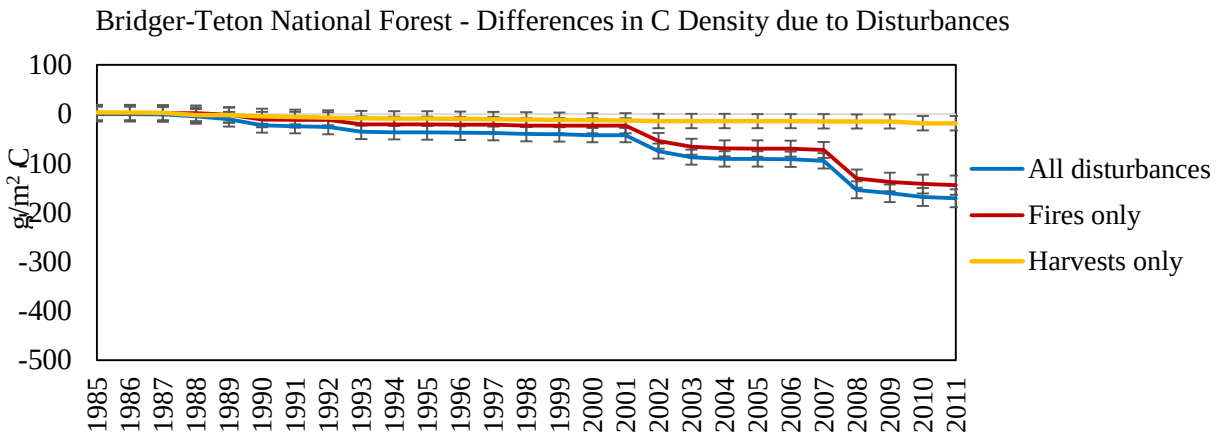

(e)

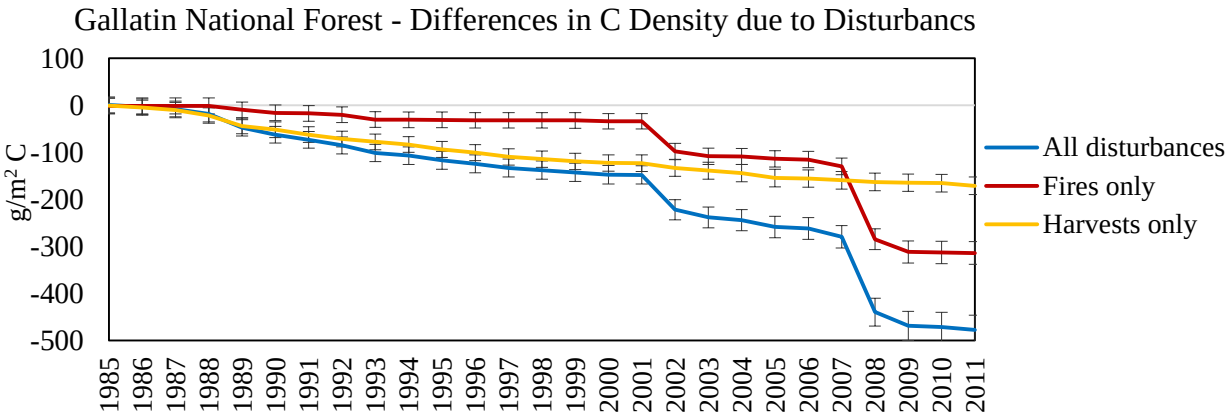

Figure 5- 6 Changes in C density due to disturbances in (a) Yellowstone National Park (b) GYE Wilderness Areas (c) Caribou-Targhee National Forest (d) Bridger-Teton National Forest (e) Gallatin National Forest. Wilderness Areas were designated by the 1964 Wilderness Act and specifically refer to Wilderness Areas within National Forest lands. National Forests here only contain timber-managed area excluding Wilderness Areas.

5.5 Discussions and Conclusions

Remote sensing can and does provide critical monitoring information for ecological models, commonly including surfaces related to biological productivity and representing vegetation structure and change. While a few efforts have been made with MC methods to account for map error in the uncertainty of model outputs, there has to date been no generic approach proposed for doing so, particularly for

maps of categorical variables. We illustrated how MC simulations of map error may be aligned with reference data at both the map unit and population levels. This importance of map error as a source of uncertainty was underscored by the significant model output variability resulting from simulation of map errors.

Fires are the dominant form of disturbance in the GYE National Parks and Wilderness Area, while harvests are usually more pronounced in GYE National Forests. Catastrophic fire events can often converts the ecosystems from a C sink to a C source. C removals from the 1988 mega fires are more than four times of C removal from harvests occurred in the past few decades in the surrounding National Forests. The fact that post-2000 fires in Wilderness Area and National Forests are more prominent than National Parks might be explained by the wide-spread forest recovery in National Parks after the 1988 fires.

There are some limitations in the study, and it should be noted that model errors do not necessarily equal to errors in reality. Insufficient data, limits in modeling capabilities and the inadequate scientific understanding of these complex interactions between natural phenomena can lead to uncertainties in this study. With proper calibration with remote sensing observations, uncertainties in this assessment are limited to input inventory data and methods related to carbon storage simulation. The known limitations of this approach include the following: 1) uncertainties from the FIA measurements were not included. Not all error sources were fully tracked for FIA plot information such as GPS location error, measurement and calculation errors; 2) soil carbon pool was not included in this assessment. Considering the large uncertainty associated with the soil carbon dynamics, much higher uncertainties are

expected once the soil carbon are taken into account; 3)the interactions between vegetation and climate was not included in the carbon modeling process. Forest carbon accumulation rates were assumed to keep constant for recent changes in greenhouse gas concentrations and the "carbon fertilization" effects were not considered; 4) Constraint values for PDF weaving were derived from FIA regional average and could potentially underestimate the impact of spatial heterogeneity on ecosystem carbon balance. All these above issues would add to the discrepancies between the simulated results and the ground truth.

In addition to the above limitations, this study only quantified the impact of disturbance and management activities on ecosystem carbon storage, which is one of the many ecosystems services provided by forests. Other ecosystems services such as erosion and flood control, decomposition, water purification, recreation, etc. are also important to human well-being and detailed assessment are required to fully understand the effects of disturbance and forest management on ecosystem functions and sustainability.

This study is an effort to assess the impact of recent forest management and disturbances on ecosystem carbon dynamics in GYE. Methods of this study can establish a good foundation for scientific research, including but not limited to carbon dynamics, landscape ecology, policy making, and climate change mitigation. Forest managers can use the produced carbon dynamics and modeling approach to develop land management goals, prioritize management activities, and quantify carbon consequences of management strategies. There is also great interests in further understanding of potential future management and disturbance on future C dynamics.

The physical mechanisms by which climate-vegetation-disturbance interactions affect ecosystem C dynamics in GYE have not been fully characterized; therefore, future investigations should address this challenge by using models capable of simulating interactions between future climate change, disturbance pattern/intensity, and C stocks/fluxes.

Chapter 6: Concluding Remarks

Forests play an important role in the terrestrial carbon cycles and are believed to account for a sustained carbon sink in recent decades (Canadell and Raupach 2008; Rhemtulla et al. 2009). International negotiations to restrict greenhouse gases require an understanding of forest C emissions and sequestration potentials in both managed and unmanaged forests (Pan et al. 2011). With increasing interests in quantifying greenhouse gas emissions and potentially managing forests to increase the rate of CO_2 sequestration, there are urgent needs to quantify current patterns of forest carbon stocks and fluxes, which also require accurate characterization of many factors affecting these stocks and fluxes, including forest management, disturbance, and recovery, as well as departure of current disturbance patterns from historical conditions (Magnani et al. 2007).

This dissertation research was designed to address the above needs. It first developed a novel approach to integrate the VCT and SVM was developed and used to map the timing, location, and agent/cause of forest disturbances on an annual basis from 1985 to 2011 for the GYE region. Then, following a comprehensive validation of the post-disturbance recovery as mapped by the VCT, the spatial and temporal patterns of post-fire and post-harvest forest recovery were evaluated and impact of environmental variables on forest recovery following the 1988 great Yellowstone fire was evaluated. Thirdly, an innovative modeling approach was developed to measure the differences between current and historical fire regimes by feeding time series remote sensing results into a landscape succession model. Finally, the above derived

results were combined with inventory and other ancillary data in an empirical C model to quantify forest C storage and flux, and the impact of disturbance and management practices. Although the Yellowstone region has been a focal point for many ecological studies (Hatala et al. 2010; Parmenter et al. 2003; Turner et al. 2003), to my knowledge this is the first systematic study over the entire GYE region that integrates field inventory data, a consistent, annualized record of forest disturbance and recovery, and a carbon model to disentangle the relative impact of disturbance and management on regional C dynamics.

Major findings of the dissertation are described in section 6. 1. Major contributions and future research directions are summarized in sections 6.2 and 6.3, respectively.

6.1 Major findings

Using Landsat time series observations, we mapped annual rates of different forest disturbance types in the GYE region by combining the VCT and SVM algorithms. This VCT-SVM approach was found effective for mapping wildfires and harvest/logging, with overall accuracy of 87% and user's accuracy ranging from 73% to 96%. The classification results revealed that forest fire was the most dominant forest change agent in GYE NPs and WAs during the study interval, while harvest was significant in the NFs. However, this approach missed most disturbances in the "other disturbance" class, which were mostly minor disturbances due to insect/disease as well as snow and wind damages. This was mainly due to the limited capability of the current version of the VCT to detect those disturbances, which was also observed in previous studies (Thomas et al. 2011).

Robust validation of the VCT recovery product indicates the ability of VCT algorithm in monitoring large scale time series forest recovery following multiple disturbance types. In general, these accuracies of VCT recovery/no-recovery maps were consistent (~80%) among different disturbance types (fires and harvests) and forest types in GYE. Spatial patterns of forest recovery following the 1988 fires were highly clustered across GYE and largely located in the lower elevations (<2,300m) where the growing season is longer and land productivity is higher. Forests in National Forests generally grow back faster than forests in National Parks and Wilderness Areas. During the two decades following the catastrophic fires in 1988, National Forests have consistently higher percentages of forest recovery than National Parks and Wilderness Areas. Results from machine learning modeling approach reveal that environmental conditions, especially topography and post-fire climate, have high prediction accuracy (ranging from 81% to 95% for major species) for modeling forest recovery condition after the 1988 fires by the year 2011.

Comparison between simulated fire regimes and satellite observations suggests that the LANDSUMv4 model is a viable vehicle for simulating the current fire regimes with inputs derived from a relatively long record of remotely sensed observations . We can compare this current fire regime data with the simulated historical fire regime data for national consistent and local relevant FRCC assessment. The comparison of historical and current fire regimes indicates that current fire regimes of most forest ecosystems in the Northern Rocky Mountains have moderately departed from historical conditions. First, out results show that current fire regimes can be described as having lower fire frequency and higher severities

compared to historical fire regimes. Secondly, fire regimes have departed the most for montane forests in the Northern Rocky Mountains which historically were dominated by frequent and nonlethal fires. Third, about half of the forest ecosystems were historically characterized by infrequent stand replacement fires. The current fire regimes of these ecosystems also experienced a moderate departure from historical fire conditions, induced by human activities, climate change or combined effects of the two. Findings of this study provide quantitative evidence to the change of fire regime conditions in the study area.

In Yellowstone National Park (YNP), fire was the dominant disturbance agent for changing ecosystem C dynamics in recent decades. C storage in Yellowstone National Park and GYE Wilderness Areas show a similar temporal trend: the 1988 fires have shown to be the major C source in the past few decades, with some additional C loss from fires after year 2000. Temporal C trend in GYE National Forests, however, tells a different story. In Caribou-Targhee National Forest, which has been heavily harvested in late 1980s to salvage trees from beetle kill, timber harvests account for more than four times C than released by fires (1.2 million metric tons vs. 0.28 million metric tons C). In Bridger-Teton and Gallatin National Forests, harvests are less pronounced in the 1980s but rather evenly distributed over the whole time series; while fires claim the primary changes of C storages in the 2000s, confirming the drastic increase in fire activities in Western United States in recent decades (Zhao et al. 2015b). Cumulative C loss due to fires from 1985 to 2011 are about 0.96 and 1.56 million metric tons in Bridger-Teton and Gallatin National

Forests. Accumulative C loss due to harvests from 1985 to 2011 are about 0.12 and 0.85 million metric tons in Bridger-Teton and Gallatin National Forests.

The mega fires in 1988 have caused the ecosystem C density to decrease about 900 g/m^2 in YNP, emitting C equivalent to more than three times that of all harvests which occurred in the surrounding National Forests, from 1985 to 2011. The effects of the 1988 fires on GYE Wilderness Area (276 g/m^2) are about one third of the same fires on National Parks. For fire activities after year 2000, the mega fires in 1988 might have caused less burns in the YNP, supported by the fact that C loss from post-2000 fires in surrounding National Forests have approached or even exceeded the effects of those fires on National Parks (140 g/m^2). Considering that fires are generally suppressed in National Forests and much less restricted in the National Parks, human management might be the driving force of increased fuel loading and higher fire risk in the National Forests, in addition to the frequent drought events in Western U.S.

The period of study, some 30+ years, is relatively short ecologically, considering the mean fire return interval for GYE vegetation ranges from 30-300 years (Turner et al. 2003; Westerling et al. 2011). Long-term continuous observations are required to further test and validate all the findings.

6.2 Major contributions

This dissertation is a synthesized study in quantifying the impact of decadal forest management and disturbances on C dynamics using forest inventory, remote sensing and C modeling approach. Although GYE has been a focal point for many ecological studies (Hatala et al. 2010; Parmenter et al. 2003; Turner et al. 2003), a

consistent annualized record of forest disturbances, recovery and the associated C implications from 1980s to the present is not available. Such a comprehensive and consistent record would be very useful for informed forest management and policy making, ecosystem conservation and restoration, biodiversity protection and carbon assessment in the region. With the availability of forest inventory, VCT disturbance maps, and C modeling capability nationwide, the modeling approach used in this dissertation can be applied to the rest of the U.S for many research and management purposes.

The disturbance products derived through the VCT-SVM approach was used as input for quantifying the carbon fluxes from the mapped disturbance events and their impact on future carbon sequestration potential in the GYE region. By providing details on both the timing and causal agents of the mapped disturbances over nearly three decades, these products can be valuable for many other applications, including forest management, biological conservation, and ecosystem restoration. SVM appeared to be an effective tool for separating different forest disturbance types after those disturbances have been detected. While it was used together with VCT in this study, it can be used with other change detection algorithms designed for detecting changes but not for separating different change types. Now that Landsat data are publically available at no data cost to users, this algorithm can be used together with VCT or other change detection algorithms to achieve annual mapping of different disturbance types for areas that have time series Landsat data.

Results from this dissertation underscore the ability of VCT algorithm in monitoring large scale time series forest recovery following multiple disturbance

types. Through temporal and spatial consistency, time series forest recovery history was characterized in GYE using the VCT forest recovery data. The spatial and temporal forest recovery trends in GYE were analyzed for different land ownership (management regimes), disturbance types, and forest types. The impact of environmental conditions, such as topography and climates, on post-disturbance forest recovery was assessed using a machine learning modeling approach. With the public availability of VCT disturbance and recovery product nationwide, this approach can be applied to other regions of US for many monitoring and management purposes.

The assessment approach, aimed at measuring departures of current to historical fire regimes, is helpful for complementing consistent and comparable large scale FRCC assessment for large scale forest management policy making (Keane et al. 2007). Knowing the differences between historical and current fire regime conditions, following the methods developed in this paper, can establish a good foundation for scientific research in many fields, including but not limited to landscape ecology, climate change, and carbon dynamics (Agee 1998; Liu et al. 2011; Spittlehouse and Stewart 2004; Westerling et al. 2011; Whitlock et al. 2003). Forest managers can also use the produced fire regime departure and condition class maps to prioritize fuel treatment and fire monitoring efforts (Hann et al. 2004; Hardy et al. 2001).

Recent advances in remote sensing of vegetation condition and change (Huang et al. 2010; Kennedy et al. 2010b; Zhu et al. 2012), along with new techniques linking remote sensing with inventory records, have allowed investigations that are much more tightly constrained to actual landscape conditions. These new capabilities are built into the Forest carbon Management Framework (ForCaMF), which is being used by the National Forest System not only to model, but to monitor across very specific

management units, the impact of different kinds of disturbance on carbon storage. In this dissertation, ForCaMF has been applied to directly compare the impact of forest management and disturbances in different land ownerships for the first time. Results from this study can be used to guide forest C management in GYE for improved adaptation and mitigation to climate change.

6.3 Future research directions

This study is a preliminary study in characterizing time series forest disturbances in GYE. The validation results suggest that major mapping uncertainty lies in low to moderate severity disturbances, such as low severity fire or thinning, and multiple disturbance events. Thus, improving characterization of forest disturbances and recovery, especially for low and moderate severity disturbances, are recommended for future work. A possible remedy lies in segmenting spatial patterns/textures and incorporating the segmentations in the classification process. Successful stories have been reported in using these information to map high resolution forest type and structure information (Franklin and Maudie 2001; Kayitakire et al. 2006), and it would be interesting to explore if these new information would help improve accuracies in GYE forest disturbance mapping. Another caveat associated with forest disturbance characterization in this study is that forest loss due to insect attacks was not included. Preliminary efforts towards mapping mountain pine beetle outbreaks in GYE showed high omission errors in the low and moderate magnitude classes. And it would also be interesting to examine the effects of spatial pattern and texture information on mapping of forest disturbances caused by insect outbreaks.

The forest recovery analysis presented in this dissertation is among one of the first attempts to track forest recovery following disturbances using time series remote

sensing images and a forest change algorithm. Given the rich information revealed from the analysis, this validation was limited in its ability to support short-term forest recovery. Additional information are needed to better determine the year of forest recovery and calibrate the algorithm to match certain forest definition (greater than 10% or 30% in canopy cover and greater than 5m in tree height). A common solution to this problem relies on forest structure information provided by ground measurements or small to medium footprint lidar remote sensing (~30m), which can be difficult to obtain for large spatial extents. Fortunately, future spaceborne lidar missions are scheduled to collect waveforms at diameters of about 15 to 20 meters at the global scale (Tang, 2015), and improved global forest structure characterization can be expected from future lidar datasets.

This study presented here indicated recent forest management and natural disturbances have diverse short term carbon implications. There is great interests in further understanding of potential future management and disturbance on future C dynamics. The physical mechanisms by which climate-vegetation-disturbance interactions affect ecosystem C dynamics in GYE have not been fully characterized; therefore, future investigation should address this challenge by using models capable of simulating interactions between future climate change, disturbance pattern/intensity, and C stocks/fluxes. It is also of great interests to use the current C modeling approach to simulate the impact of potential future management and disturbance on future C dynamics. There are a few methods to implement this goal: (1) use projected future disturbance maps, such as predicted fire or insect occurrence maps under future climate change scenarios, as inputs of ForCaMF and simulate the

impact of projected future disturbances on ecosystem C dynamics. For future forest management activities, we can use alternative forest management plans provided by the National Forests to prescribe future harvesting locations and intensities; (2) incorporate the current disturbance and management datasets into process based models, such as Ecosystem Demography (ED), LANDCLIM or FireBGC, to simulate interactions between future climate, disturbance and vegetation and conduct more comprehensive analysis for effects of future management and disturbances on regional C dynamics.

The dissertation is considered to be an initial step in evidencing the linkage between forest management, disturbances, and carbon dynamics in ecosystems with complex management regimes and environmental conditions. Despite the general success, this study was regional specific and lacked large scale carbon and forest management implications. This prompts interests to apply the forest change characterization and C modeling approach to other National Parks and surrounding ecosystems, such as the Greater Olympic National Park, Greater Yosemite National Park and Greater Smoky Mountain National Park. Comparative studies among these regions would help us understand the effects of forest management and disturbances for C dynamics in ecosystems with diverse geographic locations, forest composition and substrate conditions.

Abbreviations

BpS	Biophysical Settings
C	carbon
DEM	Digital Elevation Model
dNBR	Differenced normalized burn ratio
FAO	Food and Agriculture Organization
FIA	Forest Inventory and Analysis
ForCaMF	Forest carbon Management Framework
FRCC	Fire Regime Condition Class
FS	Forest Service (United States Department of Agriculture)
FVS	Forest Vegetation Simulator
GYE	Greater Yellowstone Ecosystem
HRV	Historical Range and Variation
IFZ	Integrated Forest Z-score
LANDSUMv4	Landscape Succession Model version 4.0
LEDAPS	Landsat Ecosystem Disturbance Adaptive Processing System
LTSS	Landsat Time Series Stacks
MFRI	Mean Fire Return Interval
MPB	Mountain Pine Beetle
MTBS	Monitoring Trends of Burn Severity
NAIP	National Agricultural Imagine Program

NDVI	Normalized Difference Vegetation Index
NFs	National Forests
NPs	National Parks
OA	Overall Accuracy
OBB	Out of Bag
PA	Producer's Accuracy
PDSI	Palmer Drought Severity Index
PVT	Potential Vegetation Type
RdNBR	Relativized Differenced Burn Ratio
RF	Random Forests
RNR	Recovery/No-recovery
SVM	Support Vector Machine
UA	User's Accuracy
VCT	Vegetation Change Tracker
WAs	Wilderness Areas
WRS	World Reference System
YNP	Yellowstone National Park

Bibliography

Agee, J.K. (1998). The landscape ecology of western forest fire regimes. *Northwest Science, 72*, 24-34

Alexander, R.R. (1974). Silviculture of subalpine forests in the central and southern Rocky Mountains: the status of our knowledge. In, *Alexander, RR: Silviculture of central and southern Rocky Mountain forests: a summary of the status of our knowledge by timber types.*

Alexander, R.R., & Edminster, C.B. (1980). Lodgepole pine management in the central Rocky Mountains. *Journal of Forestry, 78*, 196-201

Amaranthus, M., Jubas, H., & Arthur, D. (1989). Stream shading, summer streamflow and maximum water temperature following intense wildfire in headwater streams. In, *Berg, NH, tech. coord. Proceedings of the symposium on fire and watershed management. Gen. Tech. Rep. PSW-109. Albany, CA: US Department of Agriculture, Forest Service, Pacific Southwest Researce Station* (pp. 75-91)

Arno, S.F. (1980). Forest fire history in the northern Rockies. *Journal of Forestry, 78*, 460-465

Arno, S.F., Parsons, D.J., & Keane, R.E. (2000). Mixed-severity fire regimes in the northern Rocky Mountains: consequences of fire exclusion and options for the future. In, *Wilderness science in a time of change conference* (pp. 23-27)

Arora, V.K., & Boer, G.J. (2005). Fire as an interactive component of dynamic vegetation models. *Journal of Geophysical Research: Biogeosciences (2005–2012), 110*

Baker, W.L. (1992). Effects of settlement and fire suppression on landscape structure. *Ecology*, 1879-1887

Barrett, T.M. (2001). *Models of vegetative change for landscape planning: a comparison of FETM, LANDSUM, SIMPPLLE, and VDDT*. US Department of Agriculture, Forest Service, Rocky Mountain Research Station

Bond, W.J., Woodward, F.I., & Midgley, G.F. (2005). The global distribution of ecosystems in a world without fire. *New Phytologist, 165*, 525-538

Bowman, D.M., Balch, J.K., Artaxo, P., Bond, W.J., Carlson, J.M., Cochrane, M.A., D'Antonio, C.M., DeFries, R.S., Doyle, J.C., & Harrison, S.P. (2009). Fire in the Earth system. *Science, 324*, 481-484

Bradford, J.B., Jensen, N.R., Domke, G.M., & D'Amato, A.W. (2013). Potential increases in natural disturbance rates could offset forest management impacts on ecosystem carbon stocks. *Forest Ecology and Management, 308*, 178-187

Breiman, L. (2001). Random forests. *Machine learning, 45*, 5-32

Brown, J.K., & Smith, J.K. (2000). Wildland fire in ecosystems: effects of fire on flora

Brown, T.J., Hall, B.L., & Westerling, A.L. (2004). The impact of twenty-first century climate change on wildland fire danger in the western United States: an applications perspective. *Climatic Change, 62*, 365-388

Burroughs, R.H., & Clark, T.W. (1995). Ecosystem management: a comparison of Greater Yellowstone and Georges Bank. *Environmental Management, 19*, 649-663

Canadell, J.G., & Raupach, M.R. (2008). Managing forests for climate change mitigation. *Science, 320*, 1456-1457

Caspersen, J.P., Pacala, S.W., Jenkins, J.C., Hurtt, G.C., Moorcroft, P.R., & Birdsey, R.A. (2000). Contributions of land-use history to carbon accumulation in US forests. *Science, 290*, 1148-1151

Chang, C.-C., & Lin, C.-J. (2011). LIBSVM: a library for support vector machines. *ACM Transactions on Intelligent Systems and Technology (TIST), 2*, 27

Chang, Y., He, H.S., Hu, Y., Bu, R., & Li, X. (2008). Historic and current fire regimes in the Great Xing'an Mountains, northeastern China: Implications for long-term forest management. *Forest Ecology and Management, 254*, 445-453

Chen, W., Chen, J., & Cihlar, J. (2000). An integrated terrestrial ecosystem carbon-budget model based on changes in disturbance, climate, and atmospheric chemistry. *Ecological Modelling, 135*, 55-79

Clark, T.W., Amato, E.D., Whittemore, D.G., & Harvey, A.H. (1991). Policy and programs for ecosystem management in the Greater Yellowstone Ecosystem: An analysis. *Conservation Biology, 5*, 412-422

Cocke, A.E., Fulé, P.Z., & Crouse, J.E. (2005). Comparison of burn severity assessments using Differenced Normalized Burn Ratio and ground data. *International Journal of Wildland Fire, 14*, 189-198

Cohen, W.B., Yang, Z., & Kennedy, R. (2010). Detecting trends in forest disturbance and recovery using yearly Landsat time series: 2. TimeSync—Tools for calibration and validation. *Remote Sensing of Environment, 114*, 2911-2924

Cortes, C., & Vapnik, V. (1995). Support-vector networks. *Machine learning, 20*, 273-297

Council, F.E. (2009). Guidance for implementation of federal wildland fire management policy. In U.S.D.o.A.a.U.S.D.o.t. Interior (Ed.)

Covington, W.W., & Moore, M.M. (1994). Postsettlement changes in natural fire regimes and forest structure: ecological restoration of old-growth ponderosa pine forests. *Journal of Sustainable Forestry, 2*, 153-181

Cubbage, F.W., & Siegel, W.C. (1985). The law regulating private forest practices. *Journal of Forestry, 83*, 538-545

Dennison, P.E., Brewer, S.C., Arnold, J.D., & Moritz, M.A. (2014). Large wildfire trends in the western United States, 1984–2011. *Geophysical Research Letters*

D áz-Uriarte, R., & De Andres, S.A. (2006). Gene selection and classification of microarray data using random forest. *BMC bioinformatics, 7*, 3

Dixon, G.E. (2002). Essential FVS: A user's guide to the Forest Vegetation Simulator. *Fort Collins, CO: USDA-Forest Service, Forest Management Service Center*

Dudley, N. (2008). *Guidelines for applying protected area management categories*. IUCN

Eidenshink, J., Schwind, B., Brewer, K., Zhu, Z.-L., Quayle, B., & Howard, S. (2007a). project for monitoring trends in burn severity. *Fire Ecology*

Eidenshink, J., Schwind, B., Brewer, K., Zhu, Z.L., Quayle, B., & Howard, S. (2007b). A project for monitoring trends in burn severity

Everhart, W.C. (1972). *The National Park Service*. New York: Praeger Publishers Franklin, S., & Maudie, A. (2001). Using spatial co-occurrence texture to increase forest structure and species composition classification accuracy

Franks, S., Masek, J.G., & Turner, M.G. (2013). Monitoring forest regrowth following large scale fire using satellite data-A case study of Yellowstone National Park, USA. *Eur. J. Remote Sens, 46*, 551-569

Friedman, J., Hastie, T., & Tibshirani, R. (2001). *The elements of statistical learning*. Springer series in statistics Springer, Berlin

Girod, C., Hurtt, G., Frolking, S., Aber, J., & King, A. (2007). The tension between fire risk and carbon storage: evaluating US carbon and fire management strategies through ecosystem models. *Earth Interactions, 11*, 1-33

Goetz, S.J., Bond-Lamberty, B., Law, B.E., Hicke, J., Huang, C., Houghton, R., McNulty, S., O'Halloran, T., Harmon, M., & Meddens, A. (2012). Observations and assessment of forest carbon dynamics following disturbance in North America. *Journal of Geophysical Research: Biogeosciences (2005–2012), 117*

Habeck, J.R., & Mutch, R.W. (1973). Fire-dependent forests in the Northern Rocky Mountains. *Quaternary Research, 3*, 408-424

Hann, W., Shlisky, A., Havlina, D., Schon, K., Barrett, S., DeMeo, T., Pohl, K., Menakis, J., Hamilton, D., & Jones, J. (2004). Interagency fire regime condition class guidebook. *Interagency and The Nature Conservancy Fire Regime Condition Class website. USDA Forest Service, US Department of the Interior, The Nature Conservancy, and Systems for Environmental Management. Available online: www. frcc. gov*

Hann, W.J., & Bunnell, D.L. (2001). Fire and land management planning and implementation across multiple scales. *International Journal of Wildland Fire, 10*, 389-403

Hansen, A. (2006). Yellowstone bioregional assessment: understanding the ecology and land use of Greater Yellowstone. In: Technical Report

Hansen, A.J., Rotella, J.J., Kraska, M.P., & Brown, D. (2000). Spatial patterns of primary productivity in the Greater Yellowstone Ecosystem. *Landscape Ecology, 15*, 505-522

Hardy, C., Schmidt, K., Menakis, J., & Sampson, R. (2001). Spatial data for national fire planning and fuel management. *International Journal of Wildland Fire, 10*, 353-372

Harvey, B.J., Donato, D.C., Romme, W.H., & Turner, M.G. (2014). Fire severity and tree regeneration following bark beetle outbreaks: the role of outbreak stage and burning conditions. *Ecological Applications, 24*, 1608-1625

Hatala, J.A., Crabtree, R.L., Halligan, K.Q., & Moorcroft, P.R. (2010). Landscape-scale patterns of forest pest and pathogen damage in the Greater Yellowstone Ecosystem. *Remote Sensing of Environment, 114*, 375-384

Healey, S.P., Urbanski, S.P., Patterson, P.L., & Garrard, C. (2014). A framework for simulating map error in ecosystem models. *Remote Sensing of Environment, 150*, 207-217

Heinselman, M.L. (1973). Fire in the virgin forests of the Boundary Waters Canoe Area, Minnesota. *Quaternary Research, 3*, 329-382

Heinselman, M.L. (1981). Fire and succession in the conifer forests of northern North America. *Forest succession* (pp. 374-405): Springer

Houghton, R.A., Hackler, J.L., & Lawrence, K. (1999). The US carbon budget: contributions from land-use change. *Science, 285*, 574-578

Huang, C., Davis, L., & Townshend, J. (2002). An assessment of support vector machines for land cover classification. *International Journal of Remote Sensing, 23*, 725-749

Huang, C., Goward, S.N., Masek, J.G., Gao, F., Vermote, E.F., Thomas, N., Schleeweis, K., Kennedy, R.E., Zhu, Z., Eidenshink, J.C., & Townshend, J.R.G. (2009a). Development of time series stacks of Landsat images for reconstructing forest disturbance history. *International Journal of Digital Earth, 2*, 195-218

Huang, C., Goward, S.N., Masek, J.G., Thomas, N., Zhu, Z., & Vogelmann, J.E. (2010). An automated approach for reconstructing recent forest disturbance history using dense Landsat time series stacks. *Remote Sensing of Environment, 114*, 183-198

Huang, C., Goward, S.N., Schleeweis, K., Thomas, N., Masek, J.G., & Zhu, Z. (2009b). Dynamics of national forests assessed using the Landsat record: Case studies in eastern United States. *Remote Sensing of Environment, 113*, 1430-1442

Huang, C., Kim, S., Altstatt, A., Townshend, J.R.G., Davis, P., Song, K., Tucker, C.J., Rodas, O., Yanosky, A., Clay, R., & Musinsky, J. (2007). Rapid loss of Paraguay's Atlantic forest and the status of protected areas – a Landsat assessment. *Remote Sensing of Environment, 106*, 460-466

Huang, C., Ling, P.-Y., & Zhu, Z. (2015). North Carolina's forest disturbance and timber production assessed using time series Landsat observations. *International Journal of Digital Earth*, 1-23

Huang, C., Schleeweis, K., Thomas, N., & Goward, S.N. (2011). Forest dynamics within and around the Olympic National Park assessed using time series Landsat observations. In Y. Wang (Ed.), *Remote Sensing of Protected Lands* (pp. 71-93). London: Taylor & Francis

Huang, C., Song, K., Kim, S., Townshend, J.R., Davis, P., Masek, J.G., & Goward, S.N. (2008a). Use of a dark object concept and support vector machines to automate forest cover change analysis. *Remote Sensing of Environment, 112*, 970-985

Huang, C., Song, K., Kim, S., Townshend, J.R.G., Davis, P., Masek, J., & Goward, S.N. (2008b). Use of a dark object concept and support vector machines to automate forest cover change analysis. *Remote Sensing of Environment, 112*, 970-985

Hurtt, G., Pacala, S., Moorcroft, P., Caspersen, J., Shevliakova, E., Houghton, R., & Moore, B. (2002). Projecting the future of the US carbon sink. *Proceedings of the National Academy of Sciences, 99*, 1389-1394

Kane, V.R., Cansler, C.A., Povak, N.A., Kane, J.T., McGaughey, R.J., Lutz, J.A., Churchill, D.J., & North, M.P. (2015a). Mixed severity fire effects within the Rim fire: Relative importance of local climate, fire weather, topography, and forest structure. *Forest Ecology and Management, 358*, 62-79

Kane, V.R., Lutz, J.A., Cansler, C.A., Povak, N.A., Churchill, D.J., Smith, D.F., Kane, J.T., & North, M.P. (2015b). Water balance and topography predict fire and forest structure patterns. *Forest Ecology and Management, 338*, 1-13

Kayitakire, F., Hamel, C., & Defourny, P. (2006). Retrieving forest structure variables based on image texture analysis and IKONOS-2 imagery. *Remote Sensing of Environment, 102*, 390-401

Keane, R., Rollins, M., & Zhu, Z. (2007). Using simulated historical time series to prioritize fuel treatments on landscapes across the United States: The LANDFIRE prototype project. *Ecological Modelling, 204*, 485-502

Keane, R.E., Cary, G.J., Davies, I.D., Flannigan, M.D., Gardner, R.H., Lavorel, S., Lenihan, J.M., Li, C., & Rupp, T.S. (2004). A classification of landscape fire succession models: spatial simulations of fire and vegetation dynamics. *Ecological Modelling, 179*, 3-27

Keane, R.E., Cary, G.J., & Parsons, R. (2003). Using simulation to map fire regimes: an evaluation of approaches, strategies, and limitations. *International Journal of Wildland Fire, 12*, 309-322

Keane, R.E., Hessburg, P.F., Landres, P.B., & Swanson, F.J. (2009). The use of historical range and variability (HRV) in landscape management. *Forest Ecology and Management, 258*, 1025-1037

Keane, R.E., Holsinger, L.M., Pratt, S.D., & Station, R.M.R. (2006). *Simulating historical landscape dynamics using the landscape fire succession model LANDSUM version 4.0*. US Department of Agriculture, Forest Service, Rocky Mountain Research Station

Keane, R.E., Parsons, R.A., & Hessburg, P.F. (2002a). Estimating historical range and variation of landscape patch dynamics: limitations of the simulation approach. *Ecological Modelling, 151*, 29-49

Keane, R.E., Ryan, K.C., Veblen, T.T., Allen, C.D., Logan, J.A., & Hawkes, B. (2002b). The cascading effects of fire exclusion in Rocky Mountain ecosystems. *Rocky Mountain futures: an ecological perspective*, 133-152

Keane, R.E., Ryan, K.C., Veblen, T.T., Allen, C.D., Logan, J.A., Hawkes, B., & Barron, J. (2002c). The cascading effects of fire exclusion in Rocky Mountain ecosystems. *Rocky Mountain futures: an ecological perspective*, 133-152

Kendall, K.C., & Keane, R.E. (2001). Whitebark pine decline: infection, mortality, and population trends. *Whitebark pine communities: ecology and restoration. Edited by DF Tomback, SF Arno, and RE Keane. Island Press, Washington, DC*, 221-242

Kennedy, R.E., Yang, Z., & Cohen, W.B. (2010a). Detecting trends in forest disturbance and recovery using yearly Landsat time series: 1. LandTrendr—Temporal segmentation algorithms. *Remote Sensing of Environment, 114*, 2897-2910

Kennedy, R.E., Yang, Z., & Cohen, W.B. (2010b). Detecting trends in forest disturbance and recovery using yearly Landsat time series: 1. LandTrendr — Temporal segmentation algorithms. *Remote Sensing of Environment, 114*, 2897-2910

Kennedy, R.E., Yang, Z., Cohen, W.B., Pfaff, E., Braaten, J., & Nelson, P. (2012). Spatial and temporal patterns of forest disturbance and regrowth within the area of the Northwest Forest Plan. *Remote Sensing of Environment, 122*, 117-133

Kessell, S.R., Fischer, W.C., Forest, I., & Station, R.E. (1981). *Predicting Postfire Plant Succession for Fire Management Planning*. USFS

Kotrlik, J., & Higgins, C. (2001). Organizational research: Determining appropriate sample size in survey research appropriate sample size in survey research. *Information technology, learning, and performance journal, 19*, 43

Kurz, W.A., Stinson, G., Rampley, G.J., Dymond, C.C., & Neilson, E.T. (2008). Risk of natural disturbances makes future contribution of Canada's forests to the global carbon cycle highly uncertain. *Proceedings of the National Academy of Sciences, 105*, 1551-1555

Landres, P., Barns, C., Dennis, J.G., Devine, T., Geissler, P., McCasland, C.S., Merigliano, L., Seastrand, J., & Swain, R. (2008). Keeping it wild: an interagency strategy to monitor trends in wilderness character across the National Wilderness Preservation System

Lenihan, J.M., Daly, C., Bachelet, D., & Neilson, R.P. (1998). Simulating broad-scale fire severity in a dynamic global vegetation model. *Northwest Science, 72*, 91-101

Li, C., Barclay, H., Liu, J., & Campbell, D. (2005). Simulation of historical and current fire regimes in central Saskatchewan. *Forest Ecology and Management, 208*, 319-329

Li, H., Calder, C.A., & Cressie, N. (2007). Beyond Moran's I: Testing for Spatial Dependence Based on the Spatial Autoregressive Model. *Geographical Analysis, 39*, 357-375

Li, M., Huang, C., Zhu, Z., Shi, H., Lu, H., & Peng, S. (2009a). Assessing rates of forest change and fragmentation in Alabama, USA, using the vegetation change tracker model. *Forest Ecology and Management, 257*, 1480-1488

Li, M., Huang, C., Zhu, Z., Wen, W., Xu, D., & Liu, A. (2009b). Use of remote sensing coupled with a vegetation change tracker model to assess rates of forest change and fragmentation in Mississippi, USA. *International Journal of Remote Sensing, 30*, 6559-6574

Liaw, A., & Wiener, M. (2002). Classification and regression by randomForest. *R news, 2*, 18-22

Liu, S., Bond-Lamberty, B., Hicke, J., Vargas, R., Zhao, S., Chen, J., Edburg, S., Hu, Y., Liu, J., McGuire, A., Xiao, J., Keane, R., Yuan, W., Tang, J., Luo, Y., Potter, C., & Oeding, J. (2011). Simulating the impacts of disturbances on forest carbon cycling in North America: Processes, data, models, and challenges. *Journal of Geophysical Research-Biogeosciences, 116*

Loboda, T., Zhang, Z., O'Neal, K., Sun, G., Csiszar, I., Shugart, H., & Sherman, N. (2012). Reconstructing disturbance history using satellite-based assessment of the distribution of land cover in the Russian Far East. *Remote Sensing of Environment, 118*, 241-248

Logan, J.A., Macfarlane, W.W., & Willcox, L. (2010). Whitebark pine vulnerability to climate-driven mountain pine beetle disturbance in the Greater Yellowstone Ecosystem. *Ecological Applications, 20*, 895-902

Lu, D., Mausel, P., Brond ́ızio, E., & Moran, E. (2004). Change detection techniques. *International Journal of Remote Sensing, 25*, 2365-2407

Magnani, F., Mencuccini, M., Borghetti, M., Berbigier, P., Berninger, F., Delzon, S., Grelle, A., Hari, P., Jarvis, P.G., Kolari, P., Kowalski, A.S., Lankreijer, H., Law, B.E., Lindroth, A., Loustau, D., Manca, G., Moncrieff, J.B., Rayment, M., Tedeschi, V., Valentini, R., & Grace, J. (2007). The human footprint in the carbon cycle of temperate and boreal forests. *Nature, 447*, 849-851

Marks, P., & Bormann, F. (1972). Revegetation following forest cutting: mechanisms for return to steady-state nutrient cycling. *Science, 176*, 914-915

Marston, R.A., & Anderson, J.E. (1991). Watersheds and vegetation of the Greater Yellowstone Ecosystem. *Conservation Biology, 5*, 338-346

Masek, J., Goward, S., Kennedy, R., Cohen, W., Moisen, G., Schleeweis, K., & Huang, C. (2013). United States Forest Disturbance Trends Observed Using Landsat Time Series. *Ecosystems, 16*, 1087-1104

Masek, J.G., Huang, C., Wolfe, R.E., Cohen, W., Hall, F., Kutler, J., & Nelson, P. (2008). North American forest disturbance mapped from a decadal Landsat record. *Remote Sensing of Environment, 112*, 2914-2926

Masek, J.G., Vermote, E.F., Saleous, N.E., Wolfe, R., Hall, F.G., Huemmrich, K.F., Feng, G., Kutler, J., & Teng-Kui, L. (2006a). A Landsat surface reflectance dataset for North America, 1990-2000. *IEEE Geoscience and Remote Sensing Letters, 3*, 68-72

Masek, J.G., Vermote, E.F., Saleous, N.E., Wolfe, R., Hall, F.G., Huemmrich, K.F., Gao, F., Kutler, J., & Lim, T.-K. (2006b). A Landsat surface reflectance dataset for North America, 1990-2000. *Geoscience and Remote Sensing Letters, IEEE, 3*, 68-72

McGuire, A.D., Sitch, S., Clein, J.S., Dargaville, R., Esser, G., Joos, F., Heimann, M., Joos, F., Kaplan, J., Kicklighter, D.W., Meier, R.A., Melillo, J.M., Moore III, B., Prentice, I.C., Ramankutty, N., Reichenau, T., Schloss, A., Tian, H., Williams, L.J., & Wittenberg, U. (2001). Carbon balance of the terrestrial biosphere in the twentieth century: Analyses of C02, climate and land use effects with four process-based ecosystem models. *Global Biogeochemical Cycles, 15*, 183-206

McKinley, D.C., Ryan, M.G., Birdsey, R.A., Giardina, C.P., Harmon, M.E., Heath, L.S., Houghton, R.A., Jackson, R.B., Morrison, J.F., & Murray, B.C. (2011). A synthesis of current knowledge on forests and carbon storage in the United States. *Ecological Applications, 21*, 1902-1924

Miller, J.D., Knapp, E.E., Key, C.H., Skinner, C.N., Isbell, C.J., Creasy, R.M., & Sherlock, J.W. (2009). Calibration and validation of the relative differenced Normalized Burn Ratio (RdNBR) to three measures of fire severity in the Sierra Nevada and Klamath Mountains, California, USA. *Remote Sensing of Environment, 113*, 645-656

Moran, P.A.P. (1950). Notes on Continuous Stochastic Phenomena. *Biometrika, 37*, 17-23

Morgan, P., Bunting, S.C., Black, A.E., Merrill, T., & Barrett, S. (1996). Fire regimes in the Interior Columbia River Basin: past and present. *Final report for RJVA-INT-94913: Coarse-scale classification and mapping of disturbance regimes in the Columbia River Basin. Interior Columbia Basin Ecosystem Management Project*

Morgan, P., Hardy, C.C., Swetnam, T.W., Rollins, M.G., & Long, D.G. (2001). Mapping fire regimes across time and space: understanding coarse and fine-scale fire patterns. *International Journal of Wildland Fire, 10*, 329-342

Neigh, C.S., Bolton, D.K., Diabate, M., Williams, J.J., & Carvalhais, N. (2014). An Automated Approach to Map the History of Forest Disturbance from Insect Mortality and Harvest with Landsat Time-Series Data. *Remote Sensing, 6*, 2782-2808

Olofsson, P., Foody, G.M., Herold, M., Stehman, S.V., Woodcock, C.E., & Wulder, M.A. (2014). Good practices for estimating area and assessing accuracy of land change. *Remote Sensing of Environment, 148*, 42-57

Olofsson, P., Foody, G.M., Stehman, S.V., & Woodcock, C.E. (2013). Making better use of accuracy data in land change studies: Estimating accuracy and area and quantifying uncertainty using stratified estimation. *Remote Sensing of Environment, 129*, 122-131

Pal, M., & Mather, P. (2005). Support vector machines for classification in remote sensing. *International Journal of Remote Sensing, 26*, 1007-1011

Pan, Y., Birdsey, R.A., Fang, J., Houghton, R., Kauppi, P.E., Kurz, W.A., Phillips, O.L., Shvidenko, A., Lewis, S.L., & Canadell, J.G. (2011). A large and persistent carbon sink in the world's forests. *Science, 333*, 988-993

Parmenter, A.W., Hansen, A., Kennedy, R.E., Cohen, W., Langner, U., Lawrence, R., Maxwell, B., Gallant, A., & Aspinall, R. (2003). Land use and land cover change in the Greater Yellowstone Ecosystem: 1975-1995. *Ecological Applications, 13*, 687-703

Pfister, R.D., & Arno, S.F. (1980). Classifying forest habitat types based on potential climax vegetation. *Forest Science, 26*, 52-70

Pontius Jr, R.G., & Millones, M. (2011). Death to Kappa: birth of quantity disagreement and allocation disagreement for accuracy assessment. *International Journal of Remote Sensing, 32*, 4407-4429

Potapov, P., Hansen, M.C., Stehman, S.V., Pittman, K., & Turubanova, S. (2009). Gross forest cover loss in temperate forests: biome-wide monitoring results using MODIS and Landsat data. *Journal of Applied Remote Sensing, 3*

Powell, S.L., Cohen, W.B., Healey, S.P., Kennedy, R.E., Moisen, G.G., Pierce, K.B., & Ohmann, J.L. (2010). Quantification of live aboveground forest biomass dynamics with Landsat time-series and field inventory data: A comparison of empirical modeling approaches. *Remote Sensing of Environment, 114*, 1053-1068

Prasad, A.M., Iverson, L.R., & Liaw, A. (2006). Newer classification and regression tree techniques: bagging and random forests for ecological prediction. *Ecosystems, 9*, 181-199

Pratt, S., Holsinger, L., & Keane, R.E. (2006). Using simulation modeling to assess historical reference conditions for vegetation and fire regimes for the LANDFIRE prototype project. *The LANDFIRE prototype project: nationally consistent and locally relevant geospatial data for wildland fire management*, 277-314

Raymond, C.L., Healey, S., Peduzzi, A., & Patterson, P. (2015). Representative regional models of post-disturbance forest carbon accumulation: Integrating inventory data and a growth and yield model. *Forest Ecology and Management, 336*, 21-34
Reinhardt, E.D., & Crookston, N.L. (2003). The fire and fuels extension to the forest vegetation simulator

Rhemtulla, J.M., Mladenoff, D.J., & Clayton, M.K. (2009). Historical forest baselines reveal potential for continued carbon sequestration. *Proceedings of the National Academy of Sciences, 106*, 6082-6087

Rollins, M.G. (2009). LANDFIRE: a nationally consistent vegetation, wildland fire, and fuel assessment. *International Journal of Wildland Fire, 18*, 235-249

Roy, D.P., Boschetti, L., & Trigg, S.N. (2006). Remote sensing of fire severity: assessing the performance of the normalized burn ratio. *Geoscience and Remote Sensing Letters, IEEE, 3*, 112-116

Ruefenacht, B., Finco, M., Nelson, M., Czaplewski, R., Helmer, E., Blackard, J., Holden, G., Lister, A., Salajanu, D., & Weyermann, D. (2008). Conterminous US and Alaska forest type mapping using forest inventory and analysis data. *Photogrammetric Engineering & Remote Sensing, 74*, 1379-1388

Running, S.W. (2006). Is global warming causing more, larger wildfires? *Science(Washington), 313*, 927-928

Running, S.W., & Hunt, E.R. (1993). Generalization of a forest ecosystem process model for other biomes, BIOME-BGC, and an application for global-scale models. *Scaling physiological processes: Leaf to globe*, 141-158

Ryan, K.C., & Noste, N.V. (1985). Evaluating prescribed fires

Salmi, T. (2002). *Detecting Trends of Annual Values of Atmospheric Pollutants by the Mann-Kendall Test and Sen's Slope Estimates: The Excel Template Application MAKESENS*. Finnish Meteorological Institute

Savage, M., Brown, P.M., & Feddema, J. (1996). The role of climate in a pine forest regeneration pulse in the southwestern United States. *Ecoscience*, 310-318

Schoennagel, T., Turner, M.G., & Romme, W.H. (2003). The influence of fire interval and serotiny on postfire lodgepole pine density in Yellowstone National Park. *Ecology, 84*, 2967-2978

Schroeder, T.A., Wulder, M.A., Healey, S.P., & Moisen, G.G. (2011). Mapping wildfire and clearcut harvest disturbances in boreal forests with Landsat time series data. *Remote Sensing of Environment, 115*, 1421-1433

Scott, A.C., Bowman, D.M., Bond, W.J., Pyne, S.J., & Alexander, M.E. (2013). *Fire on Earth: An Introduction*. John Wiley & Sons

Singh, A. (1989). Digital change detection techniques using remotely-sensed data. *International Journal of Remote Sensing, 10*, 989-1003

Soares-Filho, B., Moutinho, P., Nepstad, D., Anderson, A., Rodrigues, H., Garcia, R., Dietzsch, L., Merry, F., Bowman, M., & Hissa, L. (2010). Role of Brazilian Amazon protected areas in climate change mitigation. *Proceedings of the National Academy of Sciences, 107*, 10821-10826

Spittlehouse, D.L., & Stewart, R.B. (2004). Adaptation to climate change in forest management. *Journal of Ecosystems and Management, 4*

Steele, B.M., Reddy, S.K., & Keane, R.E. (2006). A methodology for assessing departure of current plant communities from historical conditions over large landscapes. *ecological modelling, 199*, 53-63

Stehman, S.V. (2000). Practical implications of design-based sampling inference for thematic map accuracy assessment. *Remote Sensing of Environment, 72*, 35-45

Stehman, S.V., Wickham, J.D., Smith, J.H., & Yang, L. (2003). Thematic accuracy of the 1992 National Land-Cover Data for the eastern United States: Statistical methodology and regional results. *Remote Sensing of Environment, 86*, 500-516

Team, R.C. (2012). R: A language and environment for statistical computing

Thomas, N.E., Huang, C., Goward, S.N., Powell, S., Rishmawi, K., Schleeweis, K., & Hinds, A. (2011). Validation of North American forest disturbance dynamics derived from Landsat time series stacks. *Remote Sensing of Environment, 115*, 19-32

Turner, D.P., Ritts, W.D., Kennedy, R.E., Gray, A.N., & Yang, Z. (2015). Effects of harvest, fire, and pest/pathogen disturbances on the West Cascades ecoregion carbon balance. *Carbon balance and management, 10*, 12

Turner, M.G. (2010). Disturbance and landscape dynamics in a changing world 1. *Ecology, 91*, 2833-2849

Turner, M.G., Baker, W.L., Peterson, C.J., & Peet, R.K. (1998). Factors Influencing Succession: Lessons from Large, Infrequent Natural Disturbances. *Ecosystems, 1*, 511-523

Turner, M.G., Hargrove, W.W., Gardner, R.H., & Romme, W.H. (1994). Effects of fire on landscape heterogeneity in Yellowstone National Park, Wyoming. *Journal of Vegetation Science, 5*, 731-742

Turner, M.G., Romme, W.H., & Gardner, R.H. (1999). Prefire heterogeneity, fire severity, and early postfire plant reestablishment in subalpine forests of Yellowstone National Park, Wyoming. *International Journal of Wildland Fire, 9*, 21-36

Turner, M.G., Romme, W.H., Gardner, R.H., & Hargrove, W.W. (1997). Effects of fire size and pattern on early succession in Yellowstone National Park. *Ecological Monographs, 67*, 411-433

Turner, M.G., Romme, W.H., & Tinker, D.B. (2003). Surprises and lessons from the 1988 Yellowstone fires. *Frontiers in Ecology and the Environment, 1*, 351-358
Weaver, T. (1980). Climates of vegetation types of the northern Rocky Mountains and adjacent plains. *American Midland Naturalist*, 392-398

Westerling, A., Turner, M., Smithwick, E., Romme, W., & Ryan, M. (2011). Continued warming could transform Greater Yellowstone fire regimes by mid-21st century. *Proceedings of the National Academy of Sciences of the United States of America, 108*, 13165-13170

Westerling, A.L., Hidalgo, H.G., Cayan, D.R., & Swetnam, T.W. (2006). Warming and Earlier Spring Increase Western U.S. Forest Wildfire Activity. *Science, 313*, 940-943

White, J.D., Ryan, K.C., Key, C.C., & Running, S.W. (1996). Remote sensing of forest fire severity and vegetation recovery. *International Journal of Wildland Fire, 6*, 125-136

Whitlock, C., Shafer, S.L., & Marlon, J. (2003). The role of climate and vegetation change in shaping past and future fire regimes in the northwestern US and the implications for ecosystem management. *Forest Ecology and Management, 178*, 5-21

Wijdeven, S.M., & Kuzee, M.E. (2000). Seed availability as a limiting factor in forest recovery processes in Costa Rica. *Restoration ecology, 8*, 414-424

Wilcox, R.R. (2012). *Introduction to robust estimation and hypothesis testing*. Academic Press

Williams, D.L., Goward, S., & Arvidson, T. (2006). Landsat: Yesterday, today, and tomorrow. *Photogrammetric Engineering and Remote Sensing, 72*, 1171

Woodcock, C.E., Allen, R., Anderson, M., Belward, A., Bindschadler, R., Cohen, W., Gao, F., Goward, S.N., Helder, D., Helmer, E., Nemani, R., Oreopoulos, L., Schott,

J., Thenkabail, P.S., Vermote, E.F., Vogelmann, J., Wulder, M.A., & Wynne, R. (2008). Free Access to Landsat Imagery. *Science, 320*, 1011

Wulder, M.A., White, J.C., Goward, S.N., Masek, J.G., Irons, J.R., Herold, M., Cohen, W.B., Loveland, T.R., & Woodcock, C.E. (2008). Landsat continuity: Issues and opportunities for land cover monitoring. *Remote Sensing of Environment, 112*, 955-969

Zhao, F., Huang, C., & Zhu, Z. (2015a). Use of Vegetation Change Tracker and Support Vector Machine to Map Disturbance Types in Greater Yellowstone Ecosystems in a 1984-2010 Landsat Time Series. *Geoscience and Remote Sensing Letters, IEEE, 12*, 1650-1654

Zhao, F., Keane, R., Zhu, Z., & Huang, C. (2015b). Comparing historical and current wildfire regimes in the Northern Rocky Mountains using a landscape succession model. *Forest Ecology and Management, 343*, 9-21

Zhu, Z., Key, C., Ohlen, D., & Benson, N. (2006). Evaluate sensitivities of burn-severity mapping algorithms for different ecosystems and fire histories in the United States. US Department of Interior, Final Report to the Joint Fire Science Program: Project JFSP01-1-4-12. In. Sious Falls, SD

Zhu, Z., Woodcock, C.E., & Olofsson, P. (2012). Continuous monitoring of forest disturbance using all available Landsat imagery. *Remote Sensing of Environment, 122*, 75-91